Characterization of Tetraspanins and their Role in the Hepatitis C Virus Life Cycle

Dissertation

der Mathematisch-Naturwissenschaftlichen Fakultät
der Eberhard Karls Universität Tübingen
zur Erlangung des Grades eines
Doktors der Naturwissenschaften
(Dr. rer. nat.)

vorgelegt von
Maximilian Bunz
aus Günzburg

Tübingen
2023

Gedruckt mit Genehmigung der Mathematisch-Naturwissenschaftlichen Fakultät der Eberhard Karls Universität Tübingen.

Tag der mündlichen Qualifikation: 23.06.2023

Dekan:	Prof. Dr. Thilo Stehle
1. Berichterstatter:	Prof. Dr. Michael Schindler
2. Berichterstatter:	Prof. Dr. Ulrich Rothbauer

Summary

Although infection with the Hepatitis C virus (HCV) can be cured by application of direct acting antivirals (DAAs), it remains a severe health concern throughout the world. The research community has disentangled many aspects of HCV biology and its interaction with the immune system, yet failed to develop a protective vaccine. By understanding the interplay between virus and host in more detail, it is hoped to gain profound insights that help to tackle the current lack of a vaccine and potential future problems caused by the evolution of therapy resistant variants.

In this thesis, the tetraspanin family of proteins was investigated in the context of HCV replication. A flow cytometry-based surface expression screening revealed that levels of tetraspanins CD63 and CD81 were lower in cells expressing a full-genome viral RNA. CD81 is already well characterized as an important co-receptor for HCV entry. Further analyses were conducted to investigate how the downregulation of CD81 is mediated and to uncover potential functions. It could be demonstrated that the downregulation of CD81 in HCV expressing cells is mediated on the transcriptional level. To examine potential additional roles of CD81 in the life cycle of HCV, CD81 knock-out cells were created. In the course of their characterization it was discovered that viral constructs with impaired replication kinetics are dependent on the presence of CD81 at early stages of the viral life cycle. Subsequently, it was shown that a lack of CD81 can lead to a more pronounced integrated stress response (ISR) and higher NFκB activity. This leads to the hypothesis that HCV downregulates CD81 after the initial establishment of replication to benefit from pro-survival signals mediated through the ISR and NFκB pathways.

In summary, it was shown that CD81 is downregulated by HCV in productively replicating cells to presumably increase pro-survival signals. If further investigated in more detail, this mechanism could contribute to the understanding of how chronic HCV is established and illuminate possible points to intervene.

Zusammenfassung

Obwohl Infektionen mit dem Hepatitis C Virus (HCV) durch den Einsatz von direkt wirkenden Virostatika (Direct Acting Antivirals; DAA) geheilt werden können, bleiben Infektionen mit HCV und deren Folgen ein ernstes Gesundheitsproblem weltweit. Die Forschung hat viele Aspekte der HCV Biologie und seiner Interaktion mit dem Immunsystem erforscht, konnte jedoch bisher keinen schützenden Impfstoff entwickeln. Durch ein besseres Verständnis des Zusammenspiels zwischen Virus und Wirt erhofft man sich tiefgreifendere Erkenntnisse, die dazu beitragen können, das derzeitige Fehlen eines Impfstoffs, sowie künftige Probleme, die durch die Enstehung therapieresistenter Virusvarianten verursacht werden könnten, zu bewältigen.

In dieser Arbeit wurde die Tetraspanin Proteinfamilie im Zusammenhang mit der HCV-Replikation untersucht. Ein auf Durchflusszytometrie basierendes Screening der Oberflächenexpression ergab, dass die Konzentrationen der Tetraspanine CD63 und CD81 in Zellen niedriger waren, die eine virale, genomische RNA exprimieren. CD81 ist als wichtiger Co-Rezeptor für den Eintritt von HCV in Zellen bereits gut charakterisiert. Weitere Analysen wurden durchgeführt, um zu untersuchen, wie die Herabregulierung von CD81 zustande kommt und um mögliche Funktionen aufzudecken. Es konnte gezeigt werden, dass die Herunterregulierung von CD81 in HCV-exprimierenden Zellen auf der Transkriptionsebene vermittelt wird. Um mögliche weitere Rollen von CD81 im Lebenszyklus von HCV zu untersuchen, wurden CD81 Knock-out Zellen generiert. Im Verlauf ihrer Charakterisierung wurde festgestellt, dass virale Konstrukte mit beeinträchtigter Replikationskinetik in frühen Stadien des viralen Lebenszyklus von der Anwesenheit von CD81 abhängig sind. Anschließend wurde gezeigt, dass das Fehlen von CD81 zu einer ausgeprägteren integrierten Stressantwort (Integrated Stress Response; ISR) und einer höheren NFκB-Aktivität führen kann. Dies führt zu der Hypothese, dass nach der anfänglichen Etablierung der Replikation, CD81 von HCV herunterreguliert wird, um von überlebensfördernden Signalen zu profitieren, die durch die ISR- und NFκB-Wege vermittelt werden.

Insgesamt konnte gezeigt werden, dass CD81 durch HCV in produktiv replizierenden Zellen herunterreguliert wird, vermutlich um überlebensfördernde Signale zu verstärken. Wenn dieser Mechanismus weiter erforscht wird, könnte er zum Verständnis beitragen wie HCV Infektionen chronisch werden und aufzeigen wo mögliche Ansatzpunkte für ein Eingreifen liegen.

Contents

List of Tables

List of Figures

Abbreviations

(+)ssRNA	Positive-sense single strand RNA
aa	Amino acid
APS	Ammonium persulfate
ARE	Antioxidant response element
Arl8b	ADP-ribosylation factor-like protein 8b
ATF	Activating transcription factor
BSA	Bovine serum albumine
CFP	Cyan fluorescent protein
CHOP	C/EBP homologous protein
CKII	Casein kinase II
CLDN1	Claudin-1
COPII	Coat Protein Complex II
CoV	Coronavirus
CRE	*Cis*-acting replicating element
DAA	Direct acting antiviral
DAPI	4',6-Diamidine-2'-phenylindole dihydrochloride
DEPC	Diethyl pyrocarbonate
DMEM	Dulbecco's modified eagles medium
DMSO	Dimethylsulfoxide
DMV	Double-membrane vesicle
DTT	Dithiothreitol
EDTA	ethylenediamine tetraacetate
eIF2α	eukaryotic translation initiation factor 2α
EP	Electroporation
ER	Endoplasmatic reticulum
ERAD	ER-associated degradation
ESCRT	Endosomal sorting complex required for transport
FACS	Fluorescence assisted cell sorting
FCS	Fetal calf serum
FLuc	Firefly luciferase
FRET	Förster resonance energy transfer
G3BP1	Ras GTPase-activating protein-binding protein 1
GADD34	Growth arrest and DNA damage-inducible protein

GDP	Guanosine diphosphate
GFP	Green fluorescent protein
GLuc	*Gaussia* luciferase
GTP	Guanosine triphosphate
HBV	Hepatitis B virus
HCC	Hepatocellular carcinoma
HCV	Hepatitis C virus
HEK	Human embryonic kidney cells
HIV	Human immunodeficiency virus
HPV	Human papillomavirus
HVR	Hyper variable region
IAV	Influenza A virus
IFITM	Interferon-induced transmembrane protein
IFN	Interferon
IL	Interleucin
IMPβ1	Importin β1
IRE1α	Insositol-requiring enzyme 1α
IRES	Internal ribosome entry site
IRF	Interferon regulating factor
ISG	Interferon stimulated gene
ISR	Integrated stress response
LB	Luria-Bertani
LD	Lipid droplet
LDL	Low density lipoprotein
LDLR	LDL receptor
LEL	Large extracellular loop
LPS	Lipopolysaccharide
LUJV	Lujo virus
LVP	Lipo-viro particle
m^6A	*N*-6-methylation at adenosine
MARV	Marburg virus
MAVS	Mitochondrial antiviral-signaling protein
MDA5	Melanoma differentiation-associated protein 5
MFI	Mean fluorescence intensity
MMV	Multi-membrane vesicle
MVB	Multivesicular body
NaCl	Sodium chloride

NADPH	Nicotinamide adenine dinucleotide phosphate
NFκB	Nuclear factor kappa-light-chain-enhancer of activated B cells
NOX	NADPH oxidase
Nrf2	Nuclear factor erythroid 2-related factor 2
NS	Non-structural
NTP	Nucleoside triphosphate
OCLN	Occludin
PAGE	Polyacrylamide gel electrophoresis
PAS	Pre-autophagosomal structure
PBS	Phosphate buffered saline
PE	Phycoerythrin
PEG	Polyethylenglycol
PEI	Polyethyleneimine
PERK	PKR-like ER kinase
PFA	Paraformaldehyde
PI	Protease inhibitor
PI4Kα	Phosphatidylinositol-4-kinase α
PI4P	Phosphatidylinositol-4-phosphate
PKR	Protein kinase RNA-activated
PM	Plasma membrane
PMA	Phorbol 12-myristate 13-acetate
PRR	Pattern recognition receptor
RdRp	RNA-dependent RNA polymerase
RIDD	Regulated IRE1α-dependent decay
RIG-I	Retinoic acid-inducible gene I
RILP	Rab-interacting lysosomal protein
RLuc	*Renilla* luciferase
ROS	Reactive oxigen species
RT	Room temperature
SD	Standard deviation
SDS	Sodium dodecylsulfate
SEL	Small extracellular loop
SEM	Standard error of the mean
SG	Stress granule
SP	Signal peptide
SPP	Signal peptide peptidase
SR-B1	Scavenger receptor class B member 1

STAT1	Signal transducer and activator of transcription 1
STAU1	Double-stranded RNA-binding protein Staufen homolog 1
STX	Syntaxin
TBK1	TANK-binding kinase 1
TBS	Tris buffered saline
TEMED	*N,N,N',N'*-Tetramethylethylenediamine
TGN	Trans-Golgi network
TLR	Toll-like receptor
TMD	Transmembrane domain
TNF	Tumor necrosis factor
TNFAIP3	Tumor necrosis factor α-induced protein 3
TRAF	TNF receptor associated factor
TRIF	IR-domain-containing adapter-inducing IFNβ
Tris	Tris(hydroxymethyl)aminomethane
UPR	Untranslated protein response
UTR	Untranslated region
UVRAG	UV radiation resistance-associated gene protein
VLDL	Very low densty lipoprotein
XBP1	X-box binding protein 1
YFP	Yellow fluorescent protein

1 Introduction

Liver related diseases affect approximately 1.5 billion people worldwide and lead to death in around 2 million per year, ranking at 11^{th} (liver cirrhosis) and 16^{th} (liver cancer) in most common causes of death [1–3]. Notably, the causes of liver disease differ widely across different parts of the world. For example, while the main cause of liver disease in western Europe is diet-related, in east Asia it is mainly caused by viral hepatitis [4]. Among viral infections that cause severe liver damage and are potentially fatal, hepatitis B and C viruses are the causative agents in the vast majority of cases [5]. Although mortality rates for hepatitis B and C have decreased since 1990, the total number of deaths has increased [6]. This might be due to overall growth of the world's population from 5.2 billion in 1989 to 7.9 billion in 2021 [7]. While rising vaccine coverage for hepatitis B virus (HBV) in infants is associated with a decrease in cases of hepatocellular carcinoma (HCC), no vaccine is available for hepatitis C virus (HCV) [2, 5, 8, 9]. With a vaccine available against HBV, the prognosis for future development of HBV-caused viral hepatitis is more optimistic than for HCV-caused and non-viral hepatitis [9, 10].

1.1 Viral Hepatitis C

Hepatitis caused by HCV is still a major health concern around the world as it is estimated to have led to 290 000 deaths in 2019 [10]. With over 100 million people affected by HCV related disease and around 1.5 million new infections annually, great effort over decades is required to achieve a substantial reduction in disease burden [3, 5, 10]. Several characteristics of HCV complicate this project. First, most HCV infections stay asymptomatic, resulting in many people that are not aware of their infection. Second, a substantive portion of infections transition to chronicity which is also asymptomatic and over the span of decades can progress to cirrhosis or HCC [11, 12]. In such cases, people are unaware that they were infected and upon symptom onset the liver is already severely damaged.

1.1.1 Transmission and Epidemiology

HCV is mainly transmitted via blood. While insufficiently sterilized surgical instruments and blood transfusions were the major route of transmission in the past, today the major route is injecting drugs, followed by transmission through sexual contact [13]. Nevertheless, there are still areas in the world where contaminated medical instruments and blood transfusions cause infections [14]. The prevalence ranges between 0.5% in the western

Pacific, south-east Asian and American region, and 1.8% in the the eastern Mediterranean region [15]. While prevalence does not differ too much between regions and does not correlate with wealth indicators, access to diagnosis and treatment options does. Only 5% of HCV infected people in the African region were aware of their infection at the end of 2019 and 0.5% had access to treatment. In contrast, 22% of HCV infected people in the Americas knew about their infection and 18% had access to treatment [10]. This discrepancy associates with higher mortality rates in regions with low access rates to diagnosis and treatment [5].

There are six main genotypes of HCV, whose global distributions vary widely. While genotype 1 is dominant in the Americas, Europe, Central- and East-Asia, as well as West Africa, genotype 4 is dominant in Central, East and North Africa, as well as the Middle East, and genotype 3 is dominant in South Asia [16, 17]. All genotypes are spread around the world and even within regions their distribution can vary significantly between nations [18]. It is thought that HCV infects humanity for centuries or longer and that the pandemic spread of genotype 1 is due to the emergence of blood transfusions in the 1940s and intravenous drug abuse in the 1960s and 1970s [19].

1.1.2 Treatment Strategies and Vaccine Development

The first treatment for HCV infection was recombinant IFNα. However, with limited efficacy of less than 40%, many patients had to deal with reoccurring infection after treatment termination [20, 21]. A substantial improvement was achieved by combining IFNα with Ribavirin, a nucleoside analogon, which blocks polymerases of several DNA- and RNA-viruses [20, 21]. However, a high frequency of drug administration was necessary to achieve viral clearance. Following the introduction of PEGylation to stabilize IFNα, allowing for a lower frequency of administration, PEGylated IFNα and Ribavirin became the standard therapy of HCV treatment [20]. It was only when direct-acting antivirals (DAAs) were developed, that IFNα/Ribavirin therapy was replaced. DAAs have the feature that they specifically bind to HCV proteins (mainly protease NS3-4A and polymerase NS5B) making them highly efficient. At present, combination therapy with different DAAs leads to curing rates of over 95% [22]. Two major obstacles remain that need to be addressed in order to come within reach of HCV elimination. First, access to health care that is able to diagnose and provide efficient HCV treatment. Second, a working vaccine that limits the development of cirrhosis and HCC, or decreases the chance of an acute infection progressing to a chronic infection, or, ideally, prevents infection itself [5, 20]. While the first obstacle is addressed by politicians and non-governmental organizations, the second must be solved by the scientific community.

Many strategies of immunization have been tried but none of them resulted in a protective vaccine [23]. It has been shown that clearing a natural infection gives rise to neutralizing antibodies and specific T cells that protect against chronic disease [24]. The problems with regard to the development of a vaccine are that six genotypes exist with various antigens and high tolerance towards variations in the amino acid sequence, rapidly leading to the emergence of immune escaping variants [25, 26]. Together, these characteristics have resulted in many vaccine candidates being unsuccessful. In contrast, antigenic epitopes that are recognized by T cells are generally more conserved among genotypes and over time [23]. However, vaccines focusing on the cellular immune response alone could not show protection in clinical trials [27]. This means that a vaccine is needed that elicits strong neutralizing antibody and T cell responses [23]. In recent years considerable progress has been made in understanding the mechanisms through which HCV evades neutralizing antibodies and evolves resistance [25, 26]. For example, the hyper variable region 1 (HVR1) of the E2 glycoprotein shields the more conserved regions that mediate receptor binding from neutralizing antibodies [28, 29]. On top of this, new structural insights may help with decoding this epitope masking process and lead to the development of new vaccine design approaches [30, 31]. Indeed, studies that vaccinate with E2 structures that lack the HVR1 show promising results, although not yet in humans [32, 33].

1.2 Molecular Biology of Hepatitis C Virus

1.2.1 Structure and Organization

RNA and Genome

The HCV genome is one positively oriented single stranded RNA ((+)-ssRNA) consisting of approximately 9 600 nucleotides [34]. Although it can be directly translated by ribosomes, it differs from cellular mRNA. There is no cap structure at the 5'-end and no poly-A tail at the 3'-end [35, 36]. As such, for translation initiation it is dependent on an internal ribosomal entry site (IRES) starting in the 5'-untranslated region (UTR) and including the first 30 nucleotides of the core coding region [35, 37]. The 5'-UTR is a very important component in the regulation of viral translation and replication [36]. It harbours two binding sites for the liver-specific microRNA-122 (miR-122), which promotes the viral life cycle by stabilizing the viral RNA genome and assisting in the formation of an active IRES [37–39]. The 5'-UTR, structures in the coding region, and the 3'-UTR, as well as the interactions between them, are crucial for viral replication and translation initiation [36, 40–42]. Noteworthy at this point is the *cis*-acting replicating element (CRE), located in the NS5B coding region and interacting with the X-region in the 3'-UTR [36, 43, 44]. This interaction was shown to be very important for replication, and in addition, seems to

regulate whether genomes are replicated or packaged [43–48]. In parallel, the CRE also interacts with the IRES to regulate translation [41, 44]. Hence, it is thought that these interactions play a major role in late stages of the viral life cycle, in switching between replication and packaging of viral RNA [42–44, 47]. The HCV genome is also modified chemically. RNA originating from the NS5B polymerase has a triphosphate group at the 5'-UTR, which is recognized by cellular innate immune receptors as non-self and hence, an antiviral response is mounted [49–52]. Another modification is *N*-6-methylation at adenosine nucleosides (m^6A), which is very common in eucaryotic cells but was shown to also occur at viral RNAs [53, 54]. m^6A was reported to regulate viral translation and genome packaging on the one hand, and preventing the viral genome from being recognized by innate immune receptors on the other [54–57].

Proteins and Protein Complexes

Being a (+)-ssRNA genome, HCV viral RNA gets directly translated to a polyprotein of around 3 000 amino acids [34, 58]. The polyprotein gets post-translationally cleaved by cellular and viral proteases into three structural (core, E1, E2) and seven non structural proteins (p7, NS2, NS3, NS4A, NS4B, NS5A, NS5B) [34, 58].

Core - Capsid Protein

Core is located at the N-terminus of the polyprotein and is cleaved from it by cellular signal peptidases yielding a protein of 191 amino acids (aa). The N-terminal domain (aa 1-117) is highly hydrophilic, with many positively charged aa, and is responsible for binding of viral RNA [59]. It was found that at least parts of this domain are mainly unstructured but nevertheless, it can form nucleocapsid-like particles in the presence of RNA [60, 61]. The C-terminal domain (aa 118-191) consists of two amphiphatic α-helices connected by a lipophilic loop associating core with cellular membranes [59, 60, 62]. After initial cleavage from the polyprotein, another proteolytic step is required [63]. The cutting off of the signal peptide at the C-terminus (aa 178-191) by signal peptide peptidase (SPP) allows core localization to lipid droplets (LDs) [62, 64, 65]. Core localization to LDs is a central step in virion production and interruption leads to severe impairment of the former [63, 64, 66]. Virions are thought to bud at the ER membrane towards the ER lumen, for which the interaction of core with several viral and host proteins was proven indispensable [34, 67, 68]. In addition to its pivotal role in virion assembly, core has been found to be of key importance in counteraction of the cellular immune response [69, 70]. It was shown to inhibit IFNα-induced interferon stimulated gene (ISG) activation via interaction with STAT1 (Signal transducer and activator of transcription 1) [71, 72]. Additionally, it was reported to interfere with Toll-like receptor (TLR) and NFκB (Nuclear

factor kappa-light-chain-enhancer of activated B cells) signaling, as well as with apoptosis induction and inflammation [69, 70, 73–77].

E1 and E2 - Envelope Glycoproteins

E1/E2-heterodimers are incorporated in the envelope of the HCV particle and are thus the only proteins which are exposed to the extracellular space [25, 34]. Both E1 and E2 are type-I transmembrane proteins, whose N-terminal ectodomains face the ER lumen, followed by a short C-terminal transmembrane domain (∼30 aa) [59]. Their cleavage from the polyprotein and each other is carried out by host signal peptidases, resulting in a ∼190 (E1) and a ∼370 (E2) aa protein, respectively [59, 78–80]. The assembly process of HCV virions is not well understood, but nonetheless E1's and E2's importance in this process is undisputed [78, 81]. Their interaction with not only each other but also with other viral and host proteins is essential for viral assembly [78, 82]. Additionally, they are highly modified after translation which was proven to be important for the assembly process [31, 63, 81, 83, 84]. The E1/E2-complex binds cell surface receptors to mediate attachment and entry [85–87]. Several of the aforementioned protein-protein interactions and post-translational modifications play essential roles in the entry process as well (see Attachment and Entry) [30, 84, 88]. The glycosylations in particular have a high impact on antibody evasion and pose a serious problem for vaccine development (see 1.1.2 Treatment Strategies and Vaccine Development) [25, 28, 29].

p7 - Viroporin

The p7 protein is with 63 aa a rather small protein which consists of two membrane spanning α-helices connected by a hydrophilic loop [89–91]. It is mainly localized to the ER membrane, with N- and C-terminus facing the ER lumen and the hydrophilic loop facing the cytosol [90–92]. Many reports show that it oligomerizes to exert an ion-channel function, which is important for the production of infectious viral particles [90, 91, 93–101]. An assumption is, that it alkalizes cellular organelles to prevent pH-dependent conformational changes in newly formed particles [100–104]. p7 is also substantially involved in the formation of new viral particles, where it has proved to be important for capsid assembly and envelopment [82, 89, 100, 104–108]. Additionally, studies suggest that p7 also has immunomodulatory functions, making it a potential drug target [109–111].

NS2 - Protease and Scaffold

Non-structural (NS) protein 2 has around 184 aa. Its N-terminal domain contains three transmembrane helices, which anchor it to the ER membrane [112–114]. The C-terminal domain faces the cyctoplasmic site of the ER membrane and has proteolytic activity

[113–117]. In order to be active, NS2 needs to dimerize and interact with NS3 [116–120]. Presumably, the only cleavage site of the protease is the NS2-NS3 intersection, whose processing is essential for viral replication [112, 120]. Besides the protease activity, NS2 plays an essential role in the viral assembly process. It is seen as a scaffold that brings together viral and host proteins facilitating viral assembly and envelopment [113–115, 121–124]. At the same time, NS2 is also associated with the induction of ER stress and inhibition of cellular antiviral responses [125–128].

NS3-4A - Protease and Helicase

Full-length NS3 has a length of ∼630 aa, consisting of an N-terminal protease domain and a C-terminal helicase domain [129]. NS4A is the smallest protein encoded by HCV with a length of only 54 aa. It serves as cofactor for the NS3 protease activity, which is essential for proper polyprotein processing [112, 130, 131]. Additionally, it anchors the NS3 enzyme to the ER membrane [132]. NS3-4A is a serine protease, having a trypsin-like fold and coordinating a Zn^{2+}-ion which is indispensable for structural stability and also important for NS2 protease activity [117, 129, 133]. Junctions between viral proteins NS3/4A, 4A/4B, 4B/5A, 5A/5B are cleaved by NS3-4A making its function necessary for viral replication and propagation [130, 131, 134, 135]. On top, NS3-4A was shown to also cleave host cell substrates and thereby counteract antiviral responses, leading to higher pathogenicity [136–138]. All this makes the NS3-4A protease activity an important and successful target for therapy (see 1.1.2 Treatment Strategies and Vaccine Development) [20, 22, 129, 139]. NS3 ATP-driven helicase activity is essential for RNA unwinding during viral replication for which it is included in the replication complex [140–144]. In addition to the assistance it provides in replication, NS3 is also involved in morphogenesis of infectious viral particles and their release [145–148]. At the same time, it is a target of the cellular antiviral response and takes part in the counteraction of these mechanisms itself [127, 136, 137, 149–151].

NS4B - Membrane Organizer

The 261 aa of NS4B are nearly entirely membrane associated. NS4B comprises two N-terminal amphiphatic α-helices, followed by four membrane spanning α-helices and again two amphiphatic C-terminal α-helices [152, 153]. Amphiphatic helices have proved to be essential to NS4B oligomerization, which itself is very important for the massive membrane rearrangement that happens in HCV replicating cells [154–157]. The membrane rearrangement is termed membranous web and thought to be the location of viral replication for which NS4B oligomerization is a crucial requisite [154–159]. Having a nucleotide-binding motif, NS4B not only organizes membranes, but also functionally takes part in viral replication by interacting with viral NS5A and host proteins [160–163]. In this context,

NS4B could be involved in assembly and release processes as well [164, 165]. NS4B has been linked to autophagy induction which might cohere with the membrane organization described above [166, 167]. Besides its important role in membrane organization, many reports describe immunomodulatory actions of NS4B. For example, NS4B negatively regulates interferon signaling, but also activates the ER-stress response and NFκB signaling [168–175].

NS5A - Multifunctional Protein

NS5A has around 450 aa, starting with an N-terminal amphiphatic α-helix (aa 1-27) anchoring it in the ER membrane, followed by three cytosolic domains that are clearly separated from each other [112, 176]. Domain 1 (aa 28-213) is the best described so far, and structural data is available showing that it coordinates a Zn^{2+}-ion and comprises a disulfide bond, both of which are essential for structure and function [177, 178]. Domain 2 (aa 250-342) is less well characterized and seems to be mainly unstructured [179, 180]. However, it was also shown that NS5A can adopt α-helical structures which could allow weak SH3-domain binding, additionally to the proline-rich SH3-binding motif located at a loop between domain 2 and 3 [181–183]. For domain 3 (aa 356-450) no structural features have been described, leaving it intrinsically unstructured [184]. Dimerization of NS5A has been proposed involving domain 1, with Zn^{2+} coordination in particular playing a pivotal role [185–187]. NS5A is a part of the replication complex and plays a role (together with NS4B) in reshaping cellular membranes to create vesicular structures that harbor the replication complex, rendering it indispensable for HCV replication [159, 161, 162, 188]. It is highly phosphorylated with up to 15 possible sites described in the literature [177]. There is consensus on the fact that NS5A mainly occurs in a hypo- and hyperphosphorylated form, which happens in a sequential manner and is indicated by two bands in SDS-PAGE analysis [148, 189–191]. However, it is not fully understood which residues and kinases are involved, not to mention conditions and kinetics of these phosphorylation events [63, 112, 177]. Despite this, it has been shown that phosphorylation of NS5A is essential for its function and it is assumed that it has a regulatory effect on replication and translation [187, 190, 192, 193]. Among others, cellular kinases CKII (Casein kinase II) and PI4Kα (phosphatidylinositol 4-kinase α) have been found to phosphorylate NS5A [177, 194, 195]. Reports also suggest that NS5A is involved in the assembly process by interacting with core on LDs and is suspected to bring viral RNA to core oligomerization sites [186, 196–198]. Furthermore, several studies describe the activation of pro-survival signaling cascades by NS5A, as well as immunomodulatory functions [199–204]. Finally, NS5A is associated with the manipulation of the host lipid metabolism and induction of autophagy [205–210].

NS5B - Polymerase

The last protein encoded by the HCV genome is NS5B, the RNA-dependent RNA polymerase (RdRp). This is a 591 aa long protein whose N-terminal region (aa 1-530) forms the enzyme and whose C-terminal region (aa 531-591) anchors it to the cytosolic side of the ER membrane [59, 211]. The RdRp has a right hand polymerase shape and features finger, palm and thumb subdomains similar to other template-dependent polymerases [59, 112, 212–214]. The active site requires a bound Mg^{2+} or Mn^{2+}-ion for stabilization [215]. In contrast to other polymerases, it can adopt a conformation with an enclosed active site, which potentially facilitates *de novo* RNA synthesis without an initiation primer [212–214, 216–218]. For proper HCV genome replication it needs to be anchored to the ER membrane, as well as interact with other viral proteins, most prominently NS3-4A, NS4B and NS5A [161, 162, 219–222]. Other interaction partners, both viral and cellular, have also been found to be recruited and assist in viral replication [223–226]. As NS5B is absolutely critical for viral propagation, it is a target for cellular antiviral approaches, as well as for medical intervention (see 1.1.2 Treatment Strategies and Vaccine Development) [20, 22, 227, 228].

The Viral Particle and its Envelope

In the field of virology the HCV particle is usually termed lipo-viro particle (LVP), as it differs from other viruses by being highly associated with lipids [229, 230]. In contrast to other members of the *flaviviridae* family such as dengue and west-nile virus, which have particle sizes of ∼50 nm, LVPs are very heterogenous, with a particle size range between 40 and 100 nm, with most particles being 60-80 nm in diameter [231–233]. LVPs also have an unusually low density, being similar to very low and low density lipoprotein particles (VLDL and LDL) [232–234]. In addition to viral RNA and proteins (core, E1, E2), apolipoproteins have been detected on viral particles and seem to be vital to infectivity of LVPs [235–238]. In addition, the lipid composition of LVPs resembles that of (V)LDL, while being different to that of other enveloped viral particles [237, 239, 240]. Hence, it has been speculated that HCV hijacks the (V)LDL pathway to release its progeny [241]. Although HCV massively manipulates the host lipid metabolism and LVPs share properties with (V)LDL particles, they are probably secreted in another way (see Assembly and Release) [229, 241–243]. Notably, LVPs coming from cell culture differ considerably from those of patients, regarding density, viral RNA and apolipoprotein composition [229, 230]. There is also evidence that the lipid and lipoprotein composition of LVPs can change after being released from the cell [229, 244].

1.2.2 Viral Life Cycle

Attachment and Entry

The entry process of HCV can be divided in five steps. (1) Attachment to the cell, (2) lateral translocation to tight junctions, (3) internalization via clathrin-mediated endocytosis, (4) fusion to the endosomal membrane and (5) uncoating of the viral genome [245].

Attachment and Lateral Translocation

Several host factors are necessary to allow for the attachment of HCV LVPs to cells. Due to the similarity of LVPs to lipoprotein particles, the association with lipids, and the presence of apolipoproteins, first attachment occurs via LDL-receptor (LDLR), heparan sulfate proteoglycans (HSPGs) and scavenger receptor class B type I (SR-BI) [246]. The most abundant lipoprotein in LVPs, ApoE, was reported to interact with HSPGs, while another lipoprotein, ApoB100, which is a constituent of LDL-particles and presumably of LVPs, binds to the LDLR [237, 247–250]. The E2 glycoprotein, however, was shown to bind to HSPGs and SR-BI in the initial attachment step [86, 245, 251, 252]. After the initial attachment step, E2 binds to CD81, which is essential for lateral translocation, by forming a complex with SR-BI and EGFR (Epidermal growth factor receptor) [85, 87, 253]. EGFR activation induces Rho and Ras GTPase signaling which promotes lateral translocation of CD81 to tight-junctions [254, 255]. There, CD81 associates with the tight-junction protein Claudin-1 (CLDN1) which is a key player in virion internalization [256–258].

Internalization

Reports show that CLDN1 interacts with viral glycoprotein E1 and the E1/E2-dimer, as well as with CD81[258–260]. Additionally, another tight-junction protein, Occludin (OCLN), is recruited to the complex, but in contrast to CD81 and CLDN1 it does not bind HCV glycoproteins [261–263]. All three proteins, CD81, CLDN1 and OCLN are essential for the internalization process, although it has been reported that other Claudin proteins can promote HCV entry as well [246, 264]. It is widely accepted that internalization occurs via clathrin-mediated and dynamin-dependent endocytosis, although the molecular mechanism is not fully understood yet, as several host factors seem to be involved [245, 265–267]. Liu *et al.* reported that the second extracellular loop of OCLN interacts with Dynamin II, an important GTPase for endocytosis [267].

Fusion and Uncoating

Internalized endocytic vesicles are transported towards the perinuclear region on microtubules [268]. In this way they become acidified, which is an important prerequisite for

the fusion of the HCV LVP with the endosomal membrane [245, 246]. The current model suggests a pH-dependent conformational change of the E1/E2 heterodimer, which mediates membrane fusion [260, 269–271]. Membrane fusion of enveloped viruses usually requires a prime and a trigger. For HCV, the binding of the E2 glycoprotein to CD81 represents the prime, and low pH represents the trigger [30, 272, 273]. With several conformational changes occurring in E1, E2 and CD81, all three are crucial for the fusion process and it is unclear whether a membrane fusion motif can be mapped at E1 or E2 [30, 260, 269–273]. A putative fusion peptide in E1 has been proposed, however, the many crucial interactions of E1 and E2 point to a combined action [260, 269–271, 274, 275]. Recent findings regarding the structure of the E1/E2 heterodimer may facilitate a deeper understanding of the fusion process [31]. After fusion occurs and the capsid, together with the viral RNA genome, is released, it is thought that rapid disassembly takes place [34, 35]. Thus, the viral RNA is able to be translated by host ribosomes, giving rise to the polyprotein.

Translation and Replication

The HCV (+)-ssRNA genome can be directly translated into the polyprotein by host ribosomes after release from the capsid [34, 35]. Translation occurs via an IRES at the 5'-end of the genome and is highly regulated by, as well as highly dependent on, cellular host factors (see RNA and Genome) [35, 36, 276]. The polyprotein is translated at the rough ER where it is integrated into the membrane, and is post-translationally cleaved by host signal peptidases (core/E1, E1/E2, E2/p7, p7/NS2) and the viral proteases NS2-3 (NS2/3) and NS3-4A (NS3/4A, 4A/4B, 4B/5A, 5A/5B) [34, 58]. Several viral proteins are post-translationally modified after cleavage from the polyprotein (for details, see Proteins and Protein Complexes) [63].

In order to replicate efficiently, HCV sets up specific membrane structures to shield the replication machinery from the innate immune system and allow higher concentrations of substrates at local sites of replication [159, 219]. This membranous structure is called the membranous web and consists of vesicular structures, namely double- and multi-membrane vesicles (DMVs, MMVs), as well as LD encompassing membranes partly connected to the ER [158, 159, 219]. Buildup of the membranous web is mainly orchestrated by viral proteins NS4B and NS5A, but other viral and cellular proteins are also involved [159, 276]. Oligomerization of NS4B, as well as its interaction with NS5A, is critical for membranous web formation [154–163]. Reiss *et al.* showed that NS5A and NS5B interact with Phosphatidylinositol 4-kinase α (PI4Kα), thereby changing its localization and activity to promote membranous web formation [208]. PI4Kα and its product, phosphatidylinositol-4-phosphate (PI4P), are associated with cholesterol content in membranes, which was illustrated to be important for DMVs and viral replication [277–279]. Additionally, HCV

affects lipid metabolism to its own advantage resulting in, among other things, higher production of cholesterol [243, 280, 281]. Of note, autophagy is also upregulated in HCV infected cells and was revealed to play an important role in both replication and release [282–284]. Viral proteins interfere at several steps with the autophagy pathway. First, autophagy is mediated by HCV either indirectly by induction of ER and oxidative stress, or directly by eliciting the formation of pre-autophagosomal structures (PAS) through NS4B and NS5A activating the vesicle nucleation complex (consisting mainly of Beclin-1, ATG14L, Vps34 and Vps15) [210, 282, 285–288]. Second, autophagosome maturation is differentially regulated by HCV as it appears to form autophagosomes by homotypic fusion of PAS and recruitment of membranes from the Golgi compartment [289, 290]. Interestingly, this process seems to be slower than the usual starvation-induced autophagy, which is probably connected to differential expression of the regulatory proteins Rubicon (Run domain Beclin-1-interacting and cysteine-rich domain-containing protein) and UVRAG (UV radiation resistance-associated gene protein) [167, 279]. And third, fusion of autophagosomes and lysosomes is hindered by repositioning of lysosomes to the cellular periphery through upregulation of Arl8b (ADP-ribosylation factor-like protein 8b) and through downregulation of Syntaxin-17 (STX17), which is responsible for membrane fusion of autophagosomes and lysosomes [291–293]. With all this, autophagy presumably is an important factor in membranous web formation and hence, replication, however, many mechanisms need to be conclusively clarified.

Assembly and Release

The assembly process takes place at the LD/ER interface, in spacial proximity to replication sites [219, 294]. A prerequisite for the process is translocation of the capsid protein core to LDs, where it interacts with NS5A and possibly with viral RNA [62, 64, 196, 197]. Core is then transferred to the ER membrane where it oligomerizes, binds to viral RNA and forms the capsid [78]. The exact mechanism is to be determined, but several viral and host proteins have been identified that play important roles. Viral proteins p7 and NS2 have been reported as regulators of the assembly process through their interaction with core, but also with the E1/E2 dimer located at the ER membrane [82, 100, 105, 107, 108, 113–115, 121, 122]. NS3-4A protease and clathrin adapter AP2-M1 were associated with the translocation of core from the LD back to the ER membrane [105, 146, 147, 295–297]. It is still unclear how viral RNA travels to the assembly site and at what step packaging takes place, as several viral proteins were reported to interact with the RNA during assembly [59, 78]. Another unsolved question is the mechanism of the membrane invagination that eventually leads to budding. Several hints suggest that it is actually the E1/E2 glycoprotein dimer that "pulls" towards the ER lumen, rather than the oligomerizing

capsid that "pushes" [78, 107, 298, 299]. However, E1/E2 pulling seems not to be sufficient and it is speculated that asymmetric lipids in the membrane at the assembly site mediate membrane curvature, as well as other host factors [67, 68, 300]. The host protein ApoE is crucial for the assembly process and is thought to be recruited to assembly sites by NS5A, is integrated in viral particles and interacts with E2 [196, 235–237, 301, 302]. At this point, it is not clear when the association of the nascent viral particle with lipids and lipoproteins occurs. There is evidence that they fuse with luminal LDs directly after the assembly process, but also that the composition of lipids and lipoproteins can change after the particles have been released [205, 229, 242, 244].

The release of the HCV LVP from the site of assembly to the extracellular space is not fully elucidated. There is evidence that LVPs travel via the Golgi compartment to the endosomal compartment from where they are finally released [284]. It has been shown that COPII vesicles originating from the ER contain viral proteins and RNA [303]. These vesicles usually transport cargo from the ER to the Golgi. Additionally, regulatory proteins of COPII-dependent transport have proved to be essential for the release of LVPs [304, 305]. Likewise, other proteins responsible for Golgi transport have been reported to be crucial for particle release [304, 306]. Studies show that clathrin-mediated transport is critical for the release process, as reduction of organizing adapter proteins and clathrin heavy-chain itself diminished the amount of secreted viral RNA [123, 304, 307]. Similarly, several members of the Rab family of proteins, that connect vesicles to the cytoskeleton for transport, have been shown to be involved in HCV egress [304, 308–310]. It is thought that LVPs are transported to multi-vesicular bodies (MVBs), as some members of the ESCRT (endosomal sorting complexes required for transport) machinery have been shown to be involved as well [311–314]. Then, MVBs fuse with the plasma membrane (PM) to release vesicles and possibly LVPs to the extracellular space because Syntaxin-4 (STX4), known as a PM residing adaptor for membrane fusion, is essential for virion release [292, 315]. However, there are many results from different studies that seem to contradict the described model. For example, reports show incomplete or no modification of E1/E2 glycosylation by Golgi-residing enzymes [83, 316]. Additionally, Bayer *et al.* could not detect colocalization of typical Golgi markers with E1 [316]. As described previously (see Translation and Replication), HCV massively up- and dysregulates autophagy and there are a couple of strong indications that it is involved in viral particle egress. First, Wang *et al.* showed that phagophores undergo homotypic fusion to form autophagosomes and that they harbour active replication sites [290]. Second, at the early stage of infection, HCV impairs fusion of autophagosomes with lysosomes by moving lysosomes to the cellular periphery via upregulation of Arl8b and downregulation of STX17, which is responsible for the membrane fusion process [291–293]. However, at later stages of infection, HCV

promotes autophagosome transport towards the PM by disconnecting Rab7-positive vesicles from dynein motor proteins via cleavage of the adaptor RILP (Rab-interacting lysosomal protein) by Caspase-1 [317, 318]. This results in the transport of autophagosomes to the cellular periphery by kinesin motor proteins and increased secretion of virions [318]. Third, as mentioned above, several members of the Rab adaptor protein family are involved in LVP release, of which some are associated with secretory autophagy [308, 310, 319, 320]. Although the two models seem to contradict each other, a combined model is imaginable. For instance, there is considerable cross-talk between the Golgi compartment and autophagy during HCV infection, potentially connecting the two models [289, 321]. Additionally, HCV rearranges membranes and organelles, which renders it possible that canonical organelle functions blur and merge in some cases. Nevertheless, to finally clarify the release pathway of HCV more studies need to be conducted.

1.2.3 Reorganization of Cellular Homeostasis

Cellular Antiviral Reaction and Viral Counteraction

The cellular antiviral response is activated in several ways following a HCV infection. Viral RNA is the most potent trigger, being recognized by a plethora of cellular receptors. In the endosomal compartment, TLR-3 recognizes dsRNA, whereas TLR-7 and -8 recognize ssRNA [322]. Although they signal through different adapter proteins, their cascades induce the production of pro-inflammatory cytokines and the IFN-response [322, 323]. In the case of TLR-3, HCV counteracts the downstream signaling by cleavage of the adaptor protein TRIF (TIR-domain-containing adapter-inducing interferon-β) via the viral protease NS3-4A and, additionally, by the activation of caspase-8 through NS4B [171, 324]. Regarding TLR-7 and -8, the crucial adaptor proteins are MyD88 (Myeloid differentiation primary response 88) and TRAF6 (TNF receptor associated factor 6) [322]. While the former has been shown to be inhibited by NS5A, the latter has been reported to be degraded by HCV-induced autophagy [325, 326]. Besides the endosomal compartment, viral RNA is also recognized by cytoplasmic receptors. Many factors are involved in the cytoplasmic RNA recognition machinery, but the precise roles they play are not always fully understood [327]. The best-known receptors are MDA5 (Melanoma differentiation-associated protein 5) and RIG-I (Retinoic acid-inducible gene I) with MDA5 recognizing long RNAs over 2kb, while RIG-I has been reported to sense shorter and 3'-triphosphorylated RNA [52, 327, 328]. Following RNA recognition, both bind to the mitochondrial membrane-residing adaptor protein MAVS (Mitochondrial antiviral-signaling protein) which, in turn, serves as scaffold for downstream signaling molecules [329, 330]. One of these molecules is the Serine/threonine-protein kinase TBK1 (TANK-binding

kinase 1) which phosphorylates IRF3 (Interferon regulatory factor 3), which in turn serves as a transcription factor and induces IFNβ expression [330]. HCV NS3-4A was shown to cleave MAVS and hence, diminish downstream signaling and IFNβ expression [136, 324, 331]. Additionally, it has been suggested that NS3-4A binds to TBK1, preventing it from IRF3 phosphorylation, and that NS4B interferes with the TBK1 adaptor STING (Stimulator of interferon genes) [168, 169, 332]. The aforementioned proteins, TRAF6 and TBK1, not only lead to IRF3-mediated IFNβ transcription, but also activate the NFκB pathway, resulting in pro-inflammatory gene transcription [330, 333]. To prevent proper NFκB signaling, TRAF6 is degraded by HCV-induced autophagy, while NS3-4A degrades Importin β1 (IMPβ1), impairing the translocation of the NFκB subunit p65 to the nucleus [137, 325]. The sensing of HCV results in the secretion of pro-inflammatory cytokines (TNFα, IL-1β, IL-6), as well as type-I (IFNα, IFNβ) and type-III (IFNλ) interferons which take action in a paracrine and autocrine manner [334]. Interferons induce the Jak-STAT signaling pathway, which finally transcribes interferon-stimulated genes (ISGs) with antiviral functions [329, 333]. HCV core interferes with this pathway by binding to STAT1 impairing its nuclear translocation and transcriptional activity [71, 72]. Among the ISGs induced by this pathway, there are several that play pivotal roles in HCV infection. Protein kinase RNA-activated (PKR) is one of these. Sensing dsRNA by PKR leads to activation and subsequent phosphorylation of the eukaryotic translation initiation factor 2α (eIF2α), shutting down the cellular cap-mediated mRNA translation, which results in the accumulation of untranslated mRNAs in so called stress granules (SGs) [335]. It is still unclear whether this is beneficial or disadvantageous for the virus, as its IRES-mediated translation is independent from eIF2α [336–340]. Recent findings suggest a fine-tuned balancing of assembly and disassembly of SGs in chronic viral infection [341]. Another report showed that PKR can induce MAVS signaling, without its kinase activity, inducing IRF3-mediated gene expression [342]. In addition, it could activate NFκB signaling by interacting with the IKK complex [343, 344]. Viral proteins E2 and NS5A were reported to suppress PKR's kinase activity and impede eIF2α phosphorylation [345, 346]. Besides this and the prevention of ISG activation, HCV induces another RNA-binding protein, STAU1 (Double-stranded RNA-binding protein Staufen homolog 1), that competes with PKR for binding of viral RNA, thus reducing PKR activation [347, 348]. Other ISGs that impair the HCV life cycle are Interferon-induced transmembrane proteins 1 and 3 (IFITM1/3). IFITM1 binds to CD81 and OCLN at the PM and thereby prevents their proper interaction and hence, cell entry [349]. IFITM3 was reported to restrict the IRES-mediated translation of the HCV polyprotein [350].

Integrated Stress Response

The integrated stress response (ISR) is the reaction of a cell to stress factors that threaten its homeostasis, which can be ER stress, oxidative stress or infection. The central step of the ISR is the global shutdown of mRNA translation and expression of a set of genes that try to resolve the stressor or go into apoptosis if non-resolvable [351]. With the massive production of viral proteins at the ER membrane, ER stress induction is inevitable in HCV infection. However, HCV proteins core, E1, E2 and NS4B seem to be more potent ER stress inducers than the other viral proteins, making it tempting to speculate that they could specifically induce ER stress [352, 353]. A key factor in the induction is the ER-resident chaperone BiP (Immunoglobulin heavy-chain binding protein), which is recruited to misfolded proteins. It negatively regulates ER stress, which is activated when BiP binds to misfolded proteins [354, 355]. Thereby, misfolded proteins activate the three arms of the ER stress response, namely ATF6 (Activating transcription factor 6), PERK (PKR-like ER kinase) and IRE1α (Inositol-requiring enzyme 1 α) [351]. ATF6 is an ER resident protein which translocates to the Golgi upon accumulation of un- and misfolded proteins [355, 356]. There it is cleaved by Golgi resident proteases liberating the ATF6 transcription factor portion, which then transcribes genes from the unfolded protein response (UPR), like chaperones, and genes involved in the ER-associated degradation (ERAD) process [351, 357]. PERK is activated by dimerization and autophosphorylation, functioning as kinase of eIF2α resulting in shutdown of mRNA translation and eventually stress granule (SG) formation [351, 358]. A second effect is the upregulation of the transcription factor ATF4 which, among others, transcribes the pro-apoptotic transcription factor CHOP (C/EBP homologous protein) and GADD34 (Growth arrest and DNA damage-inducible protein) [352, 359]. ATF4 has also been linked to the expression of cell death or autophagy-inducing genes [353, 360, 361]. GADD34 is a regulatory subunit of protein phosphatase 1, which dephosphorylates eIF2α, providing negative feedback to eIF2α phosphorylation [362, 363]. Accumulation of misfolded proteins leads to activation of IRE1α via oligomerization and autophosphorylation [364, 365]. IRE1α has an endonuclease function that splices the mRNA of XBP1 (X-box binding protein 1) to enable translation of the XBP1 transcription factor, that itself expresses genes involved in UPR and ERAD [351]. There are also reports that IRE1α specifically degrades mRNAs of certain proteins (regulated IRE1α-dependent decay; RIDD), as well as ribosomal RNA to impair translation [366–368]. Additionally, IRE1α harbors a kinase domain which has been shown to activate pro-survival genes via TRAF2, JNK and NFκB [369]. Tardif *et al.* showed that HCV downregulates the IRE1α-XBP1 pathway to allow more misfolded proteins, which is likely favorable for HCV polyprotein translation [370].

In addition to ER stress, HCV also induces oxidative stress. Viral proteins core, E1, E2, NS3, NS4B and NS5A have been shown to prompt oxidative stress via several direct and indirect mechanisms, with core being the most potent inducer [172, 371–374]. It is probable that the two main mechanisms leading to production of reactive oxygen species (ROS) during HCV infection and hence, oxidative stress, are mitochondrial dysfunction and expression of NADPH oxidases (NOX) [375, 376]. Interestingly, both can be triggered by increased Ca^{2+}-levels in the cytoplasm, which is a result of HCV infection [376]. ROS usually leads to the activation of the Nrf2/ARE (Nuclear factor erythroid 2-related factor 2 / Antioxidant response element) pathway, which increases the expression of proteins that synthesize antioxidants, like glutathione [373]. If and how HCV interferes with this pathway is still under debate [372, 373, 377]. It is speculated that oxidative stress facilitates a reduced innate immune response and is therefore beneficial for HCV replication [373]. For example, increased ROS abundance can induce ER stress itself leading to PERK activation and translational shutdown of capped mRNA [378, 379]. Furthermore, Di Bona *et al.* illustrated that oxidative stress can reduce IFNα-induced antiviral gene expression [380].

As mentioned previously in Cellular Antiviral Reaction and Viral Counteraction, PKR detects dsRNA, resulting in its activation, phosphorylation of eIF2α, and shutdown of cap-dependent translation. As most cellular genes display the cap structure on their mRNA, they are highly affected by eIF2α phosphorylation, in contrast to IRES-mediated translation like the one of HCV [335, 336]. The shutdown results in the accumulation of mRNAs that are accumulating in an ordered process in stress granules (SGs). Besides mRNA, SGs consist of many proteins with RNA-binding and regulatory functions (e.g. G3BP1; Ras GTPase-activating protein-binding protein 1) [335, 381]. If the stress is not resolved and SGs disassembled, cells will activate cell death mechanisms. Although shutdown of cap-dependent translation might be beneficial for HCV as it suppresses expression of ISGs, stress cannot be permanent otherwise the host cell would die [382]. It has been shown that SGs assemble and disassemble in an oscillating manner and that this process seems to be regulated in chronic HCV [341, 383]. Therefore, HCV cannot prevent the ISR, but somehow manages to control it and may even benefit from it by shutting down ISG expression or through induction of autophagy.

Progression to cirrhosis and cancer

After decades of research it is clear that chronic HCV infection can lead to liver cirrhosis and HCC. However, the underlying cellular mechanisms have not been definitively identified. In many studies, chronic stress and inflammation of the liver was associated with liver disease and HCC [384–387]. As outlined above (Integrated Stress Response), HCV causes cellular stress in various ways, which is considered a possible link to liver damage when

HCV is chronic over years or decades [384–387]. Indeed, higher level of stress- and inflammation-associated transcripts were detected in liver samples from HCV patients, although not all studies pointed in this direction [388–391]. More recently, HCV has been shown to negatively regulate DNA damage response, leading to genomic instability, which is one hallmark of cancer development [387, 392–395]. Interestingly, HCV was reported to upregulate a number of long non-coding RNAs (lncRNAs), several of which are linked to cancer [396]. It is tempting to speculate that increased pro-survival signaling and reduced cell death mechanisms mediated in chronic HCV may contribute to cancer development.

1.2.4 Entanglement of Tetraspanins with HCV

Tetraspanins are small, membrane spanning proteins of ∼260 aa, consisting of four α-helical transmembrane domains (TMD 1-4) and a small and large extracellular loop (SEL/LEL). The N- and C-terminal tails are short peptides pointing to the cyctoplasm, and for some tetraspanins the C-terminus is palmitoylated. In humans, the tetraspanin family has 33 members [397, 398]. Available structures from CD81 and CD9 show that the transmembrane domains adopt two coiled-coil structures with TMD 1 and 2 forming one structure and TMD 3 and 4 the other [399, 400]. It has been determined that a binding site for a lipophilic ligand is located in between these structures, which probably influences and/or is influenced by the conformation of the LEL if bound or unbound [30, 399–402]. For CD81 the ligand was identified to be cholesterol, whose binding favors the "closed" conformation, while unbound cholesterol favors the "open" [399]. It is speculated that interactions with other proteins are regulated by this process. Indeed, when binding to CD19, a co-receptor in B cell activation, CD81 has been reported to adopt the open conformation and exclude cholesterol [403]. In general, tetraspanins are seen as important regulators of membrane organization and especially of cell surface receptors. They cluster in so called tetraspanin-enriched microdomains (TEMs) where they build homo- and heterodimers and higher oligomeric structures. Various interactions of cellular receptors and tetraspanins are reported and it is thought that they organize receptors and co-receptors to facilitate downstream signaling upon ligand binding [397, 398, 404]. For several viruses, tetraspanins have been shown to be essential for the entry process, for example, CD151 for human papillomavirus (HPV), CD63 for Lujo virus (LUJV) and HPV, and CD81 for influenza A virus (IAV), human coronaviruses (CoV) and HCV (see Attachment and Entry) [85, 87, 255, 404–407]. Besides the entry process, tetraspanins have also been reported to take part in later steps of viral life cycles, such as CD9, CD63, CD81 and CD82 in budding of human immunodeficiency virus (HIV), marburg virus (MARV), hepatitis B virus (HBV) and IAV [404, 405, 408, 409]. The precise mechanisms of tetraspanin involvement have not been revealed in all cases, but it is generally thought that their role in organization of

receptors and their signaling cascade is critical for entry. Furthermore, their asymmetric structure and association with membrane curvature may render them important host factors for budding processes or formation of viral compartments that require membrane bending [403–405, 410, 411].

In the case of HCV, CD81 is clearly the most important tetraspanin, given its central role in Attachment and Entry. In addition, some studies have described a role for CD81 in later steps of the HCV life cycle. Zhang *et al.* describe a role for CD81 in replication, as cells expressing low levels of CD81 were only marginally affected in entry but strongly impaired in replication [412]. Others delineate the necessity of CD81 for E1/E2 dimer maturation and secretion in exosomes, however, this was shown without other viral proteins present [413]. Nevertheless, cells releasing exosomes which contain viral proteins and RNA is plausible and it has been shown that they can play a role in transmission to other cells [414, 415]. The surface expression level of CD81 has been shown to be decreased in actively replicating cells and an accumulation within the cells was observed [416]. Zheng *et al.* monitored a downregulation of CD81 mRNA by microarray in cells stably expressing NS4B but did not further follow up on it [417]. Similarly, Tscherne *et al.* found decreased CD81 levels in replicating cells, but in contrast to the other studies they could not find any active downregulation of CD81 and hence, concluded that HCV selects for cells with lower CD81 levels [418]. Therefore, there are indications that CD81 has a role in the HCV life cycle besides the one in entry, but more studies are needed to make any conclusions. Interestingly, CD63 has also been described to have a role in HCV entry, more specifically, in the fusion process with the endosomal membrane. It was shown to interact with E2 and an antibody against CD63 was able to reduce infection [419]. CD63 has been known for a long time as component of MVBs and exosomes and is therefore used as marker for these structures, plus it has been shown to be incorporated in HCV particles [398, 420]. Recently, CD63 was directly linked to HCV release and was upregulated during infection. Its silencing decreased and overexpression increased viral particle release, indicating an important function which needs to be further deciphered [421].

2 Materials and Methods

2.1 Materials

2.1.1 Chemicals, Enzymes and Kits

Table 1: Overview of Chemicals.

Chemical	Manufacturer
2-Mercaptoethanol	Sigma-Aldrich
2-Propanol	Applichem
3 M sodium acetate pH 5.2	Promega
Acetic acid	Applichem
Acrylamide (30%)	Applichem
Agar	ThermoFisher
Agarose	Lonza
Ammonium persulfate	Sigma-Aldrich
Ampicillin	Applichem
Bafilomycin A1	AdipoGen
Brefeldin A	Biolegend
Bromphenol blue	Applichem
BSA	MP Biomedicals
Chloroform:isoamylalcohol (24:1)	Sigma-Aldrich
Coelenterazine	PJK Biotech
DAPI	Sigma-Aldrich
DEPC	Roth
di-Potassium hydrogen phosphate	Roth
di-Sodium hydrogen phosphate	Merck
Dithiothreitol	Applichem
D-Luciferin	PJK Biotech
DMEM	ThermoFisher
DMSO	Applichem
EDTA	Sigma-Aldrich
EGTA	Roth
Ethidium bromide	VWR
FCS	ThermoScientific

Geneticin (G418)	ThermoFisher
Glycerol	Applichem
Glycine	Applichem
Glycylglycine	Roth
Hoechst 33342	ThermoFisher
IFNα	R&D Systems
Ionomycin	Life Technologies
Kanamycin	Life Technologies
Lipopolysaccharide	InvivoGen
Magnesium sulfate	Roth
Methanol	Applichem
MG132	AdipoGen Life Sciences
Non-essential amino acids	Life Technologies
Non-fat dried milk powder	Applichem
OptiMEM™	Life Technologies
Paraformaldehyde (PFA)	Roth
PBS	Sigma-Aldrich
PEI	Polysciences
Penicillin/streptomycin	Life Technologies
Peptone	ThermoFisher
Phenol:chloroform:isoamylalcohol (25:24:1)	ThermoFisher
PMA	Sigma-Aldrich
PolyI:C	Sigma-Aldrich
Potassium chloride	Sigma-Aldrich
Potassium di-hydrogen phosphate	Roth
Puromycin	ThermoFisher
Sigma FAST protease inhibitor	Sigma-Aldrich
SiR-DNA	Tebu-Bio
Sodium chloride	Applichem
Sodium di-hydrogen phosphate	Applichem
Sodium dodecylsulfate	Sigma-Aldrich
Sodium hydroxide	Applichem
Sodium Pyruvate	Life Technologies
TEMED	Serva
Thapsigargin	Santa Cruz Biotechnilogy
TNFα	ImmunoTools
Top-Fluor cholesterol	Merck

Tris Base	Sigma-Aldrich
Tris-HCl	Sigma-Aldrich
Triton X-100	Sigma-Aldrich
Tunicamycin	Sigma-Aldrich
Tween 20	Applichem
VectaShield	Biozol
Yeast extract	Sigma-Aldrich

Table 2: Overview of Enzymes and Bacteria.

Enzyme / Bacterium	**Manufacturer**
BcuI	ThermoFisher
BglII	ThermoFisher
DpnI	New England Biolabs
EcoRI	ThermoFisher
Esp3I	ThermoFisher
HindIII	ThermoFisher
MluI	ThermoFisher
Pfl23II	ThermoFisher
MssI (PmeI)	ThermoFisher
SdaI	ThermoFisher
XbaI	ThermoFisher
XhoI	ThermoFisher
Fast Alkaline Phosphatase	ThermoFisher
Q5®High-fidelity DNA Polymerase	New England Biolabs
T4 Ligase	ThermoFisher
T4 Polynucleotide Kinase	ThermoFisher
NEB Stable3	New England Biolabs
NEB10β	New England Biolabs

Table 3: Overview of Kits.

Kit	**Manufacturer**
NucleoSpin Gel and PCR cleanup Kit	Macherey-Nagel
Wizard DNA Clean-Up	Promega
Neon Transfection System 10µl	Invitrogen
Neon Transfection System 100µl	Invitrogen
PureYield Plasmid Midiprep System	Promega

GeneJET Plasmid Miniprep System	ThermoFisher
T7 RiboMAX Express Large Scale RNA Production System	Promega
jetPRIME DNA & siRNA transfection reagent	Polyplus
Nano-Glo Luciferase Assay System	Promega
Rneasy Mini Kit	Qiagen
QuantiTect Reverse Transcription Kit	Qiagen
Luna® Universal qPCR Master Mix	New England Biolabs
10× Green reaction buffer	ThermoFisher
Page ruler protein ladder	ThermoFisher
GeneRuler 1 kb plus DNA ladder	ThermoFisher
2× RNA loading dye	LifeTechnologies
RNA marker 0.5 - 9 kb	Lonza
6× TriTrack DNA loading dye	ThermoFisher

2.1.2 Buffers and Antibodies

Table 4: Buffer Compositions.

Buffer	**Composition**
10× SDS-PAGE running buffer (1 l)	30 g Tris Base (250 mM)
	144 g glycine (1.92 M)
	10 g SDS (1%)
	adjust pH to 8.3 before adding SDS
	fill up to 1 l with dH_2O
1× SDS-PAGE running buffer (1 l)	100 ml 10x running buffer
	fill up to 1 l with dH_2O
50× TAE buffer (1 l)	241 g Tris Base (2 M)
	57.1 ml acetic acid
	100 ml 0.5 M EDTA (0.05 M)
	fill up to 1 l with dH_2O
1× TAE buffer (1 l)	20 ml 50× TAE buffer
	fill up to 1 l with dH_2O
0.5 M EDTA (1 l)	146.13 g EDTA
	adjust pH to 8 using NaOH
	fill up to 1 l with dH_2O
10× TBS (1 l)	78.8 g Tris-HCl (0.5 M)
	87.66 g NaCl (1.5 M)
	adjust pH to 7.5 using NaOH

	fill up to 1 l with dH_2O
1× TBS-T (1 l)	100 ml 10× TBS
	1 ml Tween 20
	fill up to 1 l with dH_2O
10× PBS (1 l)	14.7 mM NaH_2PO_4
	81mM Na_2HPO_4
	26.8 mM KCl
	1.37 M NaCl
	adjust to pH 7.4, fill up to 1 l with H_2O
1× PBS-T (1 l)	100 ml 10× PBS
	1 ml Tween 20
	fill up to 1 l with dH_2O
10× Blotting buffer (1 l)	30 g Tris Base (250 mM)
	144 g glycine (1.92 M)
	fill up to 1 l with dH_2O
1× Blotting buffer (1 l)	100 ml 10× blotting buffer
	200 ml methanol
	fill up to 1 l with dH_2O
	pH 8.1 - 8.5
6× SDS loading dye (50 ml)	0.1 g bromphenol blue (2%; w/v)
	15 ml glycerol (30%; v/v)
	5 g SDS (10%; w/v)
	35 ml 0.5 M Tris, pH 6.8
	4.65 g DTT (0.6 M)
Separating gel buffer (1 l)	181.72 g Tris Base (1.5 M)
	adjust pH to 8.8
	fill up to 1 l with dH_2O
Stacking gel buffer (1 l)	78.82 g Tris-HCl (0.5 M)
	adjust pH to 6.8
	fill up to 1 l with dH_2O
LB (1 l)	5 g NaCl
	5 g yeast extract
	10 g peptone
	fill up to 1 l with dH_2O
	autoclave
LB agar (1 l)	5 g NaCl
	5 g yeast extract

	10 g peptone
	20 g agar
	fill up to 1 l with dH_2O
	autoclave
Lysis buffer	150 mM NaCl
	50 mM Tris
	1 mM EDTA
	adjust pH to 7.4
	1× protease inhibitor
	1% (v/v) Triton X-100 added freshly
FACS buffer	1× PBS
	1% (v/v) FCS
FACS Permeabilization buffer	0.2% (v/v) saponine
	10% (v/v) normal goat serum
	in PBS
Blocking buffer	10% (v/v) normal goat serum
	in PBS
GLuc/RLuc lysis buffer	25 mM glycylglycine (pH 7.8)
	15 mM $MgSO_4$
	4 mM EGTA
	10% (v/v) glycerol
	1% (v/v) Triton X-100
	1 mM DTT before use
GLuc/RLuc assay buffer	25 mM glycylglycine (pH 7.8)
	15 mM $MgSO_4$
	4 mM EGTA
	15 mM KH_2PO_4/K_2HPO_4 (pH 7.8)
GLuc/RLuc substrate buffer	Rluc assay buffer
	7.14 µM coelenterazine
RIPA lysis buffer	10 mM Tris-HCl (pH 7.4)
	1 mM EDTA
	0.5 mM EGTA
	140 mM NaCl
	0.1% (v/v) Na-deoxychalate
	0.1% (v/v) SDS
	1% (v/v) Triton X-100
	1× protease inhibitor

	1× phosphatase inhibitor
BioID lysis buffer	10 mM Tris-HCl (pH 7.4)
	0.55% (v/v) NP-40
	1× protease inhibitor
	1× phosphatase inhibitor
FLuc lysis buffer	0.1 M KH_2PO_4 / K_2HPO_4 pH 7.8
	1% (v/v) Triton X-100
	1 mM DTT before use
FLuc assay buffer	0.1 M KH_2PO_4 / K_2HPO_4 pH 7.8
	15 mM $MgSO_4$
	5 mM ATP
FLuc substrate buffer	Fluc assay buffer
	1:50 D-Luciferin
IF permeabilization buffer	0.5% (v/v) Triton X-100
	in PBS
DEPC water	0.1% DEPC
	in dH_2O over night
4% PFA	4% (w/v) PFA
	in PBS
10% APS	10% (w/v) APS
	in dH_2O

Table 5: Western Blot Antibodies.

Target	**Clone**	**Species**	**Dilution**	**Conjugate**	**Manufacturer**
core	C7-50	Mouse MC	1:1000		Novus Biologicals
E2	AP-33	Mouse MC	1:1000		Genentech Inc.
NS5A	2F6/G11	Mouse MC	1:1000		IBT Systems
p65	D14E12	Rabbit MC	1:1000		Cell Signaling
p-p65	93H1	Rabbit MC	1:1000		Cell Signaling
eIF2a		Goat PC	1:1000		R&D Systems
p-eIF2a	849159	Rat MC	1:500		R&D Systems
GAPDH	W17079A	Rat MC	1:2000		Biolegend
Tubulin		Rabbit PC	1:2000		ThermoFisher
Mouse		Goat PC	1:15000	IRDye 680CW	LiCor Biosciences
Rabbit		Goat PC	1:15000	IRDye 800RD	LiCor Biosciences
Rat		Goat PC	1:10000	IRDye 800RD	LiCor Biosciences

Goat	Donkey PC	1:10000	IRDye 800RD	LiCor Biosciences

Table 6: Flow Cytometry and Immunofluorescence Antibodies.

Target	Clone	Species	Dilution	Conjugate	Manufacturer
CD9	HI9a	Mouse MC	1:250	PE	Biolegend
CD63	H5C6	Mouse MC	1:250	PE	Biolegend
CD81	5A6	Mouse MC	1:250	PE	Biolegend
CD81	5A6	Mouse MC	1:250		Biolegend
CD317	RS38E	Mouse MC	1:250	PE	Biolegend
CD317	E-4	Mouse MC	1:250	AF488	SantaCruz Biotechn.
core	C7-50	Mouse MC	1:250		Novus Biologicals
p65	D14E12	Rabbit MC	1:250		Cell Signaling
Mouse		Goat PC	1:250	AF594	ThermoFisher
Rabbit		Donkey PC	1:250	AF488	ThermoFisher
Mouse		Goat PC	1:250	AF488	ThermoFisher

2.1.3 Plasmids and Primers

Table 7: Constructs for FACS-based FRET Experiments.

Construct name	Protein	Tag	Source
pECFP-C1	eCFP		[422]
pECFP-C1 HCV Core	Core	eCFP	[422]
pECFP-N1 HCV E1	E1	eCFP	[422]
pECFP-C1 HCV E2	E2	eCFP	[422]
pECFP-C1 HCV p7	p7	eCFP	[422]
pECFP-C1 HCV NS2/3	NS2-3	eCFP	[422]
pECFP-N1 HCV NS3	NS3	eCFP	[422]
pECFP-C1 HCV NS4A	NS4A	eCFP	[422]
pECFP-C1 HCV NS4B	NS4B	eCFP	[422]
pECFP-N1 HCV NS5A	NS5A	eCFP	[422]
pECFP-C1 HCV NS5B	NS5B	eCFP	[422]
pECFP-N1 Staufen1	STAU1	eCFP	Schindler Lab, Tübingen
pECFP-C1 G3BP1	G3BP1	eCFP	Schindler Lab, Tübingen
pEYFP-N1	eYFP		[422]
pEYFP-N1-ECFP	eYFP-eCFP		[422]

pEYFP-C1 HCV Core	Core	eYFP	[422]
pEYFP-N1 HCV E1	E1	eYFP	[422]
pEYFP-C1 HCV E2	E2	eYFP	[422]
pEYFP-C1 HCV p7	p7	eYFP	[422]
pEYFP-C1 HCV NS2-3	NS2-3	eYFP	[422]
pEYFP-C1 HCV NS3	NS3	eYFP	[422]
pEYFP-C1 HCV NS4A	NS4A	eYFP	[422]
pEYFP-C1 HCV NS4B	NS4B	eYFP	[422]
pEYFP-C1 HCV NS5A	NS5A	eYFP	[422]
pEYFP-C1 HCV NS5B	NS5B	eYFP	[422]
pEYFP-C1 CD9	CD9	eYFP	Schindler Lab, Tübingen
pEYFP-C1 CD53	CD53	eYFP	Schindler Lab, Tübingen
pEYFP-C1 CD63	CD63	eYFP	Schindler Lab, Tübingen
pEYFP-C1 CD81	CD81	eYFP	Schindler Lab, Tübingen
pEYFP-C1 CD81 E219Q	CD81	eYFP	Schindler Lab, Tübingen
pEYFP-C1 CD82	CD82	eYFP	Schindler Lab, Tübingen
pEYFP-N1 Staufen1	STAU1	eYFP	Schindler Lab, Tübingen
pEYFP-N1 G3BP1	G3BP1	eYFP	Schindler Lab, Tübingen

Table 8: Overview of other DNA Constructs.

Construct name	**Protein**	**Tag**	**Source**
mEmerald-ER-3	ER-SP	mEmerald	Addgene #54082
mEmerald-TGNP-N-10	GalT	mEmerald	Addgene #54279
pEGFP-C1-ATG5	ATG5	eGFP	Marina Jendrach, Berlin
pEGFP-C1-ATG12	ATG12	eGFP	Marina Jendrach, Berlin
pEGFP-C1-LC3B	LC3B	eGFP	Marina Jendrach, Berlin
pWPI_BLR			[423]
pWPI-hCD81-HAHA-BLR	CD81	HA-HA	[423]
pNFkB(3x)-FLuc	FLuc		Daniel Sauter, Tübingen
pCMV-Gluc	GLuc		Daniel Sauter, Tübingen
pcDNA3.1			Schindler Lab, Tübingen
p_human IKKβ, const. act.	IKKβ		Daniel Sauter, Tübingen
p(N)FLAG-CMV2 MAVS	MAVS	Flag	Daniel Sauter, Tübingen
pEF-Bos-RIG-I 1-211-flag	RIG-I	Flag	Daniel Sauter, Tübingen

Table 9: Overview of Viral Constructs.

Construct name	Restr. sites	Source
pFK_Jc1_E1(A4)		[316]
pFK_Jc1_XbaI		[100]
pFK_Jc1_E1(A4)_XbaI		pFK_Jc1_E1(A4)
pFK_Jc1(A4)_mScarlet-E2	SdaI, Pfl23II	pFK_Jc1_E1(A4), idea [294]
pFK_Jc1(A4)_BioID2-E2	EcoRI, BglII	pFK_Jc1(A4)_mScarlet-E2
pFK_Jc1_p7-half		[100]
pFK_Jc1_R2A_p7-half	SdaI, Pfl23II	pFK_Jc1_p7-half
pFK_Jc1_R2A		[208]
pFK_Jc1_R2A_short	BcuI, XbaI	pFK_Jc1_R2A_p7-half
pFK_Jc1_mScarlet-2A_short	RF cloning	pFK_Jc1_R2A_short
pFK_Jc1_mScarlet-2A	SdaI, Pfl23II	pFK_Jc1_R2A
pFK_Jc1_NanoLuc-2A	EcoRI, BglII	pFK_Jc1_mScarlet-2A
pFK_Jc1_NS5A-GFP		[424]
pFK_Jc1_NS5A-BioID2	PmeI, XbaI	pFK_Jc1_NS5A-GFP
pFK_Jc1_NS5A-mScarlet	PmeI, XbaI	pFK_Jc1_NS5A-GFP

Table 10: Constructs for Lentiviral Production of CRISPR/Cas9 Knock-out Cells. Target Sequences are Displayed without NGG Motif.

Construct name	Target sequence (5' → 3')	Comments
psPAX2		packaging plasmid
pMD2G		envelope plasmid
LentiCRISPRv2_empty		integration plasmid
LentiCRISPRv2_CD9_1	GCCCTCACCATGCCGGTCAA	integration plasmid
LentiCRISPRv2_CD63_3	GAGGTGGCCGCAGCCATTGC	integration plasmid
LentiCRISPRv2_CD81	CATCGGCATTGCTGCCATCG	integration plasmid

Table 11: Primers used for Cloning. Bold Represents Complementary Part to the Template. Lowercase Letters Mark Restriction Sites.

Primer name	Sequence (5' → 3')	Restr. site	Insert
EcoRI-BioID2_fw	AGTgaattcC-**TTCAAGAACCTGATCTGGCT**	EcoRI	BioID2

BglII-BioID2_rev	ATCagatctGA-**TCTTCTCAGGCTGAACTCG**	BglII	BioID2
EcoRI-Nluc_fw	AGTgaattcC-**GTCTTCACACTCGAAGATTTC**	EcoRI	NanoLuc
BglII-Nluc_rev	ATCagatct-**GCCAGAATGCGTTCGCAC**	BglII	NanoLuc
XbaI-BioID2_fw	GTtctagaCCTCGAGCT-**TTCAAGAACCTGATCTGG**	XbaI	BioID2
PmeI-BioID2_rev	CACgtttaaacCC-**GCTTCTTCTCAGGCTGAACTC**	PmeI	BioID2
XbaI-mScarlet_fw	GTtctagaCCTCGAGCT-**ATGGTGAGCAAGGGCGA**	XbaI	mScarlet
PmeI-mScarlet_rev	CACgtttaaacCC-**CTTGTACAGCTCGTCCATGC**	PmeI	mScarlet
2A-reporter-mSc-RF_fw	CCAAAAGAAACACCAACCGGCG-**gaattcCGTGAGCAAGGGC**	EcoRI	mScarlet
2A-reporter-mSc-RF_rev	GAAGACTTCCCCTGCCCTCGGC-**CagatctTTGTACAGCTCGTC**	BglII	mScarlet

Table 12: Primers used for qRT-PCR. * Primer Sequence Adapted from Reference.

Primer name	**Sequence (5' → 3')**	**Target gene**	**Ref.**
qPCR_5'UTR_fw	CCTGTGAGGAACTACTGTCT	HCV-5'UTR	[425]
qPCR_5'UTR_rev	CTATCAGGCAGTACCACAAG	HCV-5'UTR	[425]
qPCR_CD81_fw	AGGGCTGCACCAAGTGC	CD81	[426]
qPCR_CD81_rev	TGTCTCCCAGCTCCAGATA	CD81	[426]
qPCR_TNFa_fw	CTGCACTTTGGAGTGATCG	TNFa	[427]
qPCR_TNFa_rev	CAACATGGGCTACAGGCTT	TNFa	[428]*
qPCR_IL-6v1_fw	CTGCTGCCTTCCCTGCC	IL-6v1	[428]*
qPCR_IL-6v1_rev	TCAGGGCTGAGATGCCGT	IL-6v1	[428]*
qPCR_GAPDH_fw	TGCACCACCAACTGCTTAGC	GAPDH	[429]
qPCR_GAPDH_rev	GGCATGGACTGTGGTCATGAG	GAPDH	[429]
qPCR_sXBP1_fw	GCTGAGTCCGCAGCAGGT	sXBP1	[430]
qPCR_uXBP1_fw	CAGACTACGTGCACCTCTGC	uXBP1	[430]

qPCR_u-sXBP1_rev	CTGGGTCCAAGTTGTCCAGAAT	s/uXBP1	[430]
qPCR_tXBP1_fw	TGAAAAACAGAGTAGCAGCTCAGA	tXBP1	[430]
qPCR_tXBP1_rev	CCCAAGCGCTGTCTTAACTC	tXBP1	[430]
XBP1_fw	CTGAAGAGGAGGCGGAAGC	XBP1	[431]
XBP1_rev	AATACCGCCAGAATCCATGG	XBP1	[431]

Table 13: Primers used for Sequencing.

Primer name	**Sequence (5' → 3')**	**Target gene**
BioID2-FP_seq_fw	TCACCGGCAAGCTGGTGG	BioID2
BioID2-FP_seq_rev	GCCTCTGCCCTTGGTCTG	BioID2
Seq_mScarlet_fw	CGTGGTGGAACAGTACG	mScarlet
Seq_mScarlet_rev	GTGCACCTTGAACCGCATG	mScarlet
HCV_seq_5'UTR_fw	CGCAAGACTGCTAGCCGAG	HCV 5'UTR
HCV_seq_NS5A-FP_fw	TATCAGAAGCCCTCCAGC	HCV NS5A
HCV_seq_E2_fw	CACCAGCTTATTTGACAT	HCV E2
HCV_seq_E2-FP_rev	CGAGCTGGATTTTCTGCC	HCV E2

2.2 Methods

2.2.1 Molecular Biology

PCR Amplification

To amplify DNA fragments, 100 ng of template DNA was use to set up a reaction with Q5® High-Fidelity DNA Polymerase (NEB) according to manufacturers instructions. Used primers are listed in Table 11.

Restriction Digestion

2-5 µg of backbone vector and insert vector were digested using respective restriction enzymes (Table 2). A sample size of 20 µl was used with 10× Green Reaction Buffer (ThermoFisher). Digestion was performed for 15min at 37°C. Samples were purified by agarose gel electrophoresis as indicated below.

Ligation

For ligation, 150 ng of purified, linearized and dephosphorylated backbone was combined with purified and linearized insert in a molar ratio of 1:7 (backbone : insert; see Equation 1). This was then mixed with 2 µl of 10× ligation buffer and 1 µl of T4 ligase. Samples were filled up to a total volume of 20 µl with purified water and incubated at RT for 1h.

$$ng\,of\,insert = \frac{ng\,of\,vector \times size\,of\,insert\,(in\,kb)}{size\,of\,vector\,(in\,kb)} \times 7 \tag{1}$$

Transformation

NEB10β or NEB Stable3 *E.coli* bacteria were thawed in ice for 5min. Then, 10 µl of ligation mix was added and bacteria were incubated on ice for 30min. Subsequently, bacteria were heat shocked for 45 s at 42°C. They were then incubated again on ice for 5min before 200 µl LB medium without antibiotics was added and they were incubated for 30-60min at 37°C. Bacteria were distributed onto LB agar plates containing either 100 µg/ml ampicillin or 50 µg/ml kanamycin, and incubated over night at 37°C.

Agarose Gel Electrophoresis and Purification

Separation of linearized DNA constructs was performed using agarose gels in 1× TAE buffer for 45-60min at 80 V. Respective bands were cut out using a scalpel and purified with the NucleoSpin® Gel and PCR cleanup Kit (Macherey-Nagel) according to manufacturers instructions, except that the washing step was performed twice and elution buffer was

heated to 70°C for elution.

Restriction-free cloning

Before cloning, a truncated version of the pFK_Jc1_R2A construct was created (pFK_Jc1-_R2A_short) that lacked everything from the end of E2. For this, pFK_R2A_p7-half was digested with BcuI, HindIII and XbaI. Subsequently, the longest fragment was purified and ends were ligated. Restriction-free cloned plasmids were created in a two-step process. Q5® High-Fidelity DNA Polymerase (NEB) was used according to manufacturers instructions unless stated differently. In the first step, hybrid primers were used to amplify the insert of interest. Ends were complementary to both the sequence of the backbone region where it should be integrated, and to the insert sequence (see Table 11). Amplification was conducted as stated above (see PCR Amplification) and the resulting product, namely the insert of interest with ends complementary to the backbone sequence, was called megaprimer. In the second step, the backbone was used as template and the product from step 1 as primer (megaprimer). 100 ng of template plasmid (pFK_Jc1_R2A_short) was mixed with megaprimer in a molar ratio of 1:20 (template : megaprimer; see Equation 1). For this, the elongation time of the PCR reaction had to be adjusted and was set to 11min and 15 cycles when pFK_Jc1_mScarlet-2A_short was constructed. Afterwards, 20 units of DpnI were added to the PCR product to digest the original plasmid (DpnI only digests methylated DNA). The PCR-DpnI mix was incubated for 2h at 37°C followed by 20min at 80°C. Transformation was carried out as stated above. Design of hybrid primers and general protocol was done using rf-cloning.org [432]. For primer sequences see Table 11.

Cloning of CRISPR/Cas9 constructs

Lentiviral constructs for CRISPR/Cas9 knock-out were designed and produced according to Sanjana *et al.* and Shalem *et al.* [433, 434]. In brief, sequences that target the gene of interest were retrieved from online tools (e.g. CHOP-CHOP [435]), specific overhangs for cloning were added and respective DNA oligos (two per target, complementary with overhangs) were produced by Metabion International AG, Germany (see Table 10). Oligos were resuspended, and both annealing and phosphorylation by T4 Polynucleotide kinase (ThermoFisher) was conducted in a single step. LentiCRISPRv2 backbone plasmid was digested with Esp3I (ThermoFisher) and dephosphorylated by FastAP (ThermoFisher). Next, digested backbone plasmid was purified as described above. 50 ng of purified plasmid was mixed with diluted, annealed oligos from above and ligated using T4 ligase (ThermoFisher). Transformation into NEB Stable3 *E.coli* was performed as stated above.

Small and Medium Scale Plasmid Preparation

Single colonies were picked (from agar plate or glycerol stock) using a pipet tip and inoculated in 5 ml (small) or 50 ml (large) overnight culture (LB medium containing respective antibiotic in concentrations indicated above). 5 ml cultures (6000 rpm, 10min, RT) and 50 ml (4000 rpm, 15min, RT) cultures were pelleted and DNA was extracted using GeneJET Plasmid Miniprep System (ThermoFisher) or PureYield™Plasmid Midiprep System (Promega), in each case according to manufacturer's instructions. DNA concentration was measured with a NanoDrop™1000 (ThermoFisher).

RNA extraction from cells

2-5×10^5 cells were used per sample for RNA extraction. Cells were detached as described below and washed once with 1× PBS. Cell pellets were frozen at -20°C until extraction took place. RNA extraction was performed using RNeasy Mini Kit (Qiagen) according to manufacturers instructions. For lysis 1% 2-mercaptoetanol was added to the lysis buffer. Extracted RNA was stored at -20°C or -80°C for long periods.

cDNA synthesis

For cDNA synthesis 200 ng of extracted RNA was used. The procedure was performed using QuantiTect Reverse Transcription Kit (Qiagen) according to manufacturer instructions. After synsthesis 40 µl of nuclease free water was added and cDNA was stored at -20°C.

XBP1-PCR for agarose gel analysis

For analysis of XBP1 splicing on agarose gels, PCR was performed using Q5® High-Fidelity DNA Polymerase (NEB) according to manufacturer's suggestions for 25 µl total sample volume. Primers XBP1_fw and XBP1_rev were used in a final concentration of 0.5 µM (Table 12). 1 µl of diluted cDNA was used as template. The PCR program used was initial denaturation at 98°C for 30 s, followed by 35 cycles of denaturation at 98°C for 10 s, annealing at 68°C for 10 s and elongation at 72°C for 10s, finalized with a 2min elongation step at 72°C. Samples were stained with 6× TriTrack DNA loading dye (ThermoFisher) and run in a 3% agarose gel together with GeneRuler 1kb DNA ladder (ThermoFisher). Gels were visualized using a GelDoc system.

qRT-PCR

All qRT-PCR measurements were conducted in duplicates, with 2 µl diluted cDNA used per well. A mastermix of according primers and Luna® Universal qPCR Master Mix (NEB)

was prepared and added to each well (0.3 µM final primer concentration, see Table 12). PCR reaction was performed on a LightCycler 480 (Roche) using the standard SYBR green protocol. Analysis was done using the ΔΔCp method with GAPDH as reference gene. The cycle number at which the signal crosses the threshold (herein called the crossing point, or Cp) is dependent on the number of gene copies. First, ΔCp needs to be calculated by subtracting the Cp value of a particular sample from that of a reference sample of the same gene (e.g. viral RNA in Mock and infected; see Equation 2). Second, to calculate the relative expression, the efficiency of the reaction is set as base and the ΔCp as exponent. The efficiency is either determined experimentally or assumed as 2 (duplication of gene copies every cycle). To calculate the gene expression in the sample relative to the reference sample corrected for total RNA amount (ΔΔCp), the relative expression of the gene of interest is divided by the relative expression of the reference gene (see Equation 3).

$$\Delta\, Cp = Cp_{\text{reference}} - Cp_{\text{sample}} \tag{2}$$

$$\Delta\Delta\, Cp = \frac{E^{\Delta\, Cp\,(sample\,gene)}}{E^{\Delta\, Cp\,(reference\,gene)}} \tag{3}$$

Preparation of Viral RNA

An adapted version of the chimeric strain Jc1 or a related construct was used (see Table 9) [298]. For preparation of viral RNA, the respective vector was amplified in bacteria and purified as described above. The vector was linearized by incubating 10 µg of vector with 10 µl of Green Buffer and 2 µl of MluI in a total volume of 100 µl. The mixture was incubated at 37°C for 30min before an extra 0.5 µl MluI was added and incubation was continued for another 30min. The linearized vector was purified using the Wizard® DNA Clean-Up System (Promega) according to manufacturer's instructions. DNA concentration was measured as mentioned above. For RNA production the T7 RiboMAX™Express Large Scale RNA Production System (Promega) was used according to manufacturer's instructions. 1 µg of linearized vector was mixed with 10 µl of 2× buffer, 2 µl of enzyme mix and 1 µl of RNAsin in a total volume of 20 µl. After incubation at 37°C for 30min, 1 µl of RQ1 RNase-free DNase was added and incubated for another 15min at 37°C to digest the DNA template. Afterwards, phenol-chloroform extraction was performed. Two reactions of the RNA production procedure were pooled and 160 µl of DEPC-water was added. Subsequently, 200 µl phenol:chloroform:isoamylalcohol (25:24:1) was added, vortexed for 1min and spun at max speed for 2min. The upper phase was transferred into a new tube and 200 µl chloroform:isoamylalcohol (24:1) was added. This tube was vortexed for 1min and spun at max speed for 2min. Then the upper phase was transferred to a new tube

and 20 µl 3 M sodium acetate pH 5.2, as well as 200 µl isopropanol was added. This was mixed and incubated on ice for 5min before being spun at max speed for 10min at 4°C. Supernatant was discarded carefully and pellet was washed with 70% ethanol. Next, a drying step at 37°C for 5min was carried out. Finally, the pellet was resuspended in 40 µl nuclease-free water, aliquoted and stored at -80°C.

DNA Sequencing

For sequencing, 100-500 ng of vector was mixed with 2.5 µl of respective primer (10 µM; Table 13) and purified water was added, for a total volume of 10 µl. The labelled tube was sent to GATC (Eurofins Genomics).

Preparation of Glycerol Stocks

Glycerol stocks were generated by pelleting a fresh culture of ∼5 ml. The pellet was resuspendet with 1 ml 70:30 LB:glycerol mixture and transferred into cryo tubes. Tubes were then labelled and stored at -80°C.

2.2.2 Cell Biology

Cell Handling

HEK 293T cells were cultured in DMEM (high glucose, GlutaMAX™) containing 10% FCS and 1% penicilin/streptomycin. Huh7.5 and Huh7-Lunet cells were cultured in DMEM (high glucose, GlutaMAX™) containing 10% FCS, 1% penicillin/streptomycin, 1% sodium pyruvate and 1% non-essential amino acids. Lentivirally transduced Huh7.5 cells stably expressing CRISPR guideRNA and Cas9 were cultured with additional 1 µg/ml puromycin. All cells were cultured in incubators providing 37°C and 5% CO_2.

Thawing Cells

One tube of frozen cells was taken from liquid nitrogen and put on ice, then thawed quickly in a 37°C water bath. Subsequently, 1 ml prewarmed medium was added and cells were transferred in a falcon containing 10 ml of prewarmed medium. Cells were spun down (300 g, 5min, RT), supernatant was discarded and cell pellet was resuspended in a suitable amount of medium and incubated overnight. The cells were split as described below for two or three days after medium change. Approximately one week after thawing, cells were fully recovered.

Maintaining Cells

To maintain HEK 293T cells, medium was aspirated and new medium was added. Cells were detached carefully by tapping the flask. Then, cells were resuspended using a serological pipet and distributed to a new flask diluted between 1:2 and 1:10 (resuspended cells : total volume). Huh7.5 medium was aspirated and cells were washed once with 1× PBS. Then, a sufficient amount of 1× trypsin was added and cells were incubated for 3-5min at 37°C to detach them. Trypsin reaction was stopped through addition of fresh medium and resuspension of cells. The cells were then spun at 300 g for 5min at RT, supernatant was discarded and cells were resuspended in new medium. Resuspended cells were distributed to a new flask diluted between 1:3 and 1:8 (resuspended cells : total volume).

Freezing Cells

For freezing, Huh7.5 cells were handled as described above and after trypsin was removed cells were resuspended in medium additionally supplemented with 10% DMSO. Then, cells were distributed to cryo tubes each containing 5×10^6 cells in 1 ml medium. Tubes were put into a styrofoam box and frozen to -80°C. About one week later cells were transferred to liquid nitrogen for storage.

Transfection

24h prior to transfection cells were seeded according to manufacturer's instructions for respective well size. Used constructs are listed in Table 7 and Table 8.

Polyethylenimine (PEI)

HEK 293T cells were seeded 24h prior to transfection. For each well in a 12-well format, 50 µl of Gibco™OptiMEM™(ThermoFisher) was mixed with 1-2 µg total DNA. A master mix was prepared, containing 2 µg of PEI for each µg of DNA in 50 µl OptiMEM for each well. Then, 50 µl of PEI mix was added to each DNA mix, thoroughly mixed and incubated for 15min at RT. Next, 100 µl of the transfection mix was dropped onto cells and cells were incubated at 37°C. After 4h-6h, or the following morning, the medium was changed and a readout was performed 24h to 48h after media change. For transfection in other formats, DNA and PEI amount was adjusted accordingly. Transfection for NFκB luciferase reporter assays was performed in a 96-well format in triplicates per condition. Per well, 100 ng of NFκB-Luc reporter, 5 ng IKKβ, 25 ng YFP or YFP-core, 50 ng pWPI_BLR empty control or CD81 and 5 ng *Gaussia* luciferase DNA was transfected, accordingly. For PolyI:C, 5 ng/well was transfected.

jetPRIME® Reagent

DNA transfections of Huh7.5 cells were performed as instructed by the manufacturer unless stated otherwise. For NFκB luciferase reporter assays the same amounts of DNA were transfected as described above.

Lentivirus Production

5×10^5 HEK 293T cells were seeded 24h prior to transfection in a 6-well format. Transfection was performed with jetPRIME as described above. 3 µg of lentiCRISPRv2 constructs (see also Table 10) was transfected together with 0.9 µg pMD2G and 2.25 µg psPAX2 per well. One well was transfected without any lentiCRISPRv2 vector and used as a negative control. Virus was harvested 24h after medium exchange by taking the supernatant and spinning it at 3200 g for 10min at RT to remove cell debris. Resulting supernatant was transferred to a new tube and used for infection.

Lenti Virus Infection

5×10^5 Huh7.5 cells were seeded 24h prior to infection in a 6-well format. Medium was aspirated and replaced with 1 ml of new medium and 1 ml of virus containing supernatant described above. Also supernatant of the negative control was used for infection. 24h after infection the medium was replaced with new medium containing an additional 1 µg/ml puromycin and maintained as mentioned above.

Electroporation

For each 10 µl electroporation (EP) 1-4×10^5 Huh7.5 cells were used and for 100 µl EP 1-4×10^6 were used. 24h prior to EP the according number of cells was seeded. The cells were detached and trypsin was removed as described above (Maintaining Cells). Three additional washing steps with 1×PBS were performed. After the last washing step, cells were resuspended in 10 µl (100 µl), plus some extra volume, for each EP in 1×PBS containing Ca^{2+} and Mg^{2+}, and the respective amount of RNA was added (0.25-1 µg per EP). The reaction chamber was filled with 3 ml of Buffer E (Buffer E2 for 100 µl tips). A gold tip was filled with 10 µl of cell/RNA suspension and pulsed once with 1300 V for 30 ms. Then, cells were transferred to prewarmed medium without any antibiotics. They were directly seeded to respective wells and incubated at 37°C and 5% CO_2. 30-60min after EP, the cells were transferred to the biological safety level 3 laboratory. 24h after EP medium was changed to a medium also containing antibiotics.

Staining with TopFluor-Cholesterol

Before fixation, living cells were incubated in medium containing 1 µM TopFluor-Cholesterol for 10min at 37°C and then washed 3× with 1×PBS.

Fixation

Medium was aspirated and the cells were washed once with 1×PBS. Cells on cover-slips or in plates for microscopy were fixed using 2% PFA for 10min at RT. Then, PFA was removed and cells were washed once with 1×PBS. All other cells were detached as described above (Maintaining Cells) and trypsin was removed using 1×PBS or FACS buffer (1×PBS supplemented with 1% FCS). Supernatants were discarded and pellets were resuspended in 50-100 µl 2% PFA, incubated for 10min at RT and stored at 4°C.

Immunofluorescence Staining

Cells on plates were permeabilized with 80% acetone (0.5% Triton X-100 for p65 translocation) for 8min at RT. Then, cells were washed with 1×PBS and blocked with 10% normal goat serum in PBS for 30min at RT. Cells were washed again with 1×PBS and stained with 40 µl anti-core or anti-p65 primary antibody (1:250 in FACS buffer) for 60min at RT. Subsequently, cells were washed 3× with 1×PBS and stained with anti-mouse secondary antibody conjugated with AlexaFluor™ 488 or AlexaFluor™ 594 for 60min at RT and in the dark. Subsequently, nuclear DNA was stained either with DAPI (1:20000, 10min, RT) or SiR-DNA red nuclear dye (1 µM, 90min, RT). Cells were then washed as before and imaged.

Mounting

Cells fixed on cover-slides were mounted on microscope slides using 8 µl of VectaShield® (Biozol) per cover-slide. Mounted slides were fixed using nail polish and dried over night at 4°C.

Luciferase Assay

Cells electroporated or infected with viral constructs harbouring a luciferase reporter gene were seeded in a 96-well format (∼8,000 cells per well, in triplicates). At the appropriate time point supernatant of cells was removed and either discarded or used for a subsequent infection. Cells were washed with 1×PBS and luciferase assay was performed according to the type of the encoded luciferase. In case of *Renilla* luciferase, cells were lysed for 10min at RT with RLuc lysis buffer (60 µl per well in 96-well format). Subsequently,

40 µl of lysed cell suspension was transferred to an opaque white 96-well plate and 60 µl of RLuc substrate buffer was added. Luminescence was measured with a Cytation® 3 Multi-Mode Microplate Reader (BioTek Instruments). In case of Nano luciferase, the Nano-Glo® Luciferase Assay System (Promega) was used. In brief, cells were lysed with NanoGlo® luciferase assay buffer (60 µl per well in 96-well format) and 40 µl of the lysed cell suspension was transferred to an opaque white 96-well plate. NanoGlo® luciferase assay buffer supplemented with NanoGlo® luciferase assay substrate according to manufacturer's instructions was added (50 µl per well) and luminescence was measured with a Cytation® 3 Multi-Mode Microplate Reader (BioTek Instruments). In case of Firefly luciferase reporter constructs, 20 µl of supernatant was transferred to an opaque white 96-well plate and 50 µl RLuc substrate buffer was added to measure the *Gaussia* luciferase signal as transfection control. Remaining supernatant was discarded, and cells washed with 1× PBS then lysed with 60 µl FLuc lysis buffer for 10min at RT. Then, 40 µl of the lysate was transferred to an opaque white 96-well plate, 40 µl of FLuc assay buffer and 40 µl of FLuc substrate buffer was added. The signal was measured using the TriStar^2 S microplate reader (Berthold Technologies).

Flow Cytometry

For flow cytometry, fixed cells were used unless otherwise stated. If cells were stained intracellularly, they were permeabilized using 0.2% saponine in 10% normal goat serum in PBS or 80% acetone for 10min at RT, followed by blocking for 30min at RT with 10% normal goat serum in PBS. Staining with primary or conjugated antibody was performed for 30min at 4°C in the dark, followed by washing 2× with FACS buffer. If applicable, staining with secondary antibody was performed for 30min at 4°C in the dark, followed by washing 2× with FACS buffer (Table 6). Measurements were performed using a MACSquant VYB machine (Miltenyi Biotech). Fixed cells were resuspended in 100 µl FACS buffer and measured. Living cells for flow cytometry-based FRET (FACS-FRET) experiments were detached in 1×PBS buffer and immediately put on ice. They were spun once (300 g, 5min, RT), resuspended in 350 µl FACS buffer, and measured as soon as possible.

SDS-PAGE and Western Blot Analysis

Cell lysates were mixed with 6× sample buffer containing SDS and denatured at 95°C for 10min. For PAGE a 12% separating gel was used. Separation was done at 80-140 V for 90-150min. Blotting was performed in a wet blotting chamber (BioRad) at 80 V for 90min. For cropping of membranes they were stained with Ponceau red for 5min and washed once with TBS-T (1×TBS with 0.1% Tween 20) or PBS-T (1×PBS with 0.1% Tween 20).

Blocking occurred in 5% milk or 1% BSA in 1×TBS or 1× PBS for 1h at RT. Primary antibodies were applied over night at 4°C while membrane was fused into a plastic foil. Secondary antibodies were applied for 1h at RT. Used antibodies and respective dilutions are depicted in Table 5. Between primary and secondary antibody application, as well as after secondary antibody application, membrane was washed 3× with TBS-T or PBS-T, respectively. Visualization was performed with an Odyssey® Fc Imaging System (LI-COR Biosciences).

Microscopy

Fixed coverslips

Microscopy was performed using a DeltaVision™OMX SR (GE Healthcare). Imaging of fixed cover-slides was performed according to the manufacturer's operating instructions using a 60× objective for confocal images.

Fixed plates

Microscopy imaging of plates was performed using a Cytation™ 3 Multi-Mode Microplate Reader (BioTek Instruments) with a 4× objective or using a IncuCyte® S3 Live-Cell Analysis System (Sartorius) with a 10× or 20× objective.

Live cell imaging of dishes

For live cell imaging, $\sim 4 \times 10^5$ Huh7.5 cells were seeded in 35mm WillCo dishes. Prior to imaging, medium was replaced by medium without phenol red. Experiments were performed at 37°C, 5% CO_2 and 40-70% humidity.

Live cell imaging of plates

Cells for live-cell imaging were seeded as usual in the respective plates and imaging was performed using a IncuCyte® S3 Live-Cell Analysis System (Sartorius) with a 10× or 20× objective at 37°C, 5% CO_2 and 80-90% humidity.

Data Analysis

Design and alignment of DNA constructs was done using SerialCloner v2.6.1 unless otherwise stated. Western blot membranes were analyzed using ImageStudio®lite. Flow cytometry data was analyzed using Flowlogic™ v8.3 (Inivai Technologies). Microscopy images were analyzed using SoftWoRx 7.0 (Cytiva), Gen5 v3.10 (BioTek Instruments) or IncuCyte® GUI v2021A (Sartorius), according to instrument, and subsequently handled with ImageJ. Statistical analysis and creation of graphs was done using Graphpad Prism 9

(GraphPad Software) and Excel 2019 (Microsoft). Design and arrangement of figures was performed with CorelDraw®X7 (Corel Corporation).

3 Results

Several points of contact between tetraspanins and HCV have been previously described (see 1.2.4 Entanglement of Tetraspanins with HCV). However, whether their expression is altered during active viral replication has not been elucidated completely. We obtained data from a surface expression screen performed by Sandra Kurz, which showed a significant downregulation of seven proteins from the surface of HCV expressing Huh7.5 cells (Figure S1A) [436, 437]. In brief, cells were electroporated with a viral genome encoding for a fluorescent protein to distinguish actively replicating cells from bystanders. Those cells were then stained with a set of antibodies (LEGEND screen) to check whether differences in surface expression levels could be observed. The two most prominently downregulated candidates belonged to the tetraspanin family of proteins, namely CD63 and CD81. Subsequently, those two candidates and other proteins of the same family were tested in a flow cytometry-based FRET interaction experiment to assess for close proximity between tetraspanins and HCV proteins (Figure S1B) [437]. There, CD9, together with CD63 and CD81, showed the highest level of FRET signal, indicating close proximity. Based on these results, the tetraspanins CD9, CD63 and CD81 were chosen for further analysis, which was conducted in this thesis.

3.1 Downregulation of Tetraspanins by HCV

3.1.1 Regulation of CD9, CD63 and CD81 Surface and Total Protein Expression

To confirm the results of the previous screen, Huh7.5 cells were electroporated with a Jc1-based viral genome that encodes a NS5A-GFP fusion protein. After 72h, cells were stained for either surface or total expression of CD9, CD63 or CD81 and levels were measured by flow cytometry. Displayed are the relative tetraspanin levels of cells that express viral proteins (GFP+) or not (GFP-). Figure 1A shows a slight increase in CD9 surface level and a slight decrease in CD63 and CD81 surface levels in HCV expressing cells. While the increase in CD9 was more prominent in the total protein level, no decrease in CD63 and CD81 total protein levels was observed. Then, YFP-tagged viral proteins E2, NS2/3, NS5A and p7 were solely expressed in HEK-293T cells and, as before, surface and total tetraspanin levels were determined by flow cytometry. Displayed are relative tetraspanin levels of cells that express no (GFP-), intermediate (GFP+) or high (GFP++) levels of the indicated viral protein. CD9 surface levels were only slightly decreased

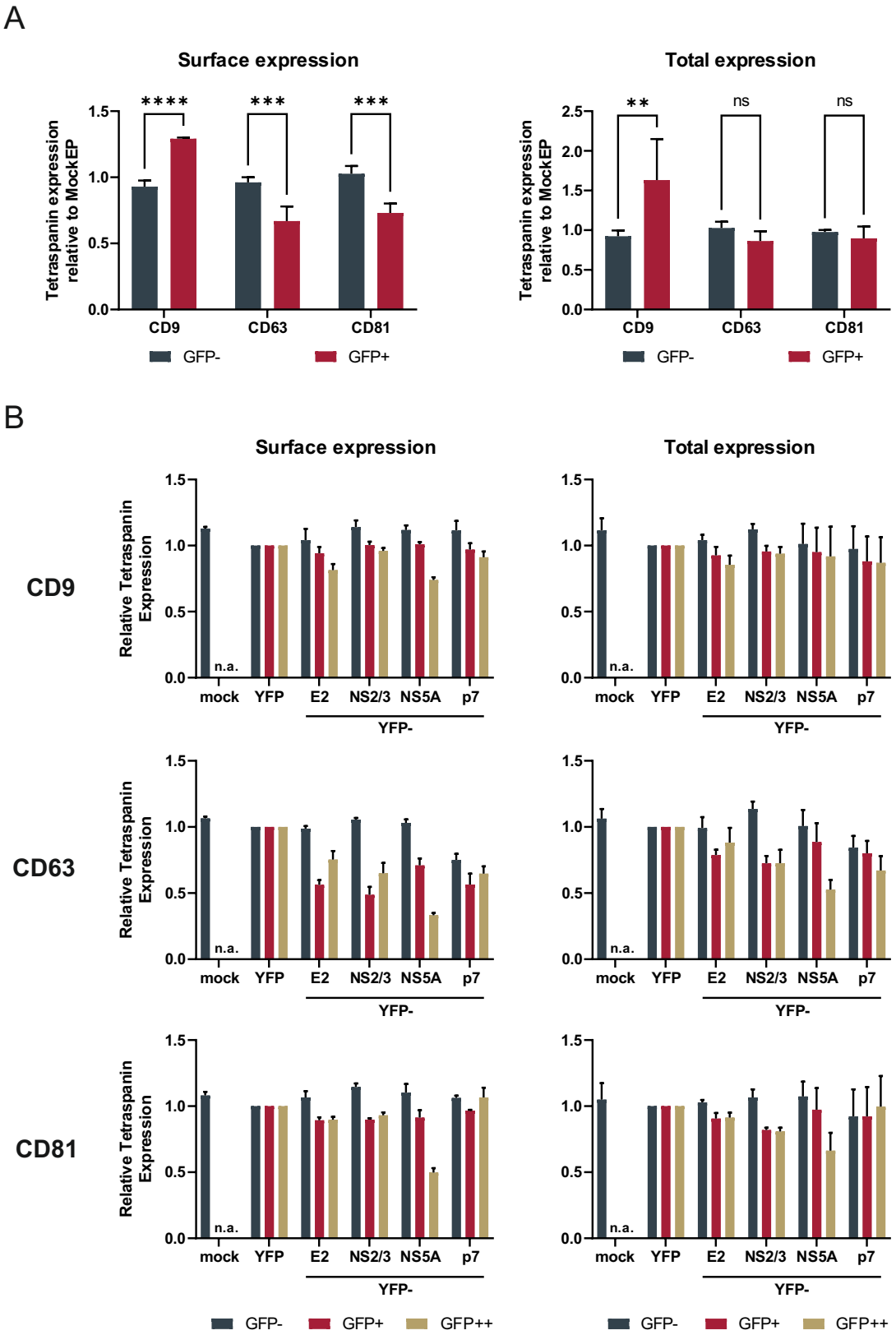

Figure 1: Regulation of Tetraspanin expression by HCV proteins.
Continued on next page.

Figure 1: (continued)
(A) Surface and total tetraspanin levels in bystander (GFP-) and HCV expressing (GFP+) cells. Huh7.5 cells were electroporated with Jc1_NS5A-GFP RNA, cultivated for 72h and subsequently fixed, permeabilized (for total staining), and stained to measure tetraspanin levels by flow cytometry. Depicted are data from 3 independent experiments. **(B)** Surface and total tetraspanin levels in bystander (GFP-) or YFP-fusion protein transfected cells with intermediate (GFP+) or high (GFP++) signal intensity. HEK-293T cells were transfected with constructs encoding different viral proteins tagged with YFP. 24h post transfection cells were fixed, permeabilized (for total staining), and stained to measure tetraspanin levels by flow cytometry. Depicted are data from 3 independent experiments. Shown are mean values ± SD. Significance was tested using two-way ANOVA with Sidak's multiple comparisons test. ns = not significant; * $p \leq 0.05$; ** $p \leq 0.01$; *** $p \leq 0.001$; **** $p < 0.0001$.

when NS5A was highly expressed and no alteration was observed in total levels of CD9 (Figure 1B, upper panel). In case of CD63, surface expression was decreased in presence of all four tested viral proteins with NS5A being the most potent one. Total protein levels decreased to a lesser extend while showing the same trend of NS5A being the most potent downregulator (Figure 1B, middle panel). Levels of CD81 were only decreased when NS5A was present. Thereby, CD81 surface expression was more decreased than the total expression (Figure 1B, lower panel). Taken together, CD9 is rather upregulated than downregulated, however, no clear effect of viral proteins could be seen. CD63 and CD81 levels are negatively affected by the presence of HCV proteins, with surface levels being more reduced than total levels. Here, CD63 appeared to be the tetraspanin most affected by presence of viral proteins. Among viral proteins, NS5A seemed to be the most potent candidate to downregulate CD63 and CD81.

3.1.2 Dynamics and Mechanism of CD81 Downregulation

Although CD63 and CD81 were both affected by the presence of HCV proteins, the investigation of the mechanism was only pursued for CD81. The reason for this is that we found no impact of CD63 on viral replication in knock-out experiments, which will be discussed in detail in the next paragraph (3.2 Characteristics of CD81KO Cells). To evaluate the dynamics of the reduced CD81 levels, Huh7.5 cells were electroporated with different Jc1-based viral genomes. They encoded a mScarlet reporter gene at the beginning of the polyprotein connected via a 2A self-cleaving site, or fused with either E2 or NS5A resulting in E2-mScarlet or NS5A-mScarlet expressing HCV-genomes. Cells were then harvested at different time points (24h, 48h, 72h, 96h and 144h) post electroporation, permeabilized and stained for total CD81 levels. Figure 2A shows Jc1 genome expressing and bystander cells (x-axis), as well as total CD81 levels (y-axis) of representative experiments. Summarized data is displayed in Figure 2B. There were no differences in CD81 levels observable at 24h post EP, while total CD81 levels were clearly reduced 48h to 96h post EP. Downregulation

seemed to be transient as CD81 levels started to rise again and reached base-line levels again between 96h and 144h post EP. Viral genome constructs encoding fusion proteins seemed to be more potent in downregulation of CD81 but at the same time caused higher cytotoxicity, as evident from lower or decreasing cell numbers (Figure 2B). The following experiment aimed to elucidate the mechanism underlying the downregulation of CD81 by HCV. Cells electroporated with the NS5A-mScarlet fusion protein were treated 48h post EP with an inhibitor of the proteasome (MG132) and one of the lysosome (Bafilomycin A1) to see if any of those are involved in the degradation process. 24h after treatment, cells were stained for total CD81. Figure 2C illustrates that none of the inhibitors were able to prevent or reverse the downregulation. Next, regulation on the transcriptional level was tested. To address this, Huh7.5 cells were electroporated with the Jc1 genome and total cellular mRNA was harvested 48h after electroporation. In Figure 2D it is evident that CD81 mRNA levels are significantly reduced in cells expressing HCV compared to Mock cells, showing that CD81 is downregulated by HCV on the transcriptional level. Together, CD81 levels could be downregulated by several different viral constructs and reach their lowest levels at 48h and 72h after EP. Inhibition of neither the proteasome, nor the lysosome could prevent this downmodulation. qRT-PCR experiments showed that mRNA levels are reduced in HCV expressing cells, suggesting that HCV-mediated regulation of CD81 happens on the transcriptional level.

3.2 Characteristics of CD81KO Cells

3.2.1 Involvement of CD81 in HCV Replication and the Role of the Cholesterol Binding Site.

To test the functional role of CD9, CD63 and CD81, Huh7.5 knock-out cell lines were created using CRISPR/Cas9. These cell lines were electroporated with a luciferase reporter construct based on the Jc1 genome (Jc1_RLuc-2A) and luciferase activity was measured 72h post EP (Figure 3A, left panel). It could be observed that cells that lack CD81 have a strongly reduced signal indicating a lower level of replication. No effect could be observed for CD9 or CD63 knock-out cells. To further evaluate this, Huh7-Lunet cells were used that lack the expression of CD81. In some cells the expression of human CD81 was reconstituted and the E219Q mutant was included, which has a diminished ability to bind cholesterol (Figure 3A, right panel) [399]. Again, cells that had low or no CD81 levels showed decreased luciferase signals, while cells with reconstituted CD81 showed signals comparable to Huh7.5 control cells. Interestingly, cells that were reconstituted with the CD81 E219Q mutant displayed no rescue effect and showed low levels of HCV replication that were comparable to cells that had low or no CD81 expression. Therefore the question

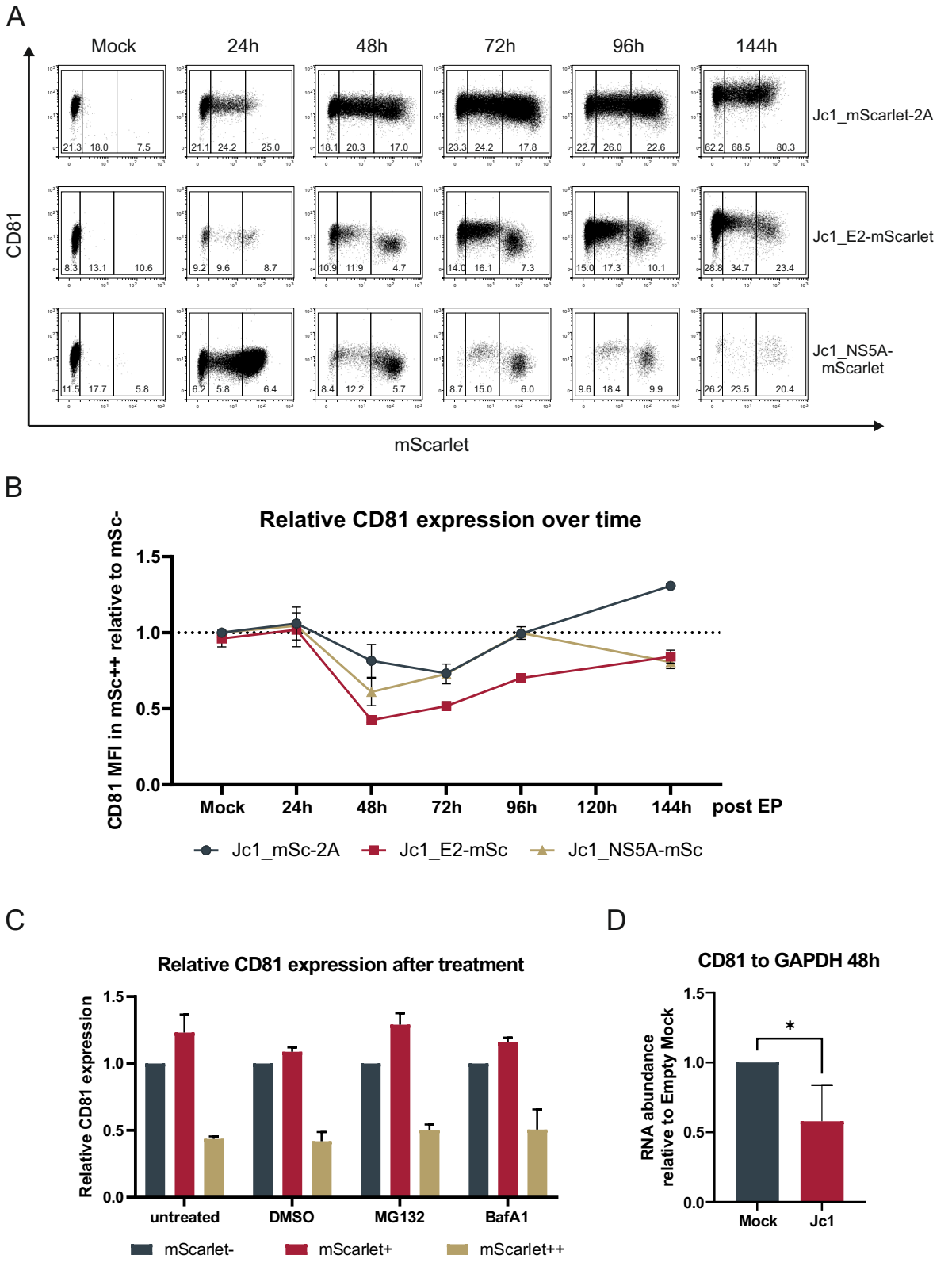

Figure 2: Dynamics of CD81 expression in HCV expressing cells and regulation at the transcriptional level.

Continued on next page.

Figure 2: (continued)
(A) Total CD81 levels in bystander (mScarlet-; left gate) or HCV expressing cells with intermediate (mScarlet+; middle gate) or high (mScarlet++; right gate) signal intensity. Huh7.5 cells were electroporated with viral genomes Jc1_mScarlet-2A, Jc1_E2-mScarlet or Jc1_NS5A-mScarlet RNA and harvested at indicated time points. Cells were fixed, permeabilized and stained for total CD81 levels and measured via flow cytometry. **(B)** Summary data of relative CD81 levels over time from 2 - 4 independent experiments. **(C)** Relative CD81 levels in cells treated with different inhibitors. Huh7.5 cells were electroporated with Jc1_NS5A-mScarlet RNA. After 48h cells were either left untreated or treated with DMSO (1 %), MG132 (1 µM) or Bafilomycin A1 (100 nM). 24h after treatment cells were fixed, permeabilized and stained for total CD81 levels to be measured by flow cytometry afterwards. Depicted are data from 3 independent experiments. **(D)** CD81 mRNA levels in Mock and Jc1 electroporated cells. Huh7.5 cells were electroporated with Jc1 RNA. 48h post EP cells were harvested and RNA was extracted to perform a qRT-PCR measurement. Relative mRNA levels were calculated using the ΔΔCp method with GAPDH as reference gene. Depicted are data from 4 independent experiments. Shown are mean values ± SD. Significance was tested using an unpaired t-test. ns = not significant; * $p \leq 0.05$.

arose whether proper cholesterol binding is important for interactions of viral proteins with CD81. Hence, HEK-293T cells were transfected with viral proteins and either CD81 or its E219Q mutant. Then, close proximity and presumably interaction was measured via flow cytometry-based FRET. Figure 3B shows diminished interaction of CD81 E219Q with core, E1 and NS5A compared to WT CD81, although the decrease for core was not significant ($p = 0.1235$). Notably, interactions with E2 and p7 seemed to be independent of the cholesterol binding ability of CD81, indicating that different interaction processes between CD81 and several HCV proteins exist. As CD81 is known for its scaffolding functions across different cellular processes the next step was to test the interaction network of HCV proteins with themselves in HEK-293T control and CD81 knock-out cells. Cells were transfected with a pair of HCV proteins and their interaction was studied using flow cytometry-based FRET (Figure 3C). Although many viral proteins interact with each other, none of those interactions was significantly altered in cells expressing no or a low amount of CD81. But this only represents the interaction of two viral proteins with each other, so alterations in the interaction of complexes of higher order with potential additional involvement of cellular proteins cannot be excluded. It can be summarized that CD81 is functionally involved in HCV replication and that its ability to bind cholesterol is important for this effect. Additionally, interaction of CD81 with E1, NS5A and also core, in a limited way, seemed to be dependent on cholesterol binding.

3.2.2 Morphology of Cells Lacking CD81

As HCV replication depends on a multitude of cellular processes (see Translation and Replication), the integrity of organelles and intracellular membranes in control and CD81 knock-out cells was analyzed. First, control and CD81 knock-out cells were checked for

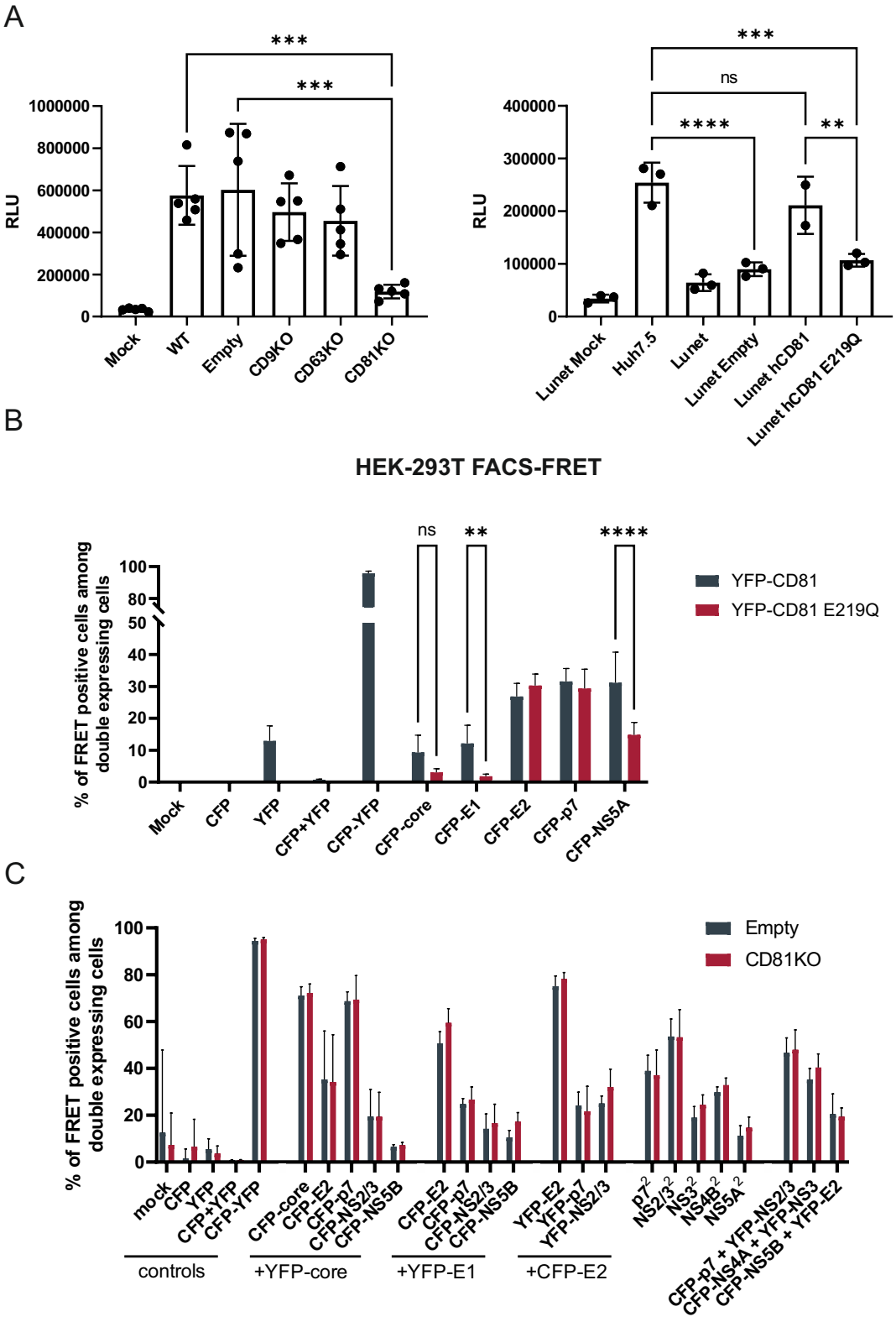

Figure 3: CD81KO functional involvement and impact of the CD81 cholesterol binding site.

Continued on next page.

Figure 3: (continued)
(A) Luciferase activity after EP in Huh7.5 tetraspanin knock-out and Huh7-Lunet CD81 reconstituted cells. Respective cell lines were electroporated with Jc1_RLuc-2A RNA and luciferase activity was measured 72h after. **(B)** Flow cytometry-based FRET signals of viral proteins with CD81 or the CD81-E219Q mutant. HEK-293T cells were transfected with a pair of constructs encoding CFP-tagged viral proteins and YFP-tagged CD81. 24h post transfection, cells were washed and FRET signals were measured via flow cytometry. Depicted are data from 4 independent experiments. **(C)** Flow cytometry-based FRET signals of different combinations of viral proteins. HEK-293T CD81KO and control cells were transfected with a pair of constructs encoding CFP- and YFP-tagged viral proteins. 24h post transfection, cells were washed and FRET signals were measured via flow cytometry. Depicted are data from 4-8 independent experiments. Shown are mean values ± SD. Significance was tested using one-way ANOVA with Tukey's multiple comparisons test for A and two-way ANOVA with Sidak's multiple comparisons test for B. ns = not significant; * $p \leq 0.05$; ** $p \leq 0.01$; *** $p \leq 0.001$; **** $p < 0.0001$.

altered organelle and autophagosome distribution. Huh7.5 control and knock-out cells were transfected with organelle markers and confocal microscopy was performed (Figure 4A). No differences in cellular distributions of ER, Golgi, early or late autophagosomes could be observed, indicating that their function is unaffected by lack of CD81. Subsequently, distribution of viral proteins was checked by transfection of YFP-tagged NS4B and NS5A plasmids in Huh7.5 control and knock-out cells (Figure 4B). NS4B and NS5A are described as playing a crucial role in formation of the membranous web (see Translation and Replication). However, no differences in distribution could be visualized. As single viral proteins alone might not be sufficient to introduce these changes, whole genome constructs were used to visualize tagged viral proteins. Electroporated Huh7.5 control and knock-out cells were imaged by confocal microscopy and both E2- and NS5A-mScarlet tagged whole genome constructs were used (Figure 4C). Again, the cellular localization seemed not to be affected by the lack of CD81, with the limitation to E2 and NS5A. In previous experiments the importance of the cholesterol binding site of CD81 in the context of interaction with HCV proteins was shown (Figure 3A and B). Hence, cells were treated with a cholesterol molecule that was fluorescently-labeled (TopFluor-Cholesterol) to visualize cholesterol rich areas. Cells that were electroporated with no or viral RNA (Jc1_E2-mScarlet, Jc1_NS5A-mScarlet) were additionally stained with TopFluor-Cholesterol and a nuclear stain before they were imaged via confocal microscopy (Figure 4D). Both cells expressing no viral RNA and those expressing either of the two viral RNAs, showed no difference in cholesterol distribution when control and CD81 knock-out cells were compared. HCV is known to dysregulate cholesterol homeostasis and its distribution, which is visible when Mock and viral RNA expressing cells are compared (Figure 4B) [243, 278, 281]. Nevertheless, lack of changes in cholesterol abundance and localization in control versus CD81 knock-out cells indicate that CD81 is probably not involved in regulation of cholesterol homeostasis. It can be concluded that the lack of CD81 did not seem to change organelle distribution,

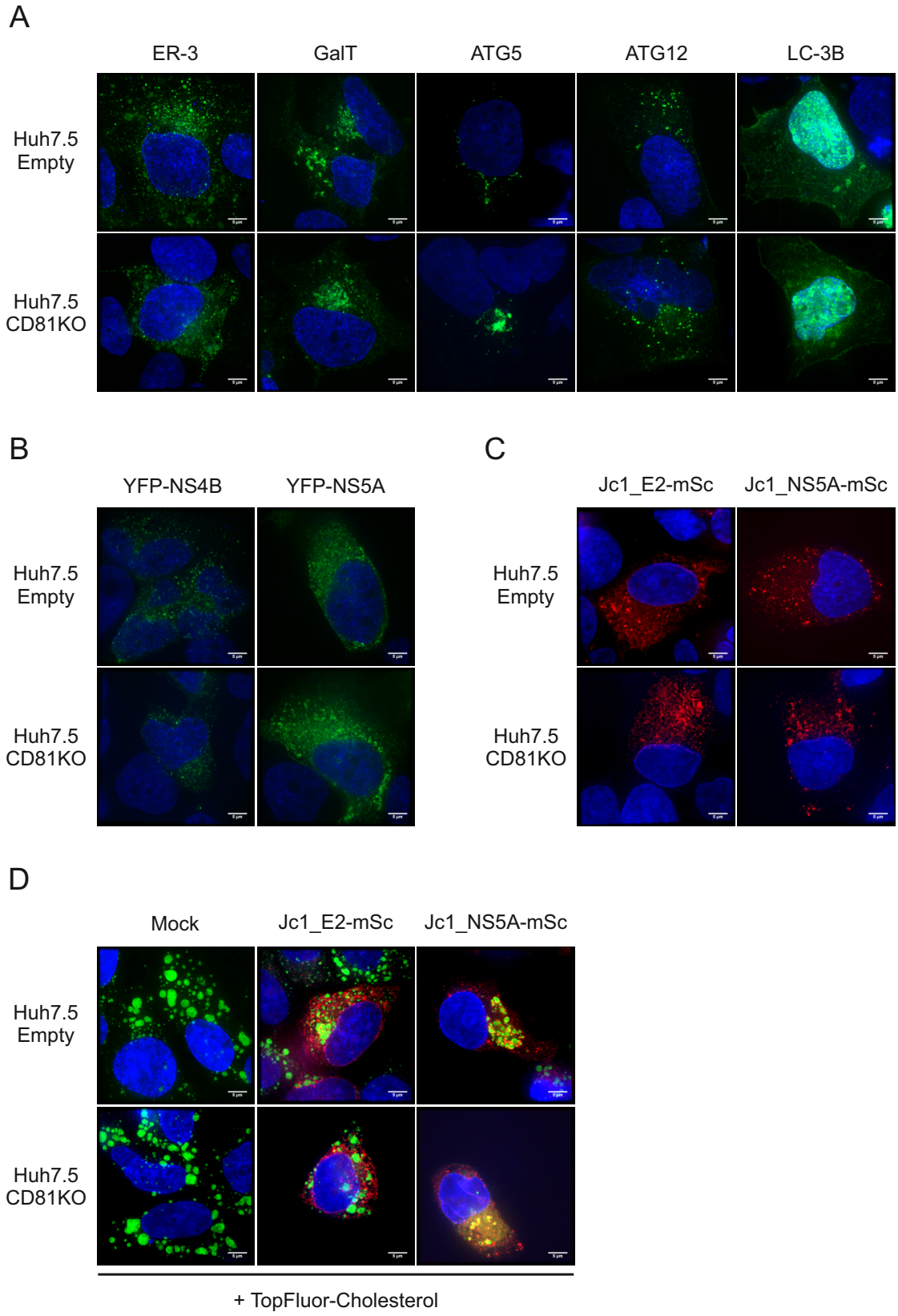

Figure 4: Cellular distribution of organelle markers in CD81KO cells.
Continued on next page.

Figure 4: (continued)
(A) Distribution of organelle markers in control and CD81KO cells. Huh7.5 control and CD81 knock-out cells were transfected with plasmids encoding fluorescently-tagged proteins (or parts thereof) with distinct cellular distribution. 24h post transfection, cells were fixed, permeabilized, the nucleus was stained and they were mounted on cover slips for confocal microscopy. Displayed are (from left to right) ER (ER-3), Golgi (GalT), early autophagosome (ATG5, ATG12), and late autophagosome (LC-3B). **(B)** Cellular distribution of viral proteins NS4B and NS5A in control and CD81KO cells. Huh7.5 control and knock-out cells were transfected with plasmids encodung YFP-tagged NS4B or NS5A. 24h post transfection, cells were fixed, permeabilized, the nucleus was stained and they were mounted on cover slips for confocal microscopy. **(C)** Cellular distribution of viral proteins E2 and NS5A in the context of full genome viral replication. Huh7.5 control and CD81 knock-out cells were electroporated with Jc1_E2-mScarlet or Jc1_NS5A-mScarlet. 72h post EP, cells were fixed, permeabilized, the nucleus was stained and they were mounted on cover slips for confocal microscopy. **(D)** Cellular distribution of cholesterol together with viral proteins E2 and NS5A in the context of full genome viral replication. 72h post EP, cells were stained for cholesterol, then fixed, permeabilized, the nucleus was stained and they were mounted on cover slips for confocal microscopy. White bars represent 5 µm.

localization of viral proteins or accumulation of cholesterol.

3.2.3 Viral Replication Depends on CD81 Expression

The reduced HCV replication in CD81 knock-out cells could not be linked to general changes in the cells morphology or cholesterol homeostasis. For a more detailed analysis of this phenomenon, control and CD81 knock-out cells were electroporated with viral RNA encoding a luciferase reporter and samples were taken after different time points. Figure 5A shows luciferase signals at indicated time points, which suggest nearly a complete absence of viral replication in CD81 knock-out cells. Indeed, no signal could be detected for viral proteins core, E2, or NS5A in these samples via western blot (Figure 5B). As the resolution of the luciferase assay and the protein detection via western blot did not allow any conclusion for the early time points, 24h and 48h, an inhibitor experiment was performed. Cells were electroporated as before and additionally treated with geneticin (G418) at 24h post EP. Geneticin interferes with the ribosome and blocks protein biosynthesis. Luciferase activity was measured at 28h or 48h post EP (4h or 24h post treatment, respectively). 4h after treatment no difference in luciferase signal of control and CD81 knock-out cells was observed, as well as no effect of geneticin on either cell line (Figure 5C, left). However, 24h post treatment control cells showed a much higher luciferase signal as CD81 knock-out cells. Interestingly, control cells that were treated with geneticin showed a comparable signal to the non-treated CD81-knock out cells. This indicates that CD81 knock-out has an inhibitory effect on viral replication early post EP. As *Renilla* luciferase is reported to have a half-life of about 4.5h, we wanted to check this effect with a reporter that has a longer half-life within cells [438]. Therefore, the *Renilla* luciferase reporter was replaced

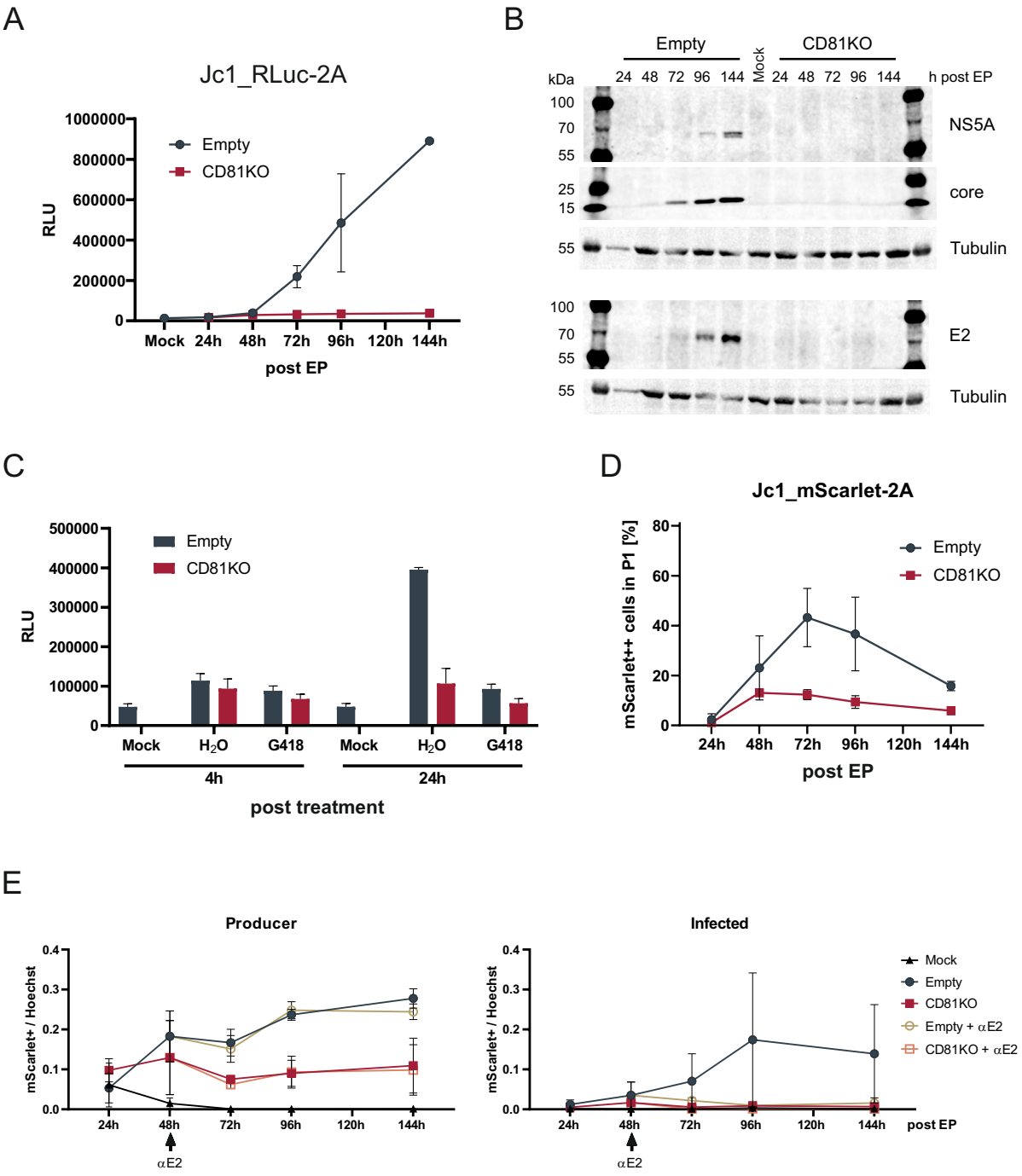

Figure 5: Viral replication depends in presence of CD81.
(A) Viral replication in control and CD81KO cells over time. Huh7.5 control and CD81KO cells were electroporated with Jc1_RLuc-2A, lysed and luciferase signal was measured at indicated time points. Depicted are data from 2 independent experiments. **(B)** Core, E2 and NS5A expression in control and CD81KO cells over time. Huh7.5 control and CD81KO cells were electroporated with Jc1_RLuc-2A, lysed and utilized for SDS-PAGE and western blot analysis. Tubulin was used as reference protein. Depicted are representative data from 2 independent experiments. Continued on next page.

Figure 5: (continued)
(C) Viral replication at early time points. Huh7.5 control and CD81KO cells were electroporated with Jc1_RLuc-2A, treated with geneticin (G418, 400 µg/ml), lysed and luciferase signal was measured. Depicted are data from 2 independent experiments. **(D)** Ratio of HCV expressing control and CD81KO cells over time. Huh7.5 control and CD81KO cells were electroporated with Jc1_mScarlet-2A, fixed, and ratio of highly mScarlet expressing cells (mScarlet++) was measured via flow cytometry. P1 gate representing living cells determined by FSC-A and SSC-A values. Depicted are data from 2 independent experiments. **(E)** Kinetics of viral replication in control and CD81KO cells and infectivity of supernatant. Huh7.5 control and CD81KO cells were electroporated with Jc1_mScarlet-2A, partly treated with an E2-targeting antibody (AP-33) at a neutralizing concentration (50 µg/ml), and supernatant was used to infect naive Huh7.5 cells. At indicated time points, cells were fixed, stained for nuclear DNA with Hoechst, and ratio of mScarlet expressing cells was measured using a plate reader. For E, data points show mean ± SEM of 2 independent experiments. Data points show mean ± SD if not mentioned otherwise.

with mScarlet, a red fluorescent protein. Control and CD81 knock-out Huh7.5 cells were electroporated with the red fluorescent reporter (Jc1_mScarlet-2A), harvested and fixed after indicated timepoints, and replicating cells were identified via flow cytometry. In Figure 5D it becomes evident that the ratio of control cells where productive replication was established is higher than in CD81 knock-out cells. Notably, the signal intensity of those cells that were identified as productively replicating is similar in control and CD81 knock-out cells (data not shown). To rule out the possibility that the shown differences between control and CD81 knock-out cells originate from the loss of spread of infection in knock-out cells, a neutralization experiment was performed. As before, cells were electroporated with Jc1_mScarlet-2A, but were additionally treated with an antibody targeting the E2 protein in a neutralizing concentration. To control for successful neutralization, supernatants were used to infect naive cells. As shown in Figure 5E (left), treatment with neutralizing antibody did not change the ratio of replicating cells in either control or in CD81 knock-out cells. At the same time, only supernatant of non-treated control cells was infectious, proving that the used antibody concentration was indeed neutralizing (Figure 5E, right). Taken together, absence of CD81 severely impairs viral replication of the used 2A reporter Jc1-based constructs. The underlying effect, that CD81 knock-out has, seems to affect early steps important for the establishment of productive viral replication. Impaired viral spread appeared not to be a major cause of the observed reduced viral replication in CD81 knock-out cells.

3.3 Kinetics of Viral Replication Define Impact of CD81

3.3.1 Expression Dynamics of Different Viral Constructs

To get a better understanding of what happens at early time points after electroporation, live-cell imaging experiments were performed. Control and CD81 knock-out cells were electroporated with viral RNA (Jc1_mScarlet, Jc1_NS5A-mScarlet, Jc1_E2-mScarlet)

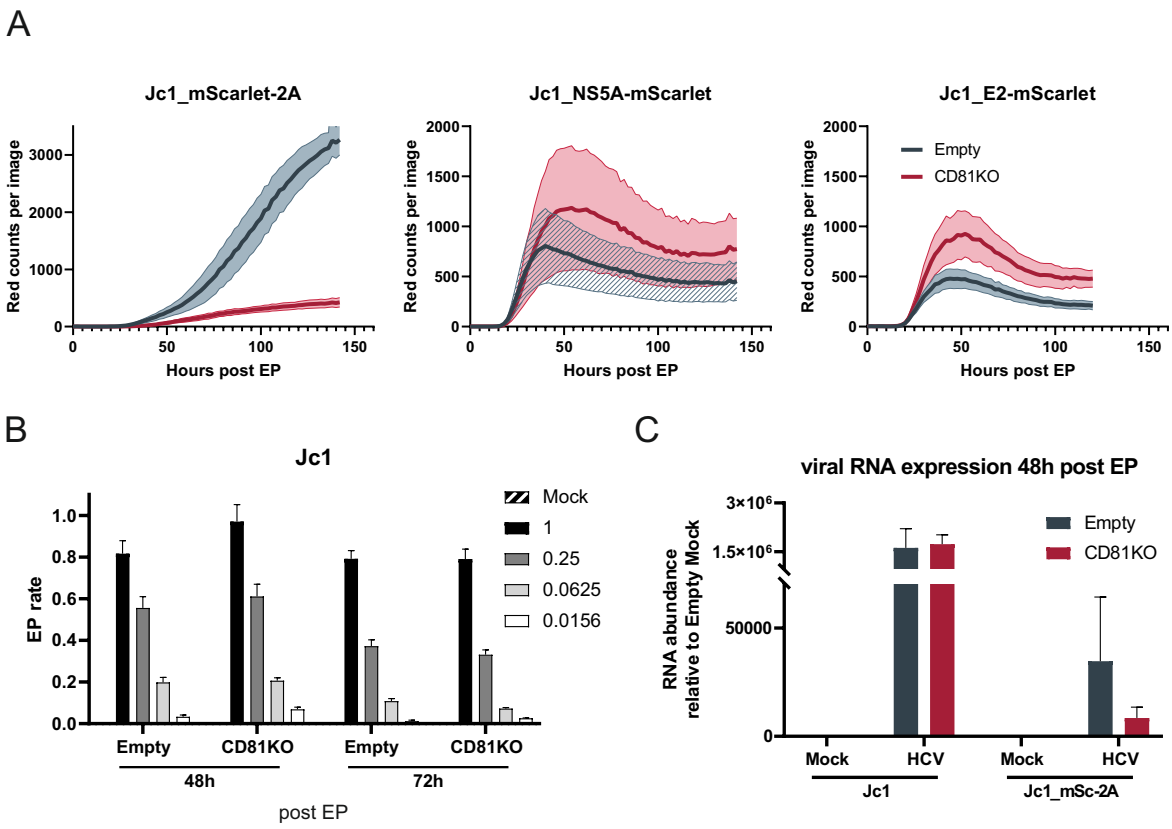

Figure 6: Impact of CD81 on viral replication is strongly dependent on the used viral construct.
(A) Kinetics of replication of different fluorescent viral constructs. Huh7.5 control and CD81KO cells were electroporated with viral RNA (Jc1_mScarlet-2A, Jc1_NS5A-mScarlet, Jc1_E2-mScarlet) and the number of red cells was counted over time. Depicted are representative data from 2-3 independent experiments. **(B)** Titration of viral RNA and respective ratio of HCV positive cells. Huh7.5 control and CD81KO cells were electroporated with indicated amounts of viral RNA (Jc1). 48h and 72h later cells were fixed, permeabilized and stained for HCV core protein and nuclear DNA. Graph represents HCV core positive cells divided by nuclear DNA positive cells. Depicted is data from one experiment in triplicates. **(C)** Comparison of viral RNA quantity in different viral RNA constructs. Huh7.5 control and CD81KO cells were electroporated with viral RNA (Jc1, Jc1_mScarlet-2A), 48h post EP, RNA was extracted and viral RNA quantified by qRT-PCR. Depicted data from 2-4 independent experiments. Data points show mean ± SD if not labelled otherwise.

and their replication dynamics (indicated by red fluorescence) were observed. Images were taken every 2h for up to 6 days post EP. Figure 6A shows red fluorescence over time for the three used constructs. Surprisingly, constructs with a fusion-protein (NS5A-mScarlet, E2-mScarlet) show a different pattern as the 2A-reporter construct. While red fluorescence in Jc1_mScarlet-2A electroporated CD81 knock-out cells stayed low compared to control cells over the measured time period, it was higher in fusion protein constructs. Of note, fusion protein constructs seemed to reach their maximum of red cells at around 50h post EP (Figure 6A, middle and right), while the 2A-construct seemed to reach a plateau after 6 days (Figure 6A, left). The overall higher number of red cells in the 2A-construct can be explained by the spread of viral particles at late time points, whereas fusion protein constructs barely produced infectious viral progeny (data not shown). To delineate CD81 dependency of wild-type HCV, unmodified viral RNA (Jc1) was used in further experiments. Electroporation of control and CD81 knock-out cells with different amounts of Jc1 viral RNA was performed, and cells were fixed and stained for HCV core 48h and 72h post electroporation. In Figure 6B the electroporation ratio of core expressing cells divided by nuclear DNA positive cells is displayed. Different RNA amounts have been used to see if massive RNA input could overcome the CD81 effect. Interestingly, control and CD81 knock-out cells showed no difference in EP ratio for any of the used concentrations or time points. Additionally, control and CD81 knock-out cells were checked for viral RNA amount 48h after they had been electroporated with viral RNA (Jc1, Jc1_mScarlet-2A; Figure 6C). In control and CD81 knock-out cells electroporated with Jc1, no difference in viral RNA amount was measured, while there was a lower RNA amount in CD81 knock-out cells that had been electroporated with the 2A-reporter construct. Importantly, the overall RNA amount in Jc1_mScarlet-2A electroporated cells was $\sim$30$\times$ lower than in Jc1 electroporated ones. All in all, these data suggest that the 2A-reporter constructs are severely impaired in viral replication and hence much slower in reaching comparable levels of viral RNA and proteins compared to the fusion protein constructs or the wild-type.

3.3.2 CD81 is not Involved in Counteraction of IFNα Signaling

With the presumably slower replication in 2A-reporter constructs, the question arose of whether viral counteraction mechanisms against cellular anti viral effects are also slower. For this, the potential impact of CD81 knock-out on viral counteraction needed to be investigated. Control and CD81 knock-out cells were electroporated with Jc1_NS5A-mScarlet viral RNA and treated 48h post EP with IFNα for 24h. As readout for successful IFNα stimulation, the surface expression of tetherin (CD317) was measured because it is a well known IFNα-stimulated gene [439, 440]. Cells that have been stimulated with IFNα displayed a distinct increase in tetherin expression (Figure 7A, Mock). In contrast,

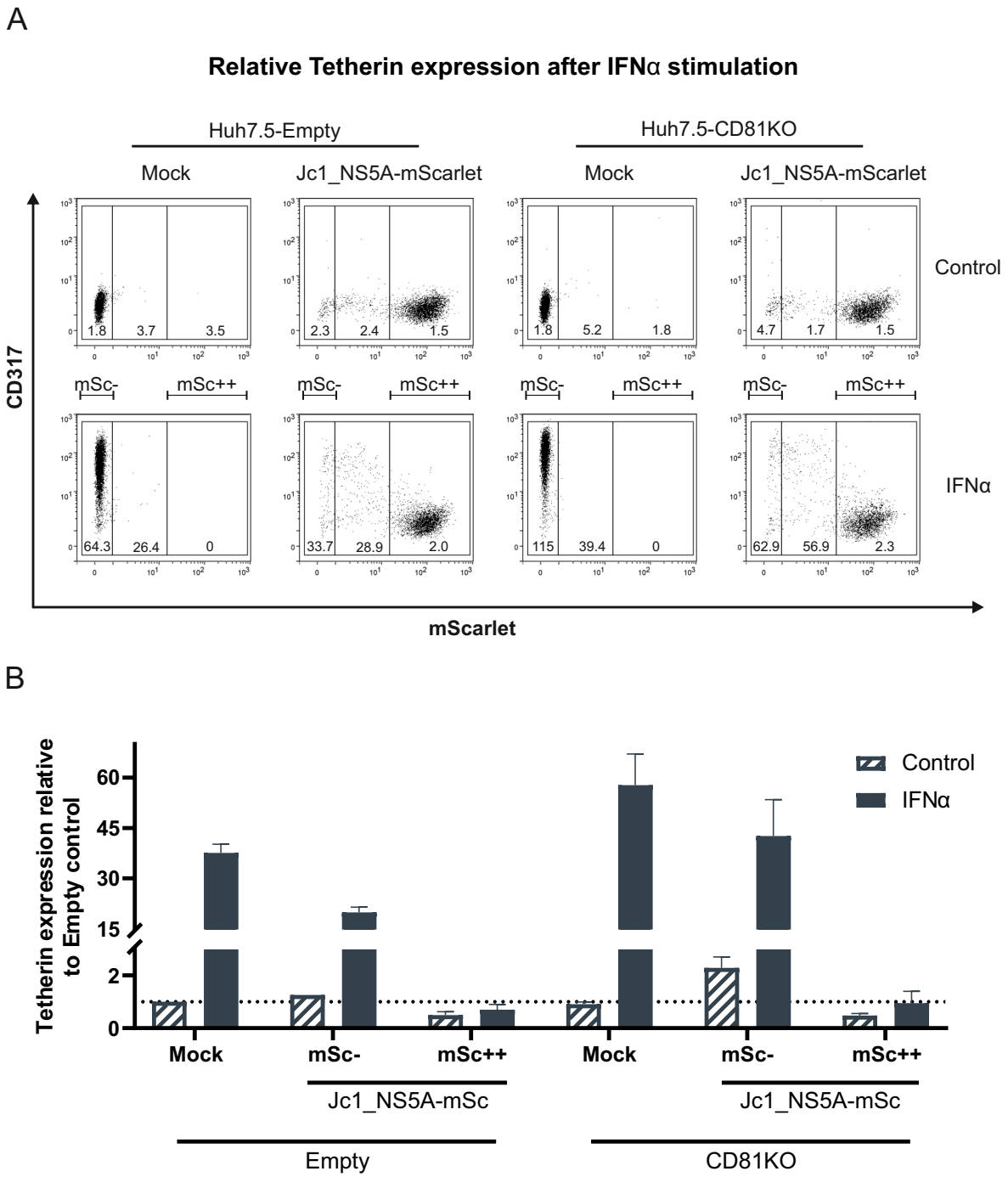

Figure 7: Conteraction of IFNα signaling is not influenced by CD81.
(A) Flow cytometry plots of tetherin (CD317) expression after IFNα treatment in Mock and HCV expressing cells. Huh7.5 control and CD81KO cells were electroporated with Jc1_NS5A-mScarlet. 48h post EP they were treated with IFNα (10 ng/ml) for 24h, stained for surface tetherin and analyzed by flow cytometry. Shown are representative data of 2 independent experiments. Numbers in gates show mean fluorescence intensity of tetherin in the particular gate. **(B)** Relative tetherin expression compared to Mock electroporated, non-treated control cells in bystander (mSc-) and cells that express high levels of NS5A-mScarlet (mSc++). Depicted data from 2 independent experiments. Data points show mean ± SD if not labelled otherwise.

upon cells that have been electroporated with viral RNA, only bystander cells (mSc-) showed an increase in tetherin expression, while cells highly expressing NS5A-mScarlet (mSc++) showed no increase (Figure 7A, Jc1_NS5A-mScarlet). In Summary, expression of viral proteins (indicated by NS5A-mScarlet) completely blocks tetherin induction by IFNα and does not differ in empty and CD81 knock-out cells (Figure 7B). At the same time, IFNα treatment had only a minor effect on the ratio of cells highly expressing NS5A-mScarlet (Figure S2). Although relative tetherin expression after IFNα stimulation seems to be higher in CD81 knock-out cells, this phenotype could not be reproduced in following experiments (data not shown). Thereof, absence of CD81 has no impact on HCV's ability to counteract IFNα induced antiviral response, which results in no effect of IFNα treatment on the amount of cells expressing viral proteins.

3.3.3 Impact of CD81 on Viral Replication Inversely Correlates with Replication Speed

The aim of the following experiment was to clarify whether slower replication of 2A-constructs would make them more susceptible to IFNα treatment. Cells were electroporated with Jc1_mScarlet-2A or Jc1_NS5A-mScarlet and treated with IFNα at indicated time points. 48h after electroporation, the ratio of mScarlet expressing cells and level of tetherin expression was determined via flow cytometry. In general, electroporated cells were more susceptible to IFNα treatment at the early time point (8h) than at the late time point (24h; Figure 8A). As expected, cells electroporated with the 2A-reporter construct were more affected by IFNα treatment, indicated by reduced mScarlet positive cells when compared with not treated ones. IFNα treatment 8h after electroporation hardly allowed any mScarlet to be expressed in the 2A-reporter cells, while NS5A-mScarlet expressing cells were reduced by half when compared with untreated cells. Additionally, IFNα treatment at 16h or 24h post electroporation had little to no effect on NS5A-mScarlet cells but mScarlet expression in 2A-reporter cells was affected negatively. Concurrently, the level of tetherin in mScarlet expressing 2A-reporter cells was not reduced when compared to bystander cells at earlier time points (8h, 16h) and only slightly reduced when IFNα was added 24h post electroporation (Figure 8B, left). In contrast to that, cells expressing NS5A-mScarlet showed reduced tetherin expression already at the earliest time point (8h) of IFNα treatment after electroporation (Figure 8B, right). In summary, 2A-reporter constructs are more affected by IFNα treatment and show less counteraction capacity at early time points after electroporation when compared with a NS5A-fusion protein expressing construct. In this context, the absence of CD81 only had an influence on the ratio of mScarlet positive cells electroporated with a 2A-reporter construct (Figure 8A, left). In conclusion, it can be hypothesized that slower replication of 2A-reporter constructs

makes them more susceptible to antiviral treatment, presumably because it takes them longer to express viral proteins at a sufficient level to counteract antiviral mechanisms.

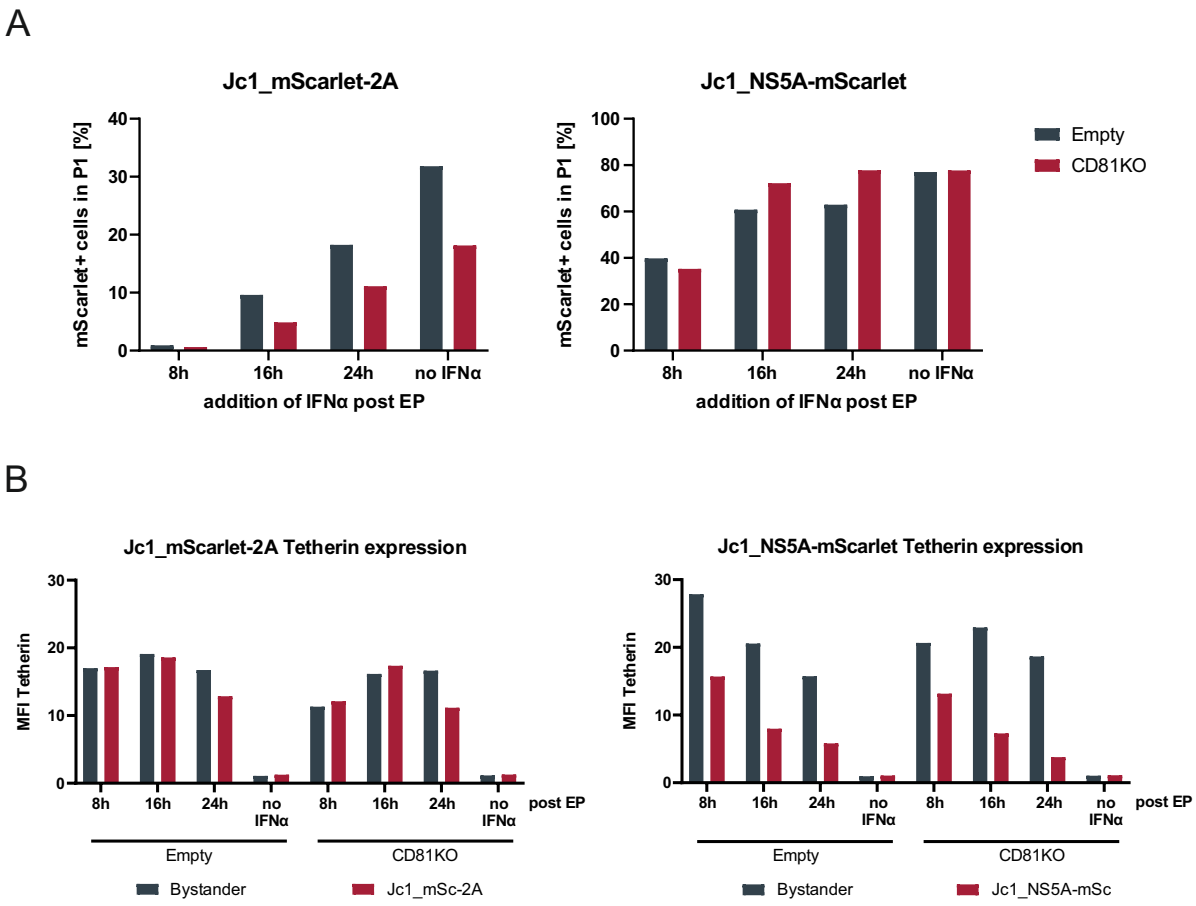

Figure 8: Replication speed defines susceptibility to INFα treatment.
(A) mScarlet or NS5A-mScarlet expressing control or CD81KO cells that were treated with IFNα at different time points. Huh7.5 control and CD81KO cells were electroporated with Jc1_mScarlet-2A or Jc1_NS5A-mScarlet and treated with IFNα at indicated time points after EP. 48h after EP, cells were fixed, stained for tetherin expression and measured by flow cytometry. Depicted data from one experiment. **(B)** Mean fluorescence intensity of tetherin expression of cells from A.

3.4 CD81KO Cells and the Integrated Stress Response

Apart from early activation of innate immunity in CD81 knock-out cells, impaired HCV protein production could also arise from an altered stress response. The integrated stress response (ISR) regulates ER homeostasis and can regulate translational capacity of cells. There are three main signaling pathways that are activated upon ER stress, namely XBP1, PERK and ATF6 (see Integrated Stress Response). In the following section the focus was on the XBP1 response.

3.4.1 Cells Lacking CD81 Have a More Pronounced XBP1 Stress Response

The main characteristic of the XBP1 stress response is splicing of XBP1 mRNA whose unspliced version is constantly expressed to allow for a fast reaction. In brief, ER-membrane resident protein IRE1α recognizes unfolded proteins in the ER lumen and, as consequence, dimerizes and becomes active. Its most prominent function is to splice already present XBP1 mRNA which, in turn, is then translated to the XBP1 transcription factor protein. XBP1 translocates to the nucleus to initiate transcription of genes responsible for ER homeostasis. In the first experiment, a chemical inducer, thapsigargin (TG), was used to artificially activate IRE1α and the subsequent XBP1 splicing. Control and CD81 knock-out cells were treated with TG for 24h and XBP1 splicing was vizualized via PCR and agarose gel electrophoresis (Figure 9A). Upper bands represent the unspliced version of XBP1 mRNA (uXBP1) while lower bands represent spliced XBP1 mRNA (sXBP1). sXBP1 to uXBP1 ratio seemed to be higher in CD81 knock-out cells when treated with TG. To corroborate this result, other potential inducers were also used to initiate XBP1 splicing (Figure 9B). This time, qRT-PCR was conducted and sXBP1 levels were set in relation to the total amount of XBP1 mRNA (tXBP1) to cope with the possibility of differences in the level of uXBP1. It could be confirmed that TG treatment induces higher levels of sXBP1 in CD81 knock-out cells when compared with control cells, while other used chemicals failed to induce XBP1 splicing or did not show a difference between control and CD81 knock-out cells. Additionally, viral proteins, either alone or in combination with one other, were tested to determine whether they induce XBP1 splicing (Figure S3A). Viral proteins core and NS4B alone, or NS4B in combination with core or E1 could induce XBP1 splicing. However, absence of CD81 did not alter this effect (Figure S3B). The next step was to analyze XBP1 splicing in the context of viral replication. Therefore, control and CD81 knock-out cells were electroporated with viral RNA (Jc1) and XBP1 splicing was monitored 24h and 48h post EP (Figure 9C). While only very weak induction of XBP1 splicing was observed at 24h, strong induction was visible at 48h post EP. Although it seemed that there was more total XBP1 mRNA in CD81 knock-out cells, the ratio of sXBP1 to uXBP1 was comparable. To investigate whether additional induction of XBP1 splicing in cells electroporated with viral RNA would have different impacts in control versus CD81 knock-out cells, the following experiment was performed. Control and CD81 knock-out cells were electroporated with viral RNA (Jc1) and 48h post EP were treated with DMSO as control or TG for an additional 24h. Treatment with TG increased XBP1 splicing on top of the already present induction by presence of replicating virus (Figure 9D, left). However, no stronger induction of XBP1 splicing in CD81 knock-out cells could be observed. Regarding HCV replication, TG treatment had neither an effect on viral

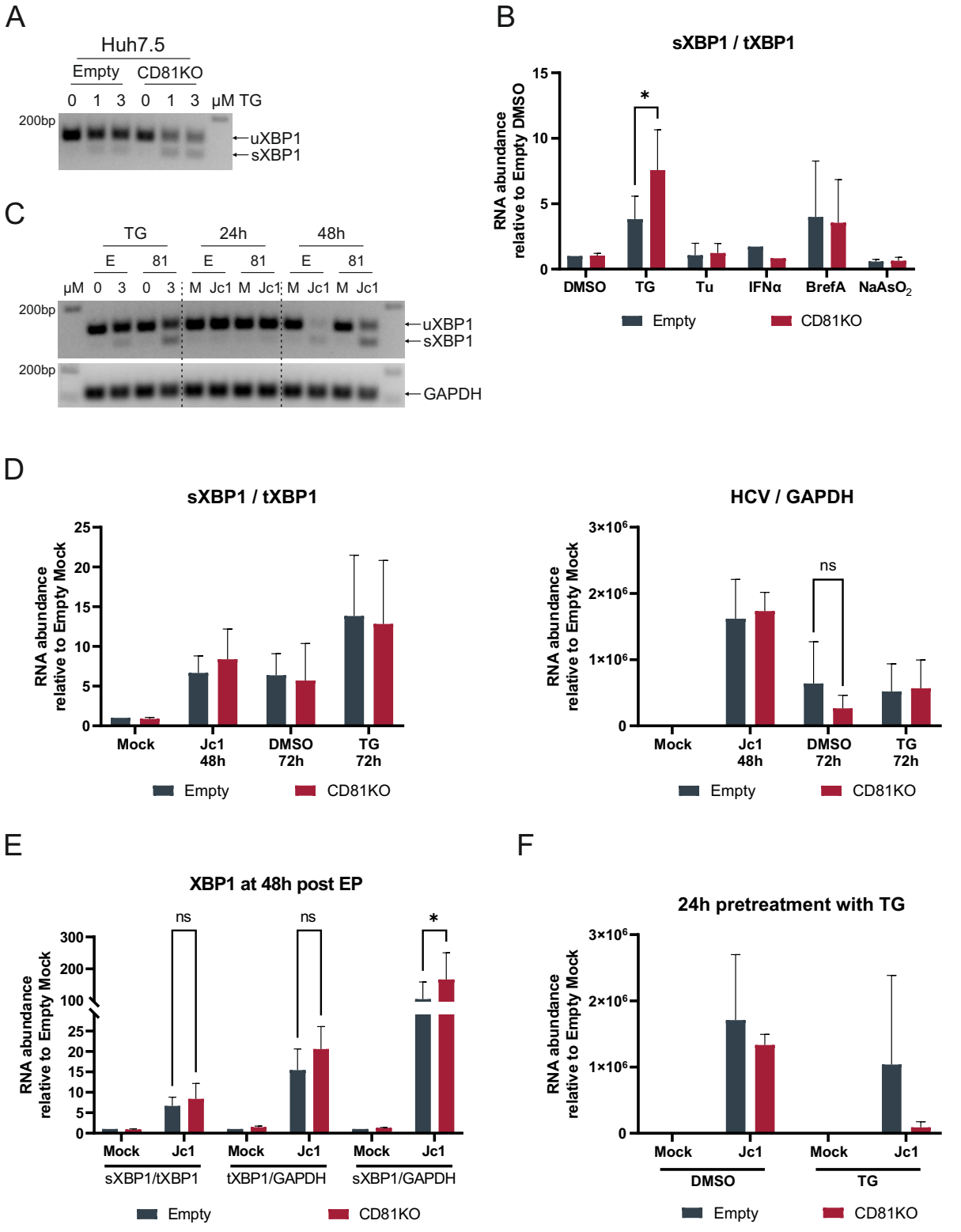

Figure 9: CD81 has a negative effect on the degree of the ER stress response. **(A)** XBP1 splicing impact upon ER stress induction with thapsigargin (TG). Huh7.5 control and CD81KO cells were treated with TG (1 or 3 µM) for 24h, subsequently cellular RNA was extracted, XBP1 mRNA was amplified and run on an agarose gel. Continued on next page.

Figure 9: (continued)
Lower band represents spliced XBP1 (sXBP1) which is 26bp shorter than the unspliced version (uXBP1). **(B)** Quantification of XBP1 splicing by qRT-PCR after treatment with potential chemical inducers. Huh7.5 cells were treated with DMSO (0.06 %), TG (3 µM), Tunicamycin (Tu; 0.8 µg/ml), IFNα (10 ng/ml), Brefeldin A (BrefA; 1×), $NaAsO_2$ (40 µM) for 24h (6h for BrefA), RNA was extracted and XBP1 mRNA was quantified via qRT-PCR. Depicted data show spliced XBP1 (sXBP1) relative to total XBP1 (tXBP1; u + sXBP1) from 1-5 independent experiments. **(C)** XBP1 splicing upon induction by TG or electroporation of Jc1 viral RNA. Huh7.5 control and CD81KO cells were treated with TG (3 µM) for 24h or electroporated with Jc1 viral RNA, and RNA was extracted 24h and 48h post EP. XBP1 and GAPDH mRNA was amplified via PCR and run on an agarose gel. Depicted is a representative dataset. **(D)** Quantified spliced XBP1 and HCV RNA at different time points with and without additional TG treatment. Huh7.5 cells were electroporated with Jc1 viral RNA. At 48h post EP, RNA of some samples was extracted and others were treated with either DMSO (0.06 %) or TG (3 µM) for additional 24h before RNA was also extracted. sXBP1, tXBP1, HCV, and GAPDH RNA was quantified via qRT-PCR. Depicted data are from 3 independent experiments **(E)** Comparison of sXBP1, tXBP1 and GAPDH between Mock and Jc1 electroporated cells at 48h post EP from experiments shown in D. **(F)** Viral RNA amount in cells pretreated with TG. Huh7.5 control and CD81KO cells were pretreated with DMSO (0.06 %) or TG (3 µM) for 24h and subsequently electroporated without (Mock) or viral RNA (Jc1). 48h after EP RNA was extracted and viral RNA amount was determined via qRT-PCR. Depicted are data from 3 independent experiments. Data points show mean ± SD if not mentioned otherwise. Significance was tested using two-way ANOVA with Sidak's multiple comparisons test. ns = not significant; * $p \leq 0.05$

RNA levels compared to the DMSO control, nor a different effect on CD81 knock-out cells compared to control cells (Figure 9D, right). Notably, viral RNA levels were decreased at 72h compared to 48h post EP, independent of TG treatment or CD81 presence. Given this observation and the one from Figure 9C, which indicated more XBP1 mRNA in Jc1 expressing cells at 48h post EP, a closer look was taken at this time point. The analysis of sXBP1 and tXBP1 in relation to the reference gene GAPDH, as well as to each other, revealed a slight trend of higher sXBP1 and tXBP1 levels in CD81 knock-out cells (Figure 9E). Moreover, when analyzing sXBP1 in relation to GAPDH, there is indeed significantly more spliced XBP1 in CD81 knock out cells that express Jc1 viral RNA compared to in control cells ($p = 0.0182$). However, this seems to be driven mainly by higher total XBP1 levels rather than higher splicing activity. Following up on this, it was hypothesized that more ER stress and hence, more XBP1 splicing, suppresses HCV replication at an early time point. Hence, control and CD81 knock-out cells were treated with TG for 24h prior to electroporation with viral RNA (Jc1). 48h after EP, viral RNA levels were measured and showed a higher impact of TG pretreatment on cells lacking CD81 (Figure 9F). Although TG pretreated cells in general show lower viral RNA levels, it was barely detectable in CD81 knock-out cells. To give a résumé, CD81 negatively impacts the ER stress response in the form of reduced XBP1 mRNA splicing when present. It was also shown that cells lacking CD81 have a slightly increased level of sXBP1 and

tXBP1 mRNA 48h after EP with viral RNA (Jc1). Finally, induction of ER stress and XBP1 mRNA splicing before electroporation resulted in reduced viral RNA levels in total, especially in CD81 knock-out cells, pointing to the involvement of CD81 in early steps of HCV replication onset.

3.4.2 HCV Interacts with STAU1 but not with Stress Granules

Another arm of the Integrated Stress Response is the PERK pathway. Eukaryotic translation initiation factor 2α kinase 3 (herein referred as PERK) is an ER membrane resident protein which, like IRE1α, senses unfolded proteins which, in turn, lead to its dimerization and phosphorylation [351]. Active PERK's most prominent function is to phosphorylate eukaryotic translation initiation factor 2α (eIF2α). When phosphorylated, eIF2α's function transitions from a cofactor to a strong inhibitor of translation. So, active PERK leads to a near complete shutdown of cellular protein biosynthesis [351]. As this process happens relatively quickly, mRNAs that were meant to be translated accumulate in the cytoplasm in so called stress granules (SGs), which are aggregates of mRNA, and certain proteins, one of these being G3BP1 (Ras GTPase-activating protein-binding protein) [335]. When investigating the potential connection of the integrated stress response, HCV, and CD81, it was of interest whether G3BP1 directly interacts with viral proteins. However, a flow cytometry-based FRET assay did not provide any indication of G3BP1 interaction with viral proteins (Figure S4). On the other hand, some viral proteins were revealed to interact with STAU1 (Double-stranded RNA-binding protein Staufen homolog 1), a protein associated with stress granule disassembly [441]. Figure 10A indicates that viral protein NS4A interacts strongly with STAU1, while E1, p7, and NS5B show weaker signals. Subsequently, the interaction of these four proteins with STAU1 was tested again in the absence of CD81. Interestingly, the interaction between E1 and NS5B with STAU1 was increased in CD81 knock-out cells while that between p7 and NS4A was unaltered (Figure 10B). With STAU1 involved in stress granule disassembly, and viral proteins interacting with it, a general influence of CD81 knock-out on stress granule formation was hypothesized. However, formation of stress granules when induced by oxidative stress through treatment with sodium arsenite ($NaAsO_2$) was not altered in cells lacking CD81 (Figure S5A). Likewise, no correlation of eIF2α phosphorylation with CD81 levels could be observed. Figure S5B shows higher eIF2α phosphorylation level in CD81 knock-out cells when stimulated with TG, but also a higher level in total eIF2α. In the same experiment, no eIF2α was detected in CD81 knock-out cells 48h after electroporation while core was expressed. Together, detection of eIF2α phosphorylation was ambiguous with no conclusions drawn. It can be summarized, that stress granules are presumably not involved in the process through which CD81 influences HCV replication. However, as interaction between viral proteins E1

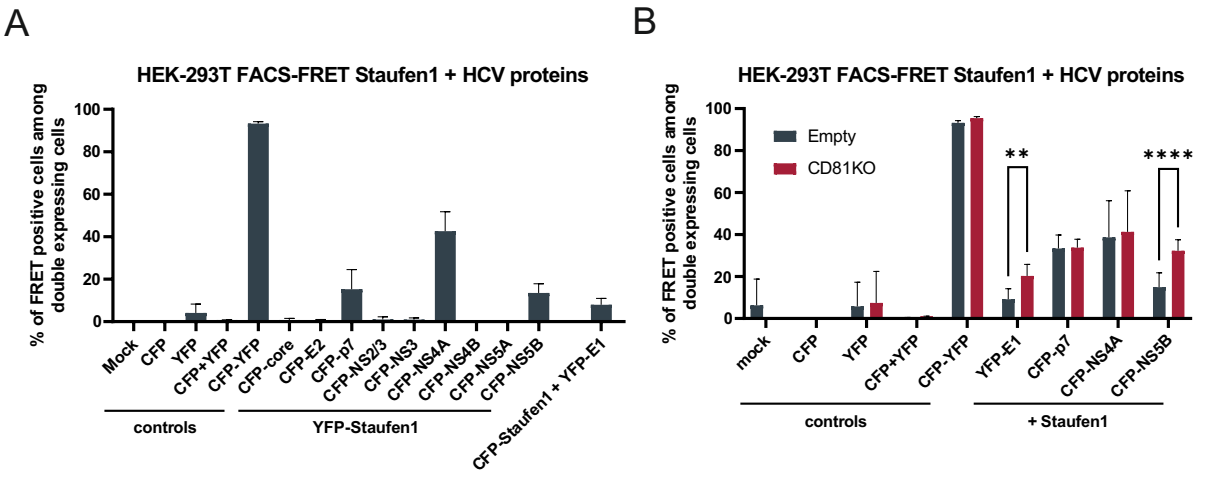

Figure 10: Several HCV proteins interact with STAU1, which is in part influenced by CD81.
(A) Interaction of HCV proteins with STAU1 measured by flow cytometry-based FRET. HEK-293T cells were transfected with pairs of plasmids encoding a CFP-tagged viral protein and YFP-tagged STAU1 (the other way round for E1). 24h post transfection, cells were harvested and FRET signals were measured via flow cytometry. Depicted are data from 3 independent experiments. **(B)** Interaction of HCV proteins with STAU1 in absence and presence of CD81. HEK-293T cells were transfected and measured as before. Depicted are data from 4 independent experiments. Data points show mean ± SD unless labelled otherwise. Significance was tested using two-way ANOVA with Sidak's multiple comparisons test. ns = not significant; * $p \leq 0.05$; ** $p \leq 0.01$; *** $p \leq 0.001$; **** $p < 0.0001$.

and NS5B was increased in CD81 knock-out cells, and given the fact that it binds dsRNA, other functions of STAU1 could be the cause for these results.

3.5 Higher Activity of NFκB in CD81KO Cells

Investigation of the integrated stress response related to HCV provided some indication of how CD81 could be involved in post-entry processes. However, there are still many open questions. More recently, the interconnection of the integrated stress response with the NFκB pathway was uncovered. Both pathways together play a major role in cellular homeostasis and in response to pathological conditions like infections or cancer development [442]. With this connection and the already described interrelation of HCV and the NFκB pathway, a potential involvement of CD81 in this pathway was investigated in the following section. Data presented in Figure 11 - Figure 14, with exception of Figure 13C, were obtained by Mona Eisele who did a Bachelor's thesis under the supervision of Maximilian Bunz [443].

3.5.1 CD81 Suppresses IKKβ- and PMA-mediated NFκB Activation

To execute their transcriptional activity, NFκB subunits need to translocate to the nucleus. In non-stress conditions they are retained in the cytoplasm and are only able to translocate if the complex that they form with a specific inhibitory protein (IκB) disassembles. In this respect, phosphorylation of IκB by the IKK (IκB kinase) complex is the most crucial step leading to its proteasomal degradation. The IKK complex, in turn, can be activated by a plethora of cellular pathways, ranging from growth factor receptors to DNA damage repair. Receptors which recognize foreign molecules, like parts of a bacterial cell wall or viral RNA, are also able to induce NFκB activity via the IKK complex. In first experiments, it was tested whether signaling of RIG-I (Antiviral innate immune response receptor RIG-I) and MAVS (Mitochondrial antiviral-signaling protein), which recognize dsRNA in the cytoplasm and induce an antiviral response, was influenced by the absence or overexpression of CD81. A firelfy luciferase-reporter was used to measure transcriptional activity of NFκB. Therefore, HEK-293T cells were transfected with the reporter plasmid and different inducer molecules. Absence of CD81 had no influence on transcriptional activity of NFκB when induced by expression of IKKβ (subunit of IKK complex), MAVS or RIG-I (Figure 11A). However, overexpression of CD81 via transfection of an additional plasmid led to a lower NFκB activation with all three tested inducers (Figure 11B). As transfection of plasmids encoding inducer proteins is a quite artificial system, chemical inducers were used to reflect less artificial conditions. HEK-293T control and CD81 knock-out cells were transfected with the NFκB luciferase reporter and treated with different chemicals, except PolyI:C (polyinosinic:polycytidylic acid), which was transfected. Figure 11C shows that only PMA (phorbol 12-myristate 13-acetate), tumor necrosis factor alpha (TNFα) and PolyI:C were able to induce NFκB activity. Within those, NFκB activity displayed significantly higher activity in CD81 knock-out cells after PMA stimulation.

Aiming for further insights into this phenomenon, HEK-293T and HeLa cells, control and CD81 knock-out cells, respectively, were transfected with the NFκB luciferase reporter and additionally with a plasmid encoding CD81 or an empty control. This was meant to result in different expression levels of CD81, assuming that CD81 knock-out cells transfected with the control plasmid have the lowest expression, while control cells transfected with the CD81 encoding plasmid have the highest. Figure 12A shows NFκB activation either mediated by transfection of IKKβ or PMA. In HEK-293T cells, there is a clear trend with high CD81 expression levels correlating with lower NFκB activity. This effect is less distinct in HeLa cells, while maintaining the overall trend, and inconclusive in Huh7.5 cells (Figure 12A and Figure S6A). It is noted that actual CD81 levels have not been determined, limiting the interpretability of the results. Given that PMA was the only chemical tested

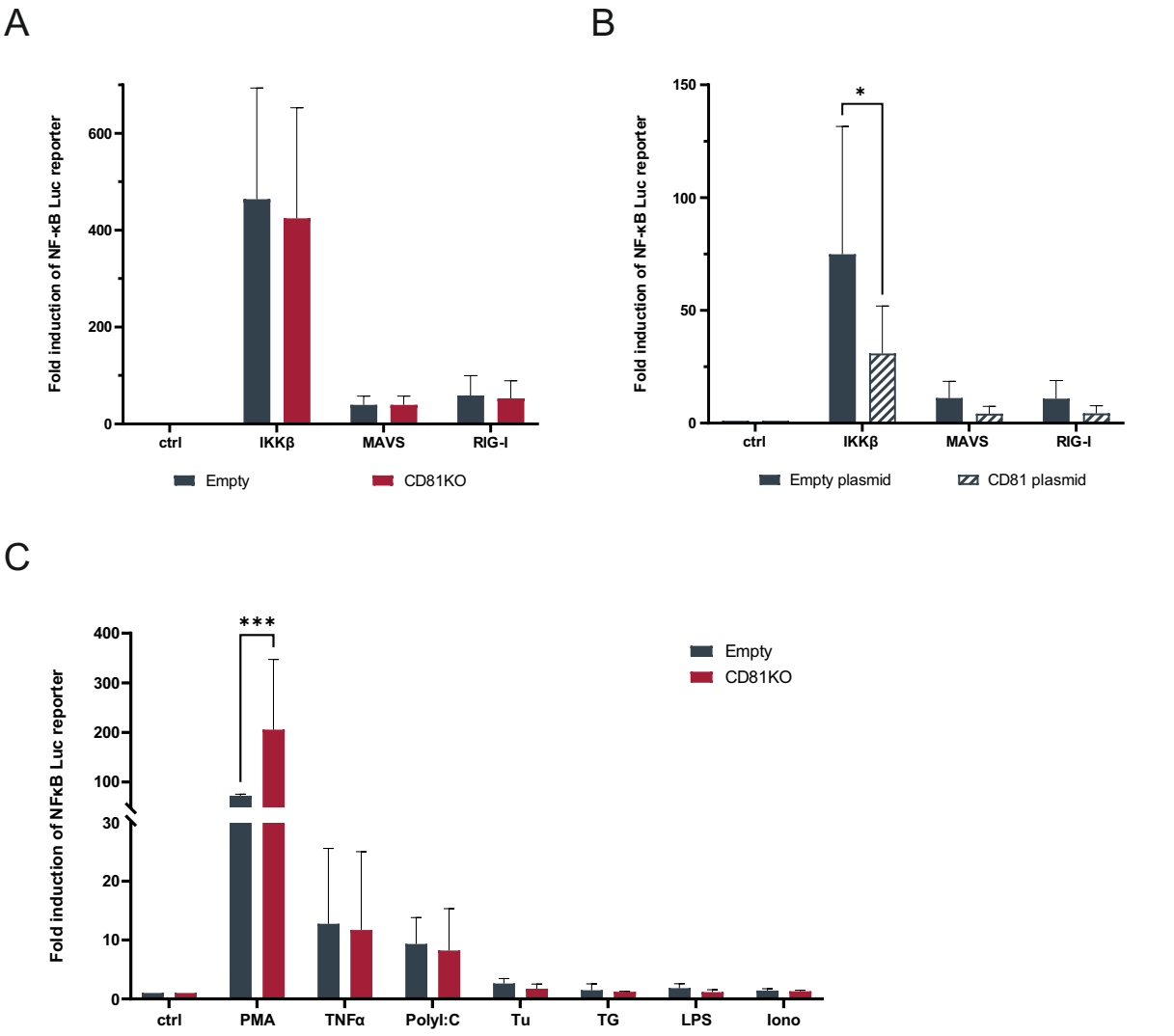

Figure 11: NFκB transcriptional activity mediated by several inducers.
(A) Induction of NFκB activity by innate immune sensors in control and CD81KO cells. HEK-293T control and CD81KO cells were transfected with plasmids encoding a firefly luciferase-reporter for NFκB, gaussia-luciferase as transfection control and an inducer (IKKβ, MAVS or RIG-I). 24h after transfection, luciferase signals were measured in the supernatant (gaussia) and the cell lysate (firefly). Depicted are data normalized to no inducer from 4-7 independent experiments. **(B)** Induction of NFκB activity by innate immune sensors in control and cells overexpressing CD81. HEK-293T cells were transfected and measured as before, with an additional plasmid encoding CD81. Depicted are data from 4 independent experiments. **(C)** Induction of NFκB activity by chemical stimuli in control and CD81KO cells. HEK-293T control and CD81KO cells were transfected and measured as in A. 4h after transfection, treatment with PMA (10 ng/ml), TNFα (10 ng/ml), Tu (1 µg/ml), TG (3 µM), LPS (100 ng/ml) and Iono (0.25 µM) started, except for PolyI:C (5 µg/ml) which was transfected together with plasmids. Depicted data are from 3 independent experiments. Data points show mean ± SD unless otherwise labelled. Significance was tested using two-way ANOVA with Sidak's multiple comparisons test. ns = not significant; * $p \leq 0.05$; ** $p \leq 0.01$; *** $p \leq 0.001$.

whose stimulation led to higher NFκB activity in CD81 knock-out cells (Figure 11C), and that the latter could be highly reduced by CD81 overexpression (Figure 12A, right), a closer look was taken at mechanisms of PMA-mediated NFκB activation. PMA activates protein kinase C (PKC) by mimicking diacylglycerol (DAG), which is a prerequisite (together with Ca^{2+}, depending on the subfamily) for PKC activity. In turn, PKCs can phosphorylate and activate the IKK complex resulting in NFκB activation.

NFκB luciferase-reporter transfected HEK-293T and HeLa cells were treated with either PMA or ionomycin (Iono), or both. Ionomycin increases intracellular Ca^{2+} levels. Figure 12B shows either CD81 knock-out cells transfected with an empty plasmid, or control cells with a CD81 encoding plasmid. Two things became evident. First, ionomycin treatment seemed not to induce NFκB activity, neither alone nor as an additional effect in combination with PMA. Second, a high level of CD81 reduced NFκB activity mediated by PMA or PMA and ionomycin together. Although this was true for HEK-293T cells, induction of NFκB was not strong enough in Huh7.5 cells to draw any conclusion (Figure S6B). To get an idea of whether CD81's negative effect on NFκB signaling might also play a role in connection with HCV, HEK-293T cells were transfected with the NFκB luciferase-reporter and YFP-tagged core or YFP alone as control. Additionally, cells were treated with TNFα before measurement of luciferase activity. While control cells treated either with TNFα or transfected with core showed a clear induction of NFκB, the combination of both had not only an additive but a synergistic effect on NFκB activity (Figure 12C). Interestingly, the overexpression of CD81 not only reduced the induction by TNFα or core alone, but also abrogated the synergistic effect of the combined treatment. Together, high levels of CD81 reduced IKKβ- and PMA-mediated NFκB activity in HEK-293T and HeLa cells. Its absence in HEK-293T cells increased PMA-mediated NFκB activity. On top of that, the synergistic effect of core expression and TNFα stimulation on NFκB activity was nearly eliminated in cells overexpressing CD81. It can be concluded that CD81 has a negative effect on NFκB activation.

3.5.2 NFκB Transcriptional Activity is Higher in CD81KO Cells

As shown previously, CD81 has a negative role in NFκB activation. The next step was, trying to decipher how control and CD81 knock-out cells differ in the execution of NFκB activation. Therefore, the following experiments should clarify whether different kinetics of nuclear translocation of p65 could explain the observed phenotype. Huh7.5 cells were stimulated for different time periods with TNFα or PMA and the p65 amount in the nuclei was quantified. Representative images of cells show a clear nuclear translocation

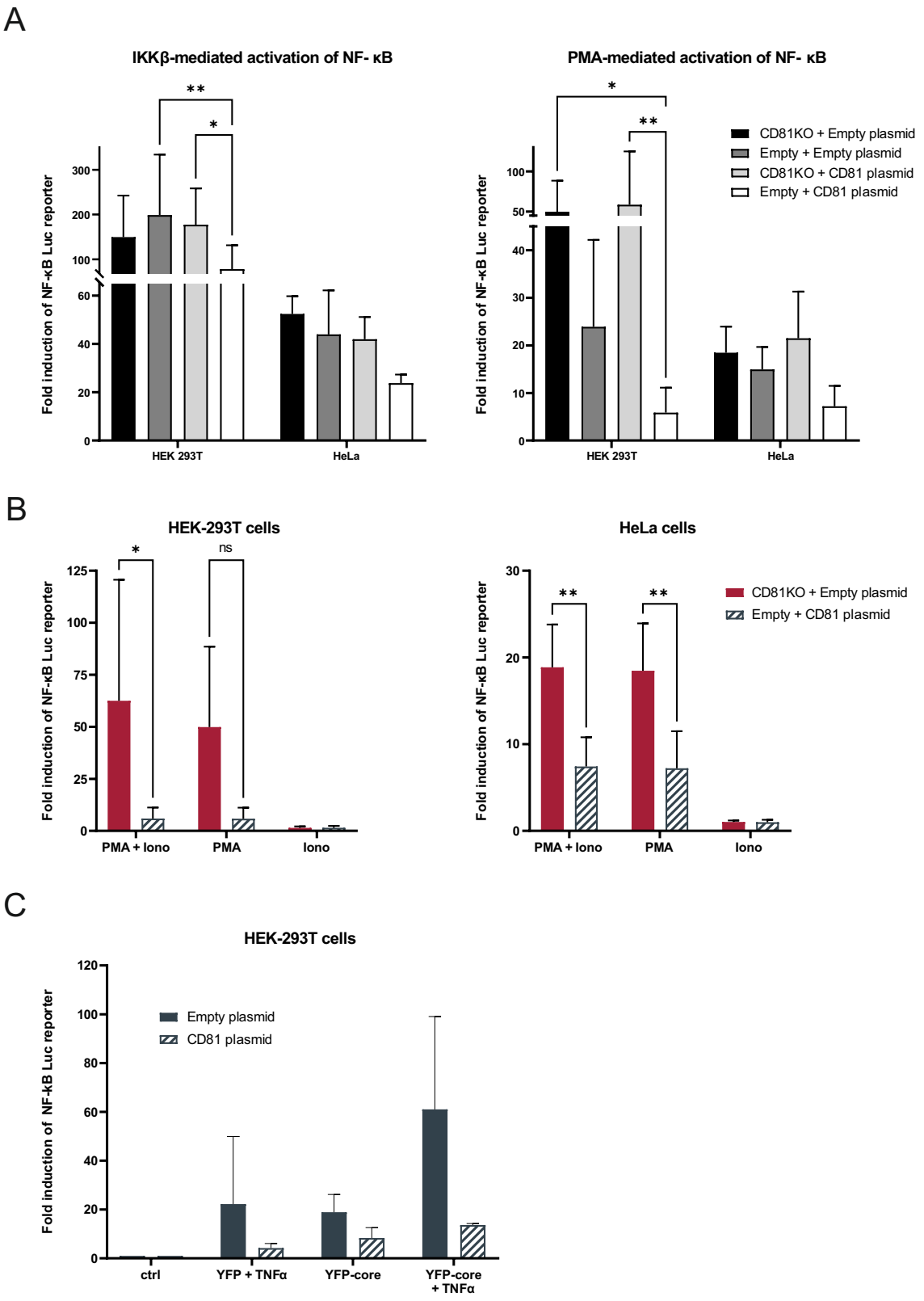

Figure 12: Negative effect of CD81 on NFκB transcriptional activity.
Continued on next page.

Figure 12: (continued)
(A) Influence of CD81 on NFκB activity in HEK-293T and HeLa cells. HEK-293T or HeLa control and CD81KO cells were transfected with plasmids encoding a firefly luciferase-reporter for NFκB and gaussia-luciferase as transfection control. NFκB activity was induced either by simultaneous transfection of IKKβ or treatment with PMA (10 ng/ml) from 4h post transfection until harvest. Additionally, cells were either transfected with a plasmid encoding CD81 or an empty control plasmid. 24h after transfection, luciferase signals were measured in the supernatant (gaussia) and the cell lysate (firefly). Depicted are data from 4 independent experiments. **(B)** Influence of CD81 on PMA-mediated activity of NFκB. HEK-293T or HeLa control and CD81KO cells were transfected as in A, except that control cells were additionally transfected with the plasmid encoding CD81 and CD81KO cells with the empty control plasmid. 4h post transfection cells were treated with PMA (10 ng/ml), Iono (0.25 µM) or both. Depicted are data from 4 independent experiments. **(C)** Induction of NFκB activity by HCV core and TNFα. HEK-293T cells were transfected with NFκB firefly luciferase-reporter, gaussia luciferase and YFP-tagged HCV core or YFP alone as control. In addition, cells were transfected with either a CD81-encoding plasmid or an empty control plasmid. 4h post transfection, some cells were treated with TNFα (10 ng/ml). Measurement was performed as in A. Depicted data are from 2 independent experiments. Data points show mean ± SD unless labelled otherwise. Significance was tested using two-way ANOVA with Sidak's multiple comparisons test. ns = not significant; * $p \leq 0.05$; ** $p \leq 0.01$.

of p65 in PMA (Figure 13A), and TNFα stimulated cells, with translocation being less prominent for TNFα (Figure S7). Quantification revealed a higher nuclear p65 signal in PMA stimulated CD81 knock-out compared to control cells (Figure 13B). However, both, control and CD81 knock-out cells, showed clear nuclear translocation of p65 already after 30min, with the only difference being that the signal increased further in the knock-out cells. As different speeds of nuclear translocation of p65 could not be observed, the questions arose of whether the underlying effect takes action one step before. Ahead of its translocation, p65 can become phosphorylated, which happens at earlier time points after stimulation than translocation. Therefore, Huh7.5 control and CD81 knock-out cells were stimulated with TNFα for 5min or 10min and subsequently prepared for SDS-PAGE and western blot analysis. Figure 13C shows higher levels of both phosphorylated, and more surprisingly, total p65 in CD81 knock-out cells. TNFα seemed not to be a good stimulus for p65 translocation (Figure 13B and Figure S7), so no influence of p65 phosphorylation status could be expected. However, higher p65 levels in CD81 knock-out cells would explain higher p65 nuclear signal and, hence, higher NFκB activity.

Finally, it was desirable to clarify whether the observed higher nuclear abundance of p65 in CD81 knock-out cells leads to higher gene expression. To do so, mRNA levels of TNFα, a target gene of NFκB, were checked. HEK-293T or Huh7.5 control and CD81 knock-out cells were stimulated with TNFα and PMA for different time periods before their cellular RNA was extracted and TNFα mRNA levels quantified via qRT-PCR. For HEK-293T cells, TNFα stimulation seemed not to be sufficient to induce TNFα mRNA transcription,

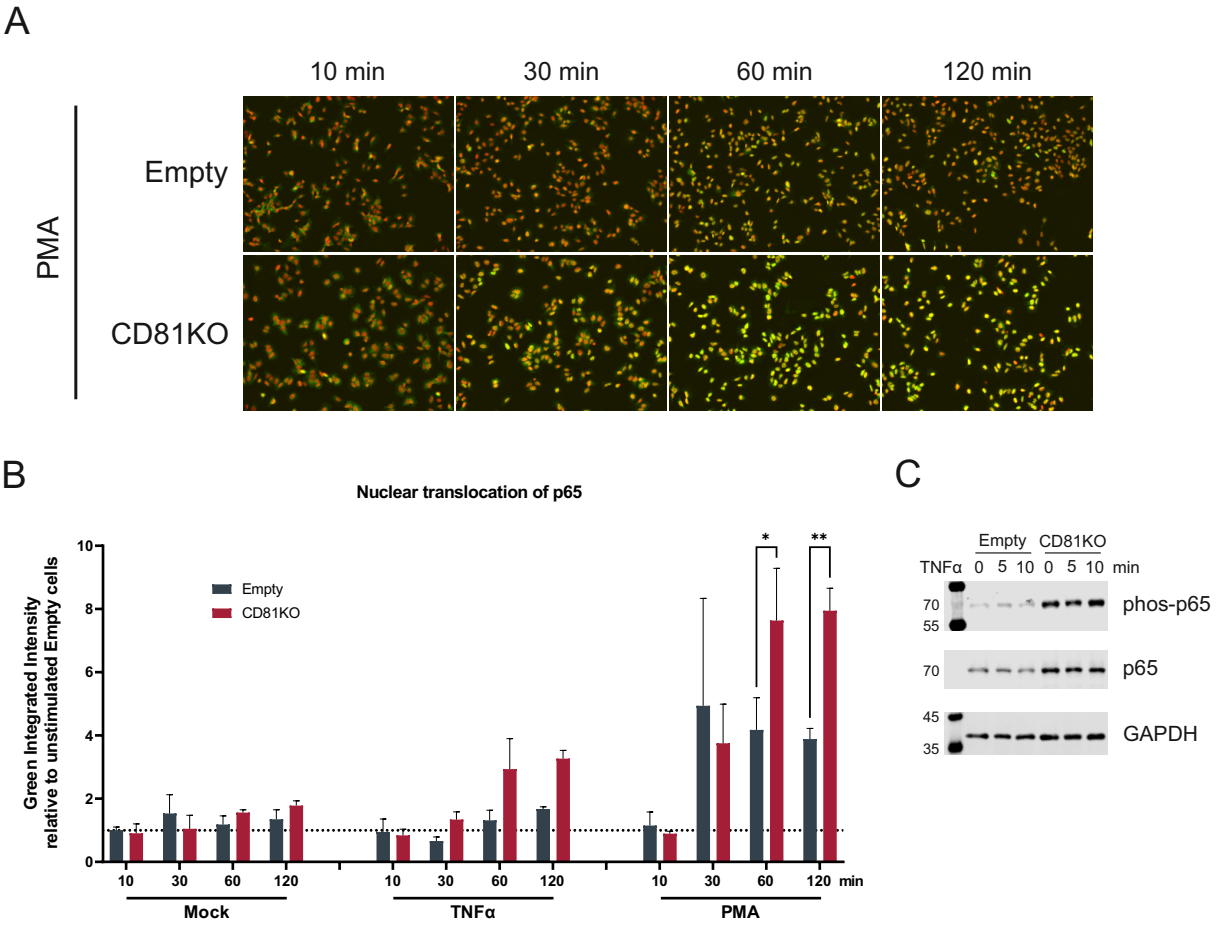

Figure 13: Nuclear translocation of p65 after PMA or TNFα stimulation.
(A) Representative images of p65 nuclear translocation after PMA stimulation. Huh7.5 control and CD81KO cells were seeded in a 96-well format and treated (or not) for the indicated time periods with PMA (100 ng/ml) or TNFα (10 ng/ml; see Figure S7). Then, cells were permeabilized and stained for endogenous p65 using antibodies and nuclear DNA using a red fluorescent dye. Images were taken using the IncuCyte® S3 Live-Cell Analysis System with a 20× objective. Shown are representative images from 3 independent experiments. **(B)** Quantification of nuclear translocation of p65 after PMA or TNFα stimulation. Shown is the integrated green fluorescence intensity (representing p65) within the overlapping area of green and red (representing nuclear DNA) relative to unstimulated cells, from 3 independent experiments. Data points show mean ± SEM. **(C)** Expression and phosphorylation of p65 in Huh7.5 cells after TNFα stimulation. Huh7.5 control and CD81KO cells were treated with TNFα for indicated time periods and subsequently lysed and prepared for SDS-PAGE and western blot. Shown is 1 representative experiment. Significance was tested using two-way ANOVA with Sidak's multiple comparisons test. ns = not significant; * $p \leq 0.05$; ** $p \leq 0.01$.

while PMA stimulation led to high levels of TNFα mRNA (Figure 14A). Notably, detected TNFα mRNA levels were strongly increased in PMA-stimulated CD81 knock-out cells when compared to control cells. In Huh7.5 cells, TNFα stimulation led to a slight increase in TNFα mRNA levels, but did not show differences between control and CD81 knock-out cells (Figure 14B). PMA stimulation however, increased TNFα mRNA levels to a greater

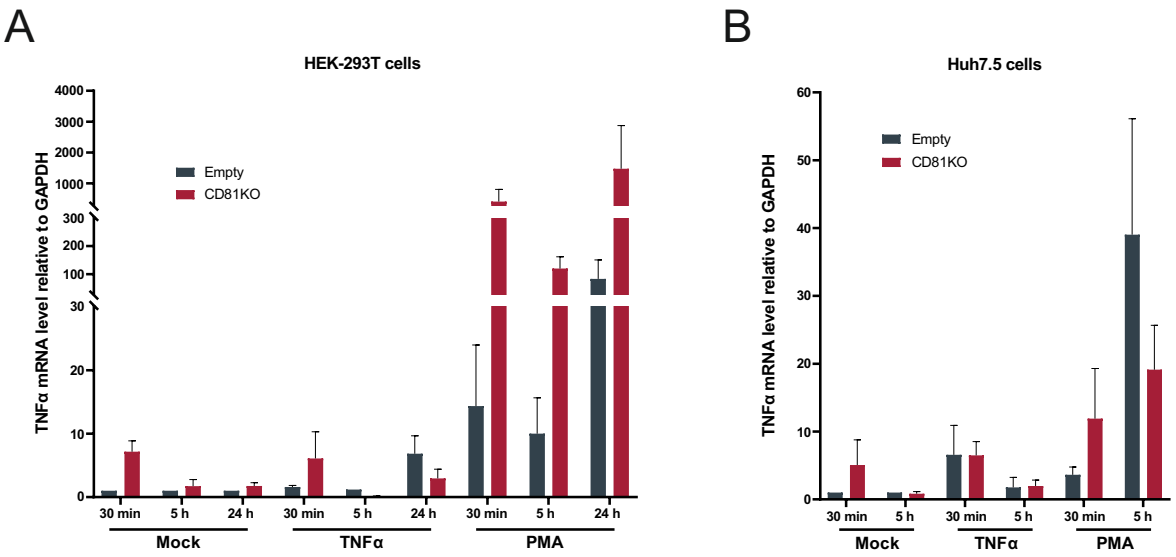

Figure 14: NFκB-mediated gene expression after PMA or TNFα stimulation. **(A)** TNFα mRNA levels in HEK-293T cells after stimulation. HEK-293T control or CD81KO cells were treated for indicated time periods with TNFα (10 ng/ml) or PMA (10 ng/ml). Subsequently, cellular RNA was extracted and TNFα mRNA was quantified via qRT-PCR. Shown is mean ± SEM relative to GAPDH and normalized to Mock treated control cells for each time point, from 3 independent experiments. **(B)** TNFα mRNA levels in Huh7.5 cells after stimulation. Huh7.5 control or CD81KO cells were treated for indicated time periods with TNFα (10 ng/ml) or PMA (10 ng/ml). Subsequently, cellular RNA was extracted and TNFα mRNA was quantified via qRT-PCR. Shown is mean ± SEM relative to GAPDH and normalized to Mock treated control cells for each time point, from 3 independent experiments.

extent than TNFα, but no clear pattern of TNFα mRNA levels and CD81 knock-out could be observed. While TNFα mRNA levels were higher in CD81 knock-out cells 30min after stimulation, the opposite result was detected 5h post stimulation. In summary, it is stated that there are higher levels of nuclear p65 in cells lacking CD81 which leads, in part, to a higher target gene transcription. A possible reason might be a higher abundance of p65 in general in those cells. It remains unclear how CD81 could be connected to overall p65 levels in cells.

4 Discussion

4.1 Transcriptional Downregulation of CD81

Given that CD63 and CD81 have been shown to be downregulated from the surface of replicating cells, an approach to decipher the associated functional importance was developed (Figure S1) [416, 436]. It was shown that surface expression of CD9, CD63 and CD81 was altered in cells expressing a full genome construct and that NS5A seems to be the viral protein mediating this effect (Figure 1A and B). However, downregulation of total protein levels seemed to be less prominent than downregulation of surface levels. Recently, an upregulation of CD63 and its potential role in virus release has been described [421]. But, as upregulation of CD63 was observed in the context of release, it is possible that this regulation was not detectable as early as 72h post EP. Additionally, the Jc1_NS5A-GFP construct used in this thesis seems to be impaired in the release of infectious particles, allowing for the possibility that regulations towards viral release are not fully active [424]. As well, only four viral proteins were tested in the context of this thesis and these may act in concert with each other or cellular proteins, which would result in a different regulation of CD63. Subsequently, a closer look was taken at the mechanism of the proposed downregulation of CD81. Different reporter and fusion protein constructs were able to transiently downregulate total CD81 protein levels with the highest effect at 48h post EP (Figure 2A and B). The recovery of CD81 levels to baseline correlates with higher cytotoxicity over time, so it must be clarified whether the recovery is due to cell death mechanisms. Figure 2C suggests, that lower levels of CD81 were not caused by protein degradation via proteasomal or lysosomal pathways. Further possibilities include transcriptional regulation or impaired binding of the CD81 antibody. The latter was shown for binding of CD19 to CD81, where CD81 could not be bound by a commercially available antibody (clone 5A6) when associated with CD19 [444]. Another possibility would be inaccessibility of the CD81 epitope because of its integration in the membranous web and insufficient permeabilization. Nevertheless, transcriptional regulation seems to be the mode of action as evidenced in Figure 2D. However, only the time point of 48h is represented, leaving the question of transient or stable downregulation unanswered. Interestingly, Zheng *et al.* showed CD81 downregulation on the transcriptional level in cells stably expressing the viral protein NS4B [417]. These results are in line with the observation that cells stably replicating sub-genomic replicons lower the levels of CD81 [416]. In contrast, Tscherne *et al.* could not find evidence for HCV-induced regulation of CD81 levels, although they found lower CD81 levels in sub-genomic replicon cells [418].

Their conclusion was that HCV selects for cells with lower CD81 expression levels to prevent superinfection, i.e. infection of an already infected cell. Under this strategy, used by many viruses and called superinfection exclusion, the established infection interferes with a possible new infection, for example, by downmodulation of the entry receptor [445–448]. Even so, not all studies have detected lower levels of CD81 and concluded that a later step in the HCV life cycle mediates superinfection exclusion, although the reduced infectivity of the Jc1_NS5A-GFP construct might have influenced the results [424]. Still, it is not clear whether, actively regulated or not, superinfection exclusion is the reason for potentially lower CD81 levels in HCV replicating cells. Analyzing patient samples for CD81 mRNA and protein expression would add important information to the context. This phenomenon of downmodulation and its potential purposes will be further discussed in the following sections.

4.2 CD81 Knock-out Characterization

Knock-out cell lines were created to evaluate functional involvement of the tetraspanins. Figure 3A (left panel) shows that knock-out of CD81 has a negative effect on replication of a luciferase reporter construct, whereas knock-out of CD9 and CD63 does not. The supernatant of those samples was used to infect naive Huh7.5 cells but the results displayed the same pattern, hence no effect on release was assumed (data not shown). Again, this seems to contradict results obtained by Gallard *et al.* who observed reduced release in CD63 silenced cells [421]. The fact that replication could be rescued in cells not expressing CD81 by stable transfection verifies the functional involvement of CD81 in HCV replication (Figure 3A, right panel). Interestingly, the CD81 cholesterol binding mutant E219Q is not able to rescue replication to the same extent. In addition, Figure 3B shows a reduced interaction of HCV core, E1 and NS5A with mutated CD81. It has been shown that binding of cholesterol affects the conformation of CD81 and thereby the interaction with binding partners [399, 403]. In addition, cholesterol binding of CD81 was revealed to be important for HCV entry [402, 423]. Hence, it is plausible that the cholesterol binding mutant E219Q affects HCV replication, although Banse *et al.* could not see an effect with sub-genomic replicons [423]. However, as sub-genomic replicons lack structural proteins and cholesterol binding seems to be important for the interaction of CD81 with core and E1, this might be an explanation for different results. Unexpectedly, the screen of intra-viral interactions in CD81 knock-out cells did not reveal any differences (Figure 3C). Even so, it is possible that it is not the interaction of two proteins but instead that of complexes of higher order, that is influenced by CD81's absence. Investigation of this possibility requires different screening methodologies, although three color FRET experiments are possible [449–451].

When checking for altered organelle distribution, markers of autophagosomes were included, due to the special role of autophagy in the HCV life cycle (see Translation and Replication) [282]. Confocal microscopy images revealed no difference in the distribution of the ER (ER-3), the Golgi (GalT), early (ATG5, ATG12) or late autophagosomes (LC-3B; Figure 4A). The same was true for viral proteins NS4B and NS5A (Figure 4B). Apparently, CD81 is not involved in organelle positioning and also not in the distribution of NS4B or NS5A alone. Similarly, the cellular localization of E2 and NS5A, when examined as fusion proteins in a whole genome context, was not modified either (Figure 4C). Coming to cholesterol, differences in cellular distribution could be observed in cells expressing viral constructs, but no alteration between control and CD81 knock-out cells was apparent (Figure 4D). Although E2 and NS5A were shown to interact with CD81 in Figure 3B, their distribution stayed similar when it was absent. However, as NS4B and NS5A act in close concert in the buildup of the membranous web, additional immunofluorescence staining for NS4B in the context of the Jc1_NS5A-mScarlet construct could have given more insight. Additionally, FRET experiments examining the interaction of NS4B with CD81 and the E219Q mutant were not performed. In Summary, CD81 does not seem to be involved in organelle integrity, or in distribution of viral proteins or cholesterol, but not all aspects have been investigated, which leaves some limitations.

To get a better idea of how the absence of CD81 influences HCV replication, the latter was examined over time using a luciferase reporter construct. While a robust, increasing luciferase signal, as proxy for HCV replication, was measured in control cells, the signal in CD81 knock-out cells was hardly above background (Figure 5A). In addition, neither core, E2 nor NS5A could be detected by western blot in cells lacking CD81 (Figure 5B). The interim conclusion was that whatever effect CD81's absence has takes place at the early steps of the life cycle, as barely any signal was detectable in CD81 knock-out cells. When cells were treated with a global inhibitor of translation, geneticin (G418), 24h after EP and measured 4h and 24h post treatment, it became evident that treatment with G418 could mimic the situation of CD81 knock-out cells in control cells (Figure 5C). 24h after treatment and 48h after EP, respectively, control treated knock-out cells and G418 treated control cells showed similar signals, hardly but clearly above background. Of note, the signal of untreated CD81 knock-out cells did not increase between the two time points. This implies that the CD81 effect takes place within the first 24h after EP. Following, a fluorescent reporter construct (Jc1_mScarlet-2A) was created and the number of highly replicating cells was determined via flow cytometry (Figure 5D). The use of a fluorescent reporter allowed the accumulation of protein, and hence signal, more easily as the half-life of fluorescent proteins is ∼24h compared to ∼4.5h of *Renilla* luciferase [438]. With this construct, it was revealed that a much lower cell number replicated

productively in CD81 knock-out cells (Figure 5D). This means that, whatever happens through the absence of CD81, takes place at the very first initiation steps of viral translation or replication, preventing productive replication in the vast majority of cells. Notably, fluorescence intensity of highly replicating cells was similar in control and CD81 knock-out cells, suggesting that the CD81 knock-out obstacle can be overcome, leading to normal replication (data not shown). However, electroporation of higher viral RNA amounts did not increase the ratio of replicating cells but did increase cytotoxicity (data not shown). In Figure 5E the possibility was ruled out that lower replication levels in CD81 knock-out cells was due to suppressed viral spread. Treatment with an E2-targeting antibody in a neutralizing concentration did not decrease the ratio of replicating cells. Even if it had, neutralizing antibodies cannot prevent direct cell-to-cell transmission [452, 453]. At the moment, it is assumed that most of the cellular factors that are required for cell-free spread are also required for cell-to-cell transmission [452–457]. However, whether CD81 is among them is still controversial. Different reports show contradictory results regarding the need for CD81 in cell-to-cell transmission [452–460]. It was estimated that ∼40% of cell-to-cell transmission events are CD81-independent, whereas ∼60% are CD81-dependent [453, 455, 460]. At this point, it should be noted that in co-culture settings, a transfer of CD81 molecules from expressing to non-expressing cells was observed, making it even more difficult to decipher the role of CD81 in cell-to-cell transmission [455]. Another thing to take into account is the fact that CD81, together with CD9 and CD63, is part of exosomes, which might provide an explanation for the transfer of molecules between cells [461]. In addition, HCV can be transmitted via exosomes between cells [415]. Taking this into account, there is probably more cell-to-cell transmission in control cells versus CD81 knock-out cells. However, as the effect of CD81's absence was narrowed down to very early steps of the translation or replication, this does not change the validity of the results shown.

4.3 Replication Kinetics and CD81

The subsequently performed live cell imaging experiments were carried out with the objective of obtaining higher resolution data of replication dynamics. Interestingly, major differences in the replication dynamics were observed, indicated by the number of fluorescent cells per well of Jc1_mScarlet-2A and the fusion protein constructs (Jc1_NS5A-mScarlet, Jc1_E2-mScarlet). While the number of fluorescent cells increases slowly to reach an exponential growth phase between 70h and 120h post EP in Jc1_mScarlet-2A electroporated cells, they quickly reach a peak at approximately 50h post EP in the fusion protein constructs (Figure 6A). Surprisingly, a negative influence of CD81 knock-out could only be observed in Jc1_mScarlet-2A electroporated cells, while it seemed negligible

(Jc1_NS5A-mScarlet) or rather beneficial (Jc1_E2-mScarlet) in cells electroporated with a fusion protein construct. Furthermore, when cells were electroporated with different amounts of wild type Jc1 RNA, no difference in the number of actively replicating cells was detected (Figure 6B). This excludes the possibility that electroporation of high amounts of viral RNA could overcome a potential CD81 knock-out effect, as cells electroporated with low RNA amounts show no difference either. These results rather suggest no effect of CD81 knock-out on viral replication. In addition, no difference between control and CD81 knock-out cells in the amount of viral RNA was detected 48h post EP with Jc1 (Figure 6C, left). However, in cells that were electroporated with Jc1_mScarlet-2A, a lower viral RNA amount was detected in CD81 knock-out cells compared to control cells (Figure 6C, right). Strikingly, Jc1 electroporated cells had levels of viral RNA 30 times higher than for Jc1_mScarlet-2A electroporated cells. In conclusion, although they give rise to infectious viral progeny, viral 2A reporter constructs seem to have a much slower replication kinetic than the wild-type, non-tagged, or fusion protein constructs. A possible explanation could be an improper secondary structure of viral RNA. The sequences encoding the reporter proteins were introduced at the beginning of the coding region for the polyprotein directly after the 5'UTR, which is known to form secondary structures important for translation initiation (see RNA and Genome) [36, 40–42]. Although the first 18 aa of the core coding region were added in front of the reporter to cope with RNA secondary structures and RNA-RNA interactions, the sheer length of the reporter insert could interfere with these interactions. With lengths of ∼1000 and ∼700 nucleotides for *Renilla* luciferase and mScarlet, respectively, the whole viral genome is extended by 10% or 7%, which could interfere with long range RNA-RNA interactions. One of these long range interactions between the CRE, located in the NS5B coding region, and the IRES, located at the 5'UTR and core coding region, has been revealed to regulate translation [41, 44]. Preliminary results with a Nano luciferase reporter construct did not show differences in replication between control and CD81 knock out cells (data not shown), though the performance of this construct has not been evaluated in comparison to other viral constructs. Interestingly, insertion at other parts of the genome, like E2 or NS5A fusion proteins, did not indicate impairment of viral replication, but lower infectious titers [294, 424]. To be sure that the insertion site is responsible for the lower replication fitness of 2A-reporter constructs, more experiments are needed.

With replication being slower in reporter constructs, it was apparent that they could be more susceptible to the cellular antiviral response. Before this question could be addressed, the one of whether CD81 has any influence on viral counteracting mechanisms, had to be answered. Figure 7A illustrates that IFNα treatment increases the expression of tetherin (CD317) to a great extent, but only in cells that do not actively replicate

Jc1_NS5A-mScarlet (mSc-), as cells that replicate (mSc++) show no increased tetherin expression upon IFNα treatment. As evident from Figure 7B, tetherin expression remains at base level upon IFNα treatment in control and CD81 knock-out cells. Additionally, the ratio of actively replicating cells was similar between control and CD81 knock-out cells, and unaltered upon IFNα treatment (Figure S2). These results indicate that the counteraction of ISG activation is unaffected by the absence or presence of CD81. Potential counteraction mechanisms, for example via core, NS3-4A or NS5A described in the literature, have not been investigated in this context [72, 127, 149, 345].

Next, as viral counteraction of ISG activation via IFNα was not affected by CD81 knock-out, susceptibility of Jc1_mScarlet-2A and Jc1_NS5A-mScarlet to IFNα was tested. It became clear that Jc1_mScarlet-2A is highly susceptible to IFNα treatment even if it occurs 24h post EP (Figure 8A, left). In contrast, Jc1_NS5A-mScarlet is insusceptible from 16h post EP on (Figure 8A, right). This goes along with high tetherin expression in Jc1_mScarlet-2A electroporated cells, independent from the time point when IFNα was added (Figure 8B, left). In cells electroporated with Jc1_NS5A-mScarlet, tetherin expression was reduced already when IFNα was added as early as 8h post EP (Figure 8B, right). A reduction in the ratio of replicating cells, together with the lack of ISG counteraction, indeed suggests that 2A-reporter constructs replicate slower than their fusion protein counterparts or wild-type Jc1. Usually, (+)-ssRNA viruses start translation of their proteins directly after the RNA has been released to the cytosol. The viral proteins then start to reprogram the host cells metabolism and counteract any antiviral mechanisms that might have been triggered. There, it is decided whether the cell gets productively infected or its defense mechanisms can prevent it. Hence, viruses that are somehow impaired to counteract the host cells antiviral response have a higher chance of being eliminated. Whatever the precise role of CD81 is, it seems to increase the antiviral response resulting in a lower ratio of cells with productive replication after EP (compare Figure 5D, Figure 6A, Figure 8A). However, CD81's absence could also hinder a specific viral counteraction at an early step, which is less important later on as cells that are productively replicating show similar fluorescence intensity and hence, a similar amount of viral proteins (data not shown). At this point, more experiments are required to understand the mechanisms that take place in CD81 knock-out cells early after EP as HCV not only dysregulates antiviral response but also other pathways triggered upon infection.

4.4 Influence of CD81 on the ISR

One of the non-immunity pathways that is triggered by HCV is the Integrated Stress Response (ISR). Able to influence several cellular processes that are considered essential to

HCV replication, such as ER capacity and autophagy, the ISR is a potential candidate for CD81 impact. As illustrated in Figure 9A and B, induction of ER stress by thapsigargin (TG) leads to a higher ratio of sXBP1 mRNA in CD81 knock-out cells than in control cells. Because other potential ER stress inducers and combinations of viral proteins showed no effect when CD81 was absent, it was considered a rather specific function (Figure 9B and Figure S3). TG blocks the SERCA (sarco/endoplasmic reticulum Ca^{2+}-ATPase) which actively transports Ca^{2+} from the cyctosol to the ER [462]. Inhibition leads to Ca^{2+}-depletion in the ER and higher levels in the cytosol, resulting in ER stress [463]. The results obtained from Jc1 electroporated cells gave less clear results regarding XBP1 mRNA splicing, except that viral induced splicing happens 48h rather than 24h after EP (Figure 9C). Treatment 48h post EP was able to boost XBP1 mRNA splicing by a factor of around 2, but did not have any influence on viral RNA abundance, neither in control, nor in CD81 knock-out cells (Figure 9D). However, the ability to boost XBP1 mRNA splicing indicates that the ER was not fully stressed by replicating HCV. Hence, as TG depletes Ca^{2+} from the ER, the Ca^{2+} homeostasis was still present upon HCV replication. In addition, HCV replication results in higher total levels of spliced XBP1 mRNA without affecting the abundance of viral RNA itself, indicating that an established productive replication can cope with potentially higher sXBP1 mRNA levels in CD81 knock-out cells (Figure 9D and E). Interestingly, establishing a new productive replication in cells pre-treated with TG seems to be more difficult (Figure 9F). Although viral RNA levels were diminished in control cells treated with TG prior to electroporation when compared with DMSO treated ones, the viral RNA levels in CD81 knock-out cells were barely detectable. Therfore, pre-treatment with TG impairs the establishment of productive replication in general, but prevents it nearly completely in CD81 knock-out cells. Whether this phenotype is caused by higher levels of sXBP1 mRNA (and XBP1 protein) or due to generally increased levels of Ca^{2+} in the cytosol after TG treatment, needs to be clarified in further experiments.

As activation of the ISR during HCV infection eventually leads to translational shutdown via eIF2α phosphorylation, the potential subsequent assembly of SGs was investigated as well. Flow cytometry-based FRET experiments revealed that none of the viral proteins interact with the SG component G3BP1 (Figure S4). However, E1, p7, NS5B and, most prominently, NS4B showed an interaction with STAU1 which is involved in a plethora of cellular functions including disassembly of SGs (Figure 10A) [441]. Repeating the experiments in control and CD81 knock-out cells revealed an increased interaction of E1 and NS5B with STAU1 in CD81 knock-out cells (Figure 10B). Indeed, STAU1 was reported to be important for HCV as depletion of STAU1 clearly reduced HCV replication [347]. Additionally, Dixit *et al.* could show that it binds viral RNA, on the one hand

preventing PKR from binding and on the other, regulating translation [348]. PKR binds foreign RNA and phosphorylates eIF2α upon recognition, hence STAU1 prevents eIF2α phosphorylation and SG assembly. However, the assembly of SGs after induction of oxidative stress through $NaAsO_2$ did not display any differences between control and CD81 knock-out cells (Figure S5A). Similarly, the phosphorylation pattern of eIF2α did not allow any conclusion as there was no correlation between phosphorylation, expression of viral proteins or CD81 knock-out observable (Figure S5B). Up to now, the increased interaction of E1 and NS5B with STAU1 could not be definitely explained. Nevertheless, the binding of viral RNA by STAU1 renders its interaction with NS5B plausible, which was also shown by Dixit *et al.* [348]. Even so, an interaction of CD81 with STAU1 was not detected (data not shown). As pointed out by Ruggieri *et al.* and Klein *et al.*, SG assembly and disassembly is highly dynamic, tightly controlled and, most importantly, asynchronous in cells, which could explain the ambiguous results regarding eIF2α phosphorylation [341, 383]. Taken together, although SG dynamics and STAU1 play an important role in HCV replication, they seem not to be directly connected to CD81.

4.5 NFκB Signaling in Connection to CD81

In recent years a connection between the ISR and the NFκB signaling pathway has been uncovered [442]. The NFκB family of transcription factors transcribe a set of pro-inflammatory genes when activated. With their potential activation through the ISR or the innate immune response, the NFκB pathway represents a reasonable candidate that could explain the CD81 knock-out effect early after EP (see Cellular Antiviral Reaction and Viral Counteraction). Figure 11A and B illustrate that NFκB activation via IKKβ, MAVS and RIG-I is possible with IKKβ being the most potent activator. While CD81 knock-out could not alter NFκB activity, its overexpression led to reduced NFκB activity (Figure 11A and B). To prevent possible maximum activation, chemical inducers were used that induce the NFκB pathway further upstream. Interestingly, induction with PMA (phorbol 12-myristate 13-acetate) not only showed the highest activity of NFκB, it was also further increased in CD81 knock-out cells (Figure 11C). TNFα and PolyI:C induced NFκB activity as well but to a much lesser extent. Further experiments showed that a trend exists where CD81 levels inversely correlate with NFκB activity. When CD81 knock-out cells transfected with an empty plasmid (low level) are compared to control cells transfected with a CD81-encoding plasmid (high level), it can be appreciated that high CD81 levels correlate with lower NFκB activity (Figure 12A). This is true for HEK-293T and HeLa cells, however, only in the former was the effect significant. The effect was also more prominent in PMA-stimulated than in IKKβ overexpressing cells. Subsequently, a closer look was taken at PMA-stimulation of cells, which was also combined with

ionomycin (Iono) stimulation, as some PKC isoforms are only activated in the presence of diacylglycerol (DAG), mimicked by PMA, and Ca^{2+}, released by Iono [464]. In Figure 12B it becomes evident that Iono alone is not able to induce NFκB activation and that it does not have an additional effect on PMA-mediated activation. Still, overexpression of CD81 in control cells reduced NFκB activation compared to CD81 knock-out cells significantly (Figure 12B). The described effect was measurable in HEK-293T and HeLa cells but not in Huh7.5 cells, where overall activation was very low (Figure S6). The fact that Iono does not have an impact on NFκB activation here, indicates that the responsible PKC isoform belongs to the subfamily of novel PKCs, as it is not required to bind Ca^{2+} in order to be activated [464]. However, to identify the PKC isoform(s) responsible, further analyses must be conducted. In theory, it is possible, albeit unlikely, that Ca^{2+} levels in the cytosol were already high enough to activate conventional PKC isoforms as well. In the context of HCV, core was reported to be able to induce NFκB signaling which even increased synergistically together with TNFα [73]. Hence, the experiment was reproduced and cells were additionally transfected with CD81 to test whether a reduction in NFκB activation could be observed. Indeed, cells overexpressing CD81 displayed a lower NFκB activation than control plasmid transfected cells (Figure 12C). In their study, Chung *et al.* identified a TRAF2-IKKβ pathway to mediate NFκB activation induced by HCV core and TNFα [73]. Of note, IRE1α was also reported to induce NFκB activation via a TRAF2-dependent pathway [369]. Additionally, Fink *et al.* revealed that IRE1α activity is important for HCV replication as it regulates cell survival, presumably by degrading the pro-apoptotic miR-125a [465]. They further showed that knock-out of XBP1 with simultaneous activation of IRE1α by NS4B renders cells resistant to the intrinsic pathway of apoptosis, characterized by mitochondrial outer membrane permeabilization. Together with the study of Tardif *et al.*, this connects higher IRE1α activity with a NFκB-mediated potential pro-survival activity that is prevented from apoptosis by the blockage of XBP1 transcriptional activity and IRE1α-mediated degradation of miR-125a [370, 465]. As shown before in Figure 9B, more XBP1 mRNA is spliced in CD81 knock-out cells after TG treatment. However, cells electroporated with wild-type Jc1 only display a slight increase in spliced XBP1 mRNA, potentially because it is controlled by viral proteins (Figure 9D and E) [370]. It is tempting to speculate that absence of CD81 might allow for increased IRE1α activity, which could be even advantageous for HCV in later steps of the life cycle, but fatal in early steps for an attenuated construct like the 2A-reporters. The viral proteins that potentially control XBP1 transcriptional activity and NFκB might not be expressed in a sufficient amount at early time points after 2A-reporter EP.

As CD81 plays a negative role in NFκB activation the question, at which point of the signaling cascade the influence takes place, remains open. To be transcriptionally

active, NFκB subunits must translocate to the nucleus. Checking for the kinetic of the translocation of the NFκB subunit p65 to the nucleus in control and CD81 knock-out cells revealed two things. First, the translocation of endogenous p65 is more potently induced by PMA than by TNFα and, second, a higher p65 nuclear signal was measured in CD81 knock-out cells (Figure 13A and B, Figure S7). Interestingly, the kinetic seems not to be influenced, as 30min after PMA treatment a comparable signal was measured in control and CD81 knock-out cells, however, it increased further in the latter giving a higher signal in CD81 knock-out cells at 1h and 2h post stimulation (Figure 13B). So, it seems like translocation takes place at the same speed but in CD81 knock-out cells continues after most p65 in the control cells has already translocated. In Figure 13A it appears that 30min after PMA treatment some p65 is left in the cytosol of CD81 knock-out cells, while hardly any signal can be seen in the cytosol of control cells. This goes along with the western blot analysis of p65 phosphorylation which occurs prior to translocation. Although levels of phosphorylated p65 did not change, as TNFα is an insufficient stimulus, p65 levels in general seemed to be higher in CD81 knock-out cells (Figure 13C). Higher levels of p65 could explain the differences that have been observed in NFκB activity between CD81 knock-out cells and control cells. However, it is not clear whether more p65 would then lead to higher transcriptional activity of NFκB targeted genes. Of note, the indications of higher p65 levels in CD81 knock-out cells have been obtained in Huh7.5 cells while several of the previous experiments have been performed with HEK-293T and HeLa cells. As readout for NFκB transcriptional activity TNFα, mRNA was chosen. PMA stimulation led to a massive increase in TNFα mRNA abundance in HEK-293T CD81 knock-out compared to control cells (Figure 14A). Curiously, in Huh7.5 cells, an increase of TNFα mRNA in CD81 knock-out cells compared to control cells could only be observed at 30min after stimulation, whereas it was reversed at the 5h time point (Figure 14B). Furthermore, the detected TNFα mRNA levels in Huh7.5 cells were a multiple lower than in HEK-293T cells. A decrease in TNFα mRNA was also detected in HEK-293T cells between the 30min and the 5h time point, but levels in CD81 knock-out cells remained increased by a factor of 10 (Figure 14A). It remains unclear if more nuclear p65 leads to higher NFκB gene expression, as Huh7.5 cells show ambiguous results. However, nuclear p65 has not been detected at 5h post treatment, leaving the possibility that p65 translocation back to the cytoplasm is also altered in CD81 knock-out cells. For the target genes of NFκB, there are also inhibiting factors that terminate NFκB activity, usually between 1h and 2h after activation. Nonetheless, constant activation leads to an oscillating pattern of NFκB activity [466]. If this pattern differs between control and CD81 knock-out cells, it could explain the differences of the TNFα mRNA expression pattern. Another layer of complexity is added by the fact that HCV was reported to influence the abundance of

the ubiquitin-editing enzyme Tumor necrosis factor alpha-induced protein 3 (TNFAIP3), best known as A20. It was shown that HCV induces TNFAIP3 to prevent NFκB signaling and to support its own replication [467, 468]. Hence, to assess CD81's role in NFκB activation, more data is needed. For example, displaying NFκB gene expression in a higher temporal resolution, together with live cell imaging of p65 nuclear translocation, could reveal differences in the oscillating patterns of control and CD81 knock-out cells. Additionally, detection of p65 levels in other cell lines could clarify whether higher general levels of p65 are responsible for the observed phenotype.

4.6 Conclusion

Everything together leads us to the following overall hypothesis. As demonstrated, the lack of CD81 results in higher NFκB activation, either through higher p65 levels or another, yet undiscovered, mechanism (Figure 12 and Figure 13). Additionally, following ER stress, the activity of IRE1α is also increased in CD81 knock-out cells, illustrated by more XBP1 mRNA splicing (Figure 9). Higher IRE1α activity in concert with impaired XBP1 transcriptional activity is associated with survival of infected cells [370, 465]. Hence, viral constructs that are attenuated, as demonstrated for the 2A-reporters, are not able to counteract XBP1 transcriptional activity, because translation of a sufficient amount of viral proteins takes too long. This is indicated by the susceptibility to IFNα treatment (Figure 8). As a result, few cells manage to overcome the increased IRE1α and NFκB activity, leaving a lower ratio of productively replicating cells in CD81 knock-out versus control cells (Figure 5 and Figure 6). However, viral constructs that are not attenuated were not affected by the lack of CD81 and did even show a partially increased ratio of productively replicating cells (Figure 6). Finally, this brings us back to the transcriptional downregulation of CD81 (Figure 2). At later steps of the viral life cycle, lower CD81 levels could be beneficial for viral replication, as the antiviral and stress response are under control and higher IRE1α and NFκB activity could boost a pro-survival environment, allowing for HCV chronicity.

5 Supplement

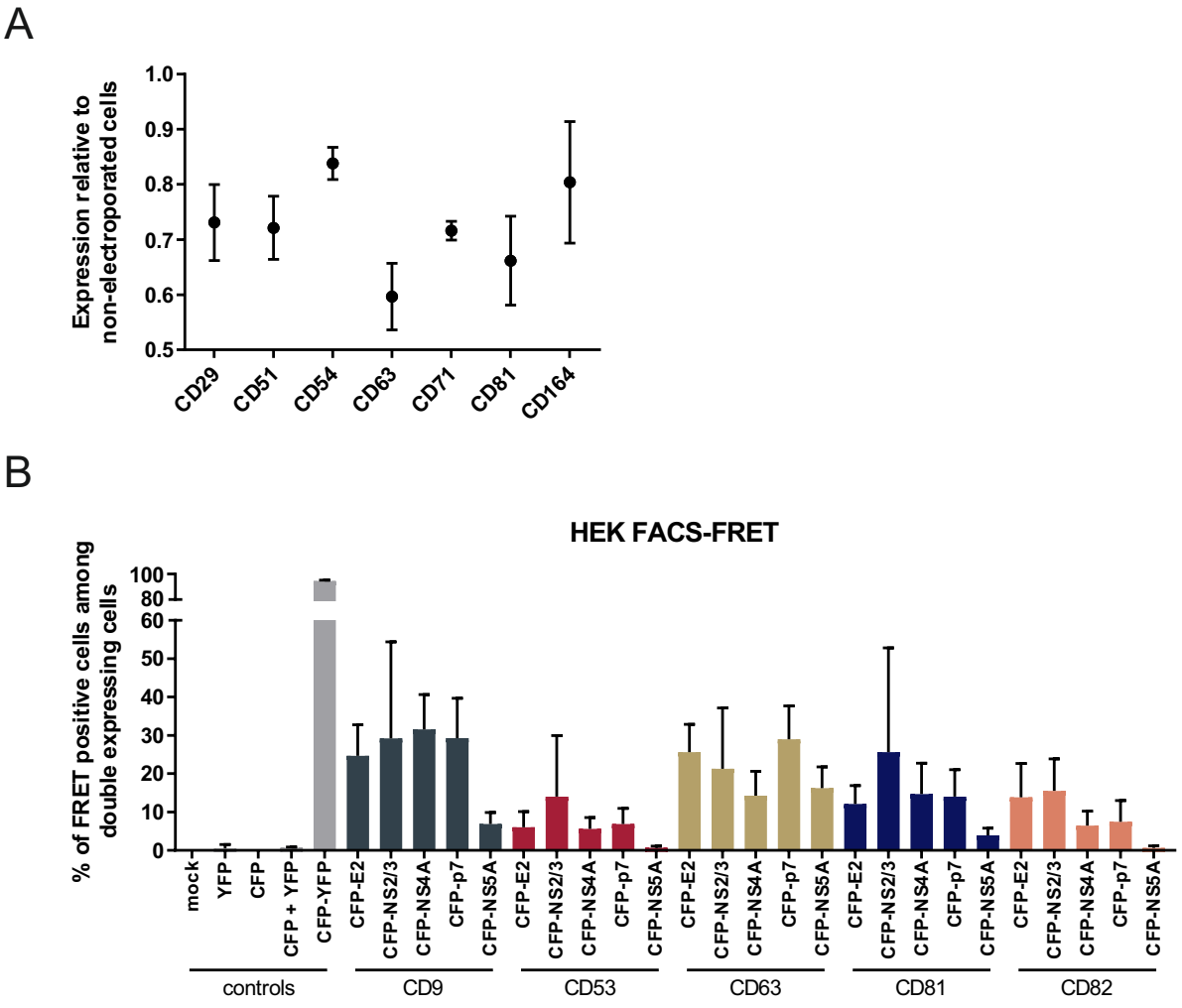

Figure S1: Previous experiments.
(A) Proteins whose surface expression was significantly downregulated in cells expressing a full-length viral genome. Huh7.5 cells were electroporated with Jc1_mtagBFP-NS5A and harvested 48h later. Cells were added to reconstituted antibody solutions in a 96-well format (LEGEND screen), fixed and measured by flow cytometry. Depicted are data from 3 independent experiments performed by Sandra Kurz [436]. **(B)** Flow cytometry-based FRET data of viral proteins with tetraspanins. HEK-293T cells were transfected with different pairs of constructs encoding a CFP-tagged viral protein, and a YFP-tagged tetraspanin, each. 24h after transfection cells were harvested and FRET signals were measured via flow cytometry to indicate close proximity and interaction. These results have been obtained in [437]. Depected are data from 3 independent experiments. Data points show mean ± SD unless labelled otherwise.

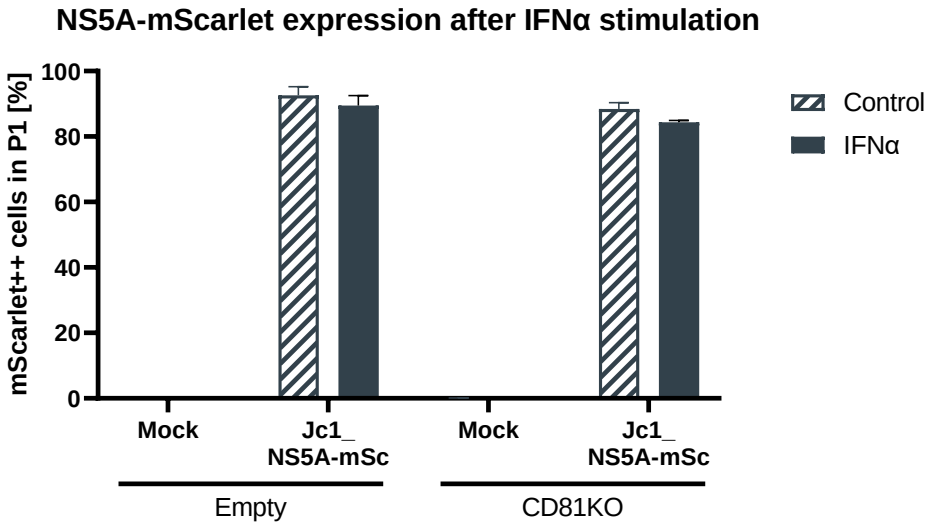

Figure S2: Ratio of cells highly expressing NS5A-mScarlet after IFNα treatment. Huh7.5 control and CD81KO cells were electroporated with Jc1_NS5A-mScarlet. 48h post EP they were treated with IFNα (10 ng/ml) for 24h, then fixed and stained for tetherin. NS5A-mScarlet and tetherin expression was measured via flow cytometry. Depicted are ratios of cells highly expressing NS5A-mScarlet as mean ± SD from 2 independent experimets. Matching tetherin expression data is displayed in Figure 7.

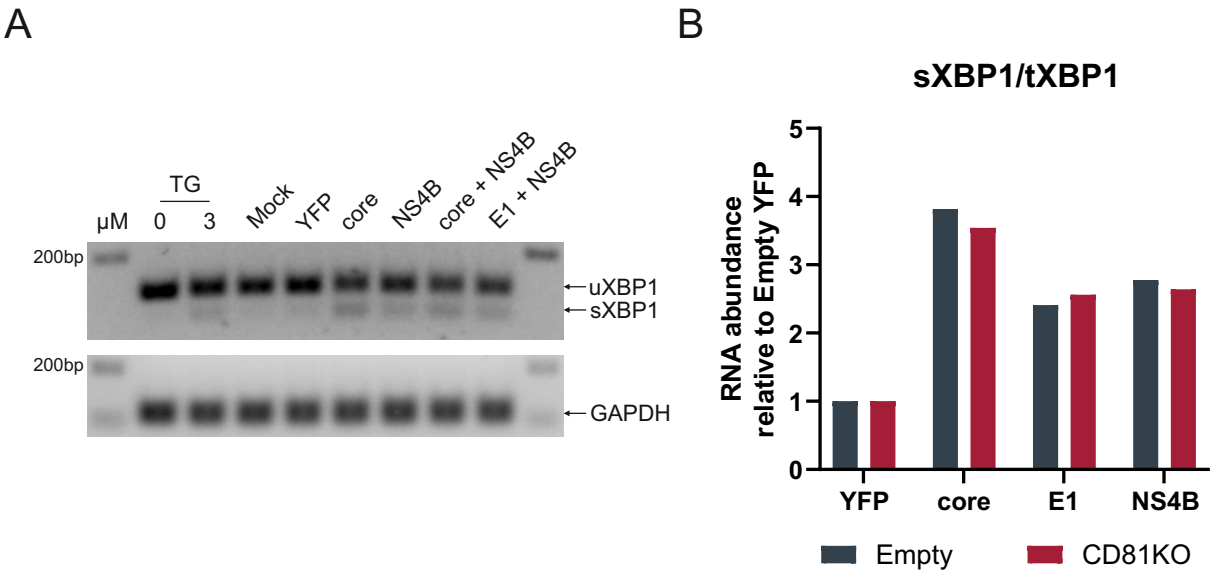

Figure S3: Viral proteins alone induce ER stress independent of CD81.
(A) XBP1 splicing after transfection of viral proteins. Huh7.5 cells were either treated with TG (3 μM) for 24h, transfected with one or two YFP-tagged viral proteins or with YFP alone. 24h after transfection cellular RNA was extracted, XBP1 mRNA amplified via PCR and visualized in an agarose gel. Lower band in the upper panel represents spliced XBP1 (sXBP1) while the upper band represents its unspliced version (uXBP1).

Figure S3: (continued)
(B) Quantification of XBP1 splicing after transfection of viral proteins. Huh7.5 control and CD81KO cells were transfected with YFP-tagged viral proteins or YFP alone. 24h after transfection cellular RNA was extracted and XBP1 solicing was quantified via qRT-PCR. Depicted is data from 1 experiment.

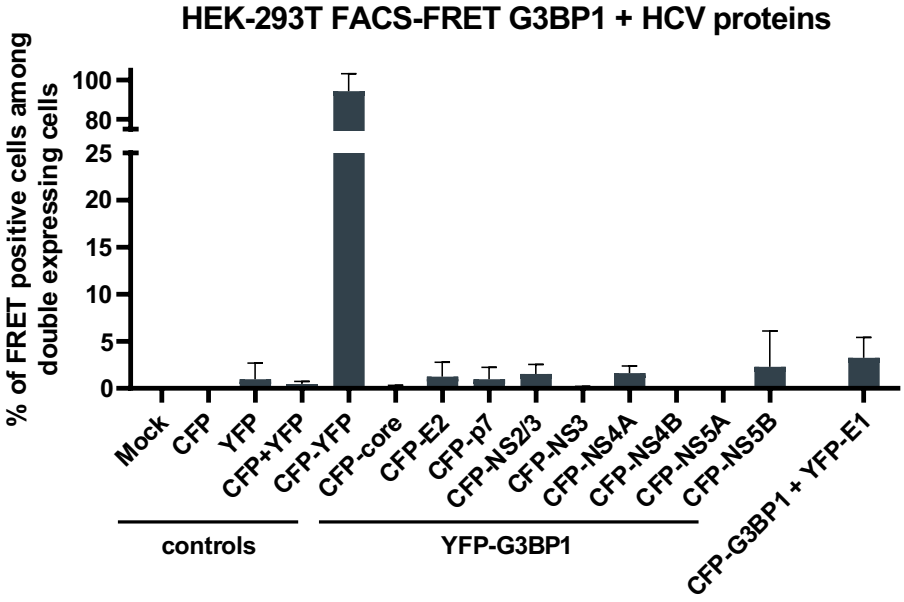

Figure S4: Stress granule protein G3BP1 does not interact with any HCV protein. HEK-293T cells were transfected with plasmid pairs encoding CFP-tagged HCV proteins and YFP-tagged G3BP1. 24h after transfection cells were harvested and potential FRET signals were measured using flow cytometry indicating close proximity and hence interaction. Depicted is mean ± SD of 3 independent experiments.

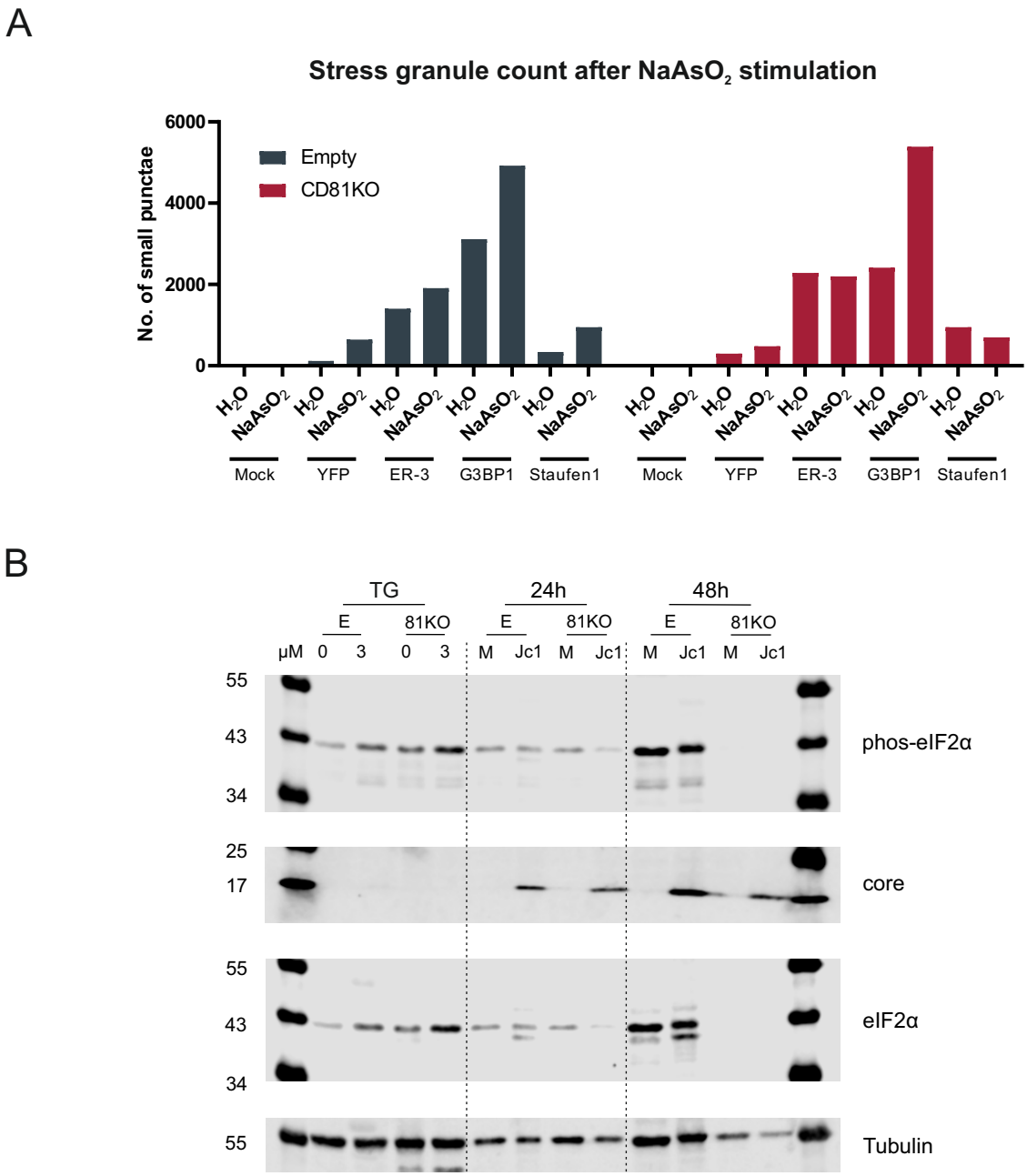

Figure S5: Stress granule formation and phosphorylation of eIF2α seem not to be connected with CD81.

(A) Stress granule induction by sodium arsenite treatment in control and CD81KO cells. HEK-293T control and CD81KO cells were transfected with plasmids encoding cellular proteins tagged with GFP-like proteins. YFP alone and ER-3 as ER marker were transfected as controls, while G3BP1 and STAU1 are involved in stress granule formation and their clearance, respectively. 24h post transfection cells were treated with $NaAsO_2$ for 1h and subsequently fixed and imaged for small green fluorescent punctae which indicate stress granules. Depicted data are from one experiment. Continued on next page.

Figure S5: (continued)
(B) eIF2α phosphorylation in cells expressing Jc1 or were treated with TG. Huh7.5 control and CD81KO cells were treated with TG (3 µM) for 24h or electroporated with Jc1 viral RNA and samples were lysed and prepared for SDS-PAGE and western blot analysis 24 and 48h post EP. Depicted is data from 1 experiment.

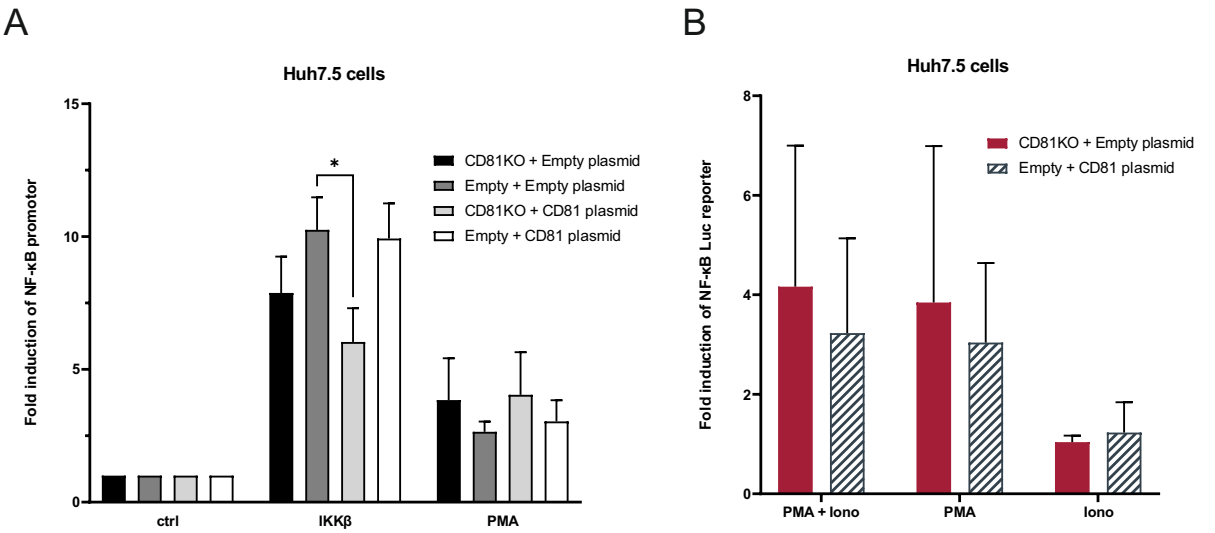

Figure S6: Influence of CD81 on NFκB activity in Huh7.5 cells.
(A) Huh7.5 control and CD81KO cells were transfected with plasmids encoding a firefly luciferase-reporter for NFκB and gaussia-luciferase as transfection control. NFκB activity was induced either by simultaneous transfection of IKKβ or treatment with PMA (10 ng/ml) from 4h post transfection until harvest. Additionally, cells were either transfected with a plasmid encoding CD81 or an empty control plasmid. 24h after transfection luciferase signals were measured in the supernatant (gaussia) and the cell lysate (firefly). Depicted are data from 4 independent experiments. **(B)** Huh7.5 control and CD81KO cells were transfected as in A, except that control cells were additionally transfected with the plasmid encoding CD81 and CD81KO cells with the empty control plasmid. 4h post transfection cells were treated with PMA (10 ng/ml), Iono (0.25 µM) or both. Depicted are data from 4 independent experiments. Data points show mean ± SD unless labelled otherwise. Significance was tested using two-way ANOVA with Sidak's multiple comparisons test. ns = not significant; * $p \leq 0.05$.

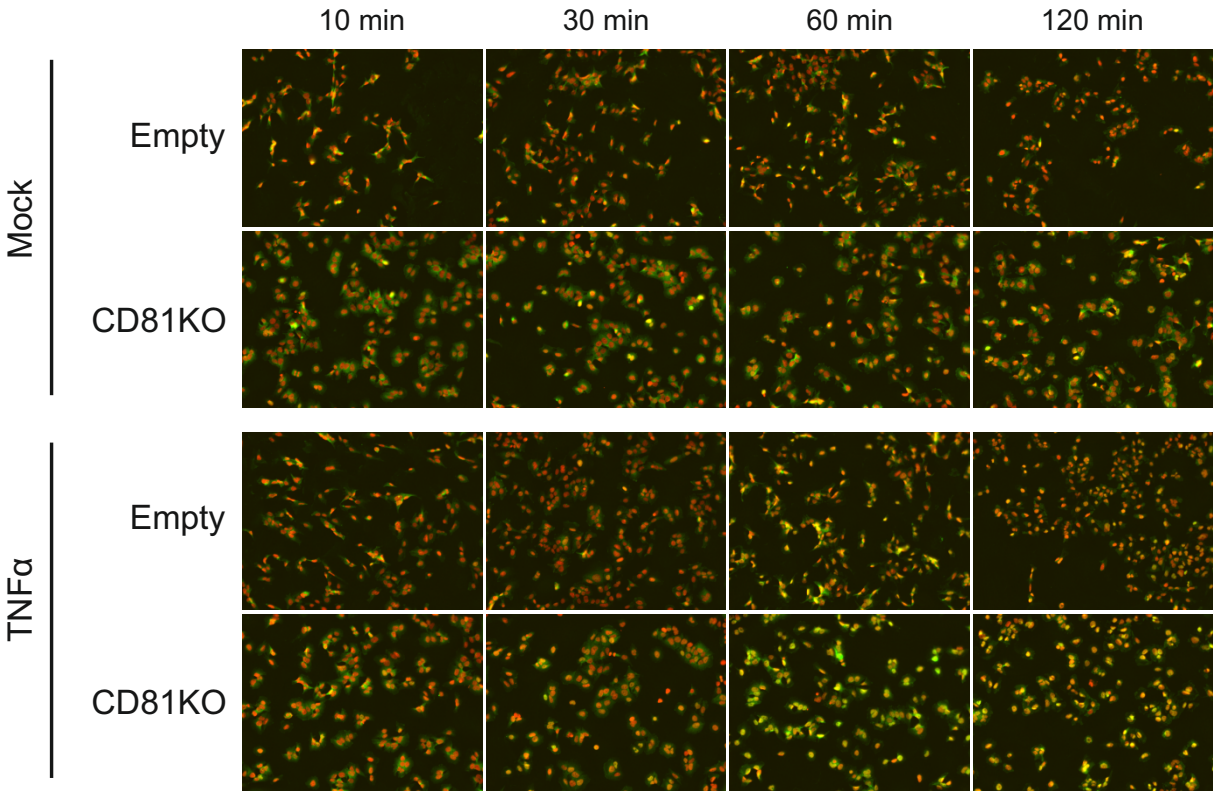

Figure S7: p65 nuclear translocation over time after stimulation with TNFα in Huh7.5 cells.
Huh7.5 control and CD81KO cells were seeded in a 96-well format and fixed after no or stimulation with TNFα (10 ng/ml) for indicated time periods. Cells were permeabilized and stained for endogenous p65 using antibodies and nuclear DNA using a red fluorescent dye. Images were taken by the IncuCyte® S3 Live-Cell Analysis System with a 20× objective. Shown are representative images of 3 independent experiments.

Acknowledgements

First, I want to thank Michael Schindler for giving me the opportunity to conduct my research in his lab and in particular for constant support and inspiring discussions. Thank you for great supervision and continuous confidence. Furthermore, I would like to thank Ana Garcia-Saez and Ulrich Rothbauer for being my second supervisors.

Special thanks is due to all the lab members over the time who always had a helping hand. In particular, Natalia, George, Dan, Ramona, Johanna and Elena for listening to my problems and having great ideas to solve them. Additionally, I want to thank the third floor's office for surviving summers and winters with me, the 2.3.05 lab for great team work and all my students who helped shaping my projects. And of course, special thanks to the BBQ and Asien Haus connections for great dinners and lunches.

I also would like to thank all the researchers who provided materials, cells, viruses and information, which allowed me to do my experiments.

I am very thankful for my flat mates Björn, Christian, Moritz, Christoph and Tim for listening to my complaints and always improving my mood. And thanks again to Tim and Björn for critical reading of the manuscript and Elena for providing her Latex template.

Finally, I want to thank my family and friends who never expressed the slightest doubt that I will finish this thesis. All of you made the hard PhD student times an experience I do not want to miss.

References

[1] Moon, A. M., Singal, A. G., & Tapper, E. B. Contemporary Epidemiology of Chronic Liver Disease and Cirrhosis. *Clinical Gastroenterology and Hepatology: The Official Clinical Practice Journal of the American Gastroenterological Association*, **18**(12): 2650–2666 (2020). doi:10.1016/j.cgh.2019.07.060. 1

[2] Asrani, S. K., Devarbhavi, H., Eaton, J., & Kamath, P. S. Burden of liver diseases in the world. *Journal of Hepatology*, **70**(1): 151–171 (2019). doi:10.1016/j.jhep.2018.09.014. 1

[3] Global Burden of Disease Collaborative Network. Global Burden of Disease Study 2019 (GBD 2019) Reference Life Table (2021). doi:10.6069/1D4Y-YQ37. Type: dataset. 1

[4] GBD 2017 Cirrhosis Collaborators. The global, regional, and national burden of cirrhosis by cause in 195 countries and territories, 1990-2017: a systematic analysis for the Global Burden of Disease Study 2017. *The Lancet. Gastroenterology & Hepatology*, **5**(3): 245–266 (2020). doi:10.1016/S2468-1253(19)30349-8. 1

[5] World Health Organization. Global hepatitis report 2017. World Health Organization, Geneva (2017). ISBN 978-92-4-156545-5. 1, 2

[6] Cheemerla, S. & Balakrishnan, M. Global Epidemiology of Chronic Liver Disease. *Clinical Liver Disease*, **17**(5): 365–370 (2021). doi:10.1002/cld.1061. 1

[7] Roser, M., Ritchie, H., Ortiz-Ospina, E., & Rodés-Guirao, L. World Population Growth. *Our World in Data* (2013). Https://ourworldindata.org/world-population-growth. 1

[8] Ni, Y.-H. & Chen, D.-S. Hepatitis B vaccination in children: The Taiwan experience. *Pathologie Biologie*, **58**(4): 296–300 (2010). doi:10.1016/j.patbio.2009.11.002. 1

[9] Pattyn, J., Hendrickx, G., Vorsters, A., & Van Damme, P. Hepatitis B Vaccines. *The Journal of Infectious Diseases*, **224**(Supplement_4): S343–S351 (2021). doi:10.1093/infdis/jiaa668. 1

[10] World Health Organization. Global progress report on HIV, viral hepatitis and sexually transmitted infections, 2021: accountability for the global health sector strategies 2016–2021: actions for impact. World Health Organization, Geneva (2021). ISBN 978-92-4-002707-7. Section: xii, 92 p. 1, 2

[11] Manns, M. P., Buti, M., Gane, E., Pawlotsky, J.-M., *et al.* Hepatitis C virus infection. *Nature Reviews Disease Primers*, **3**(1): 17006 (2017). doi:10.1038/nrdp.2017.6. 1

[12] Micallef, J. M., Kaldor, J. M., & Dore, G. J. Spontaneous viral clearance following acute hepatitis C infection: a systematic review of longitudinal studies. *Journal of Viral Hepatitis*, **13**(1): 34–41 (2006). doi:10.1111/j.1365-2893.2005.00651.x. 1

[13] European Centre for Disease Prevention and Control. Hepatitis C. In: ECDC. Annual epidemiological report for 2020. ECDC, Stockholm (2022). 1

[14] Alter, M. HCV Routes of Transmission: What Goes Around Comes Around. *Seminars in Liver Disease*, **31**(04): 340–346 (2011). doi:10.1055/s-0031-1297923. 1

[15] World Health Organization. Global progress report on HIV, viral hepatitis and sexually transmitted infections, 2021: accountability for the global health sector strategies 2016–2021: actions for impact: web annex 1: key data at a glance. World Health Organization, Geneva (2021). ISBN 978-92-4-003098-5. 2

[16] Blach, S., Zeuzem, S., Manns, M., Altraif, I., *et al.* Global prevalence and genotype distribution of hepatitis C virus infection in 2015: a modelling study. *The Lancet Gastroenterology & Hepatology*, **2**(3): 161–176 (2017). doi:10.1016/S2468-1253(16)30181-9. 2

[17] Paraskevis, D., Kostaki, E. G., Kramvis, A., & Magiorkinis, G. Classification, Genetic Diversity and Global Distribution of Hepatitis C Virus (HCV) Genotypes and Subtypes. In Hatzakis, A. (ed.), Hepatitis C: Epidemiology, Prevention and Elimination, pp. 55–69. Springer International Publishing, Cham (2021). ISBN 978-3-030-64648-6 978-3-030-64649-3. doi:10.1007/978-3-030-64649-3_3. 2

[18] Petruzziello, A., Marigliano, S., Loquercio, G., & Cacciapuoti, C. Hepatitis C virus (HCV) genotypes distribution: an epidemiological up-date in Europe. *Infectious Agents and Cancer*, **11**(1): 53 (2016). doi:10.1186/s13027-016-0099-0. 2

[19] Karamitros, T., Paraskevis, D., & Magiorkinis, G. Hepatitis C Virus Origin. In Hatzakis, A. (ed.), Hepatitis C: Epidemiology, Prevention and Elimination, pp. 45–53. Springer International Publishing, Cham (2021). ISBN 978-3-030-64648-6 978-3-030-64649-3. doi:10.1007/978-3-030-64649-3_2. 2

[20] Manns, M. P. & Maasoumy, B. Breakthroughs in hepatitis C research: from discovery to cure. *Nature Reviews Gastroenterology & Hepatology*, **19**(8): 533–550 (2022). doi:10.1038/s41575-022-00608-8. 2, 6, 8

[21] Basyte-Bacevice, V. & Kupcinskas, J. Evolution and Revolution of Hepatitis C Management: From Non-A, Non-B Hepatitis Toward Global Elimination. *Digestive Diseases*, **38**(2): 137–142 (2020). doi:10.1159/000505434. 2

[22] Janjua, N. Z., Wong, S., Abdia, Y., Jeong, D., *et al.* Impact of direct-acting antivirals for HCV on mortality in a large population-based cohort study. *Journal of Hepatology*, **75**(5): 1049–1057 (2021). doi:10.1016/j.jhep.2021.05.028. 2, 6, 8

[23] Bailey, J. R., Barnes, E., & Cox, A. L. Approaches, Progress, and Challenges to Hepatitis C Vaccine Development. *Gastroenterology*, **156**(2): 418–430 (2019). doi:10.1053/j.gastro.2018.08.060. 3

[24] Osburn, W. O., Fisher, B. E., Dowd, K. A., Urban, G., *et al.* Spontaneous Control of Primary Hepatitis C Virus Infection and Immunity Against Persistent Reinfection. *Gastroenterology*, **138**(1): 315–324 (2010). doi:10.1053/j.gastro.2009.09.017. 3

[25] Frumento, N., Flyak, A. I., & Bailey, J. R. Mechanisms of HCV resistance to broadly neutralizing antibodies. *Current Opinion in Virology*, **50**: 23–29 (2021). doi:10.1016/j.coviro.2021.07.003. 3, 5

[26] Sepulveda-Crespo, D., Resino, S., & Martinez, I. Hepatitis C virus vaccine design: focus on the humoral immune response. *Journal of Biomedical Science*, **27**(1): 78 (2020). doi:10.1186/s12929-020-00669-4. 3

[27] Page, K., Melia, M. T., Veenhuis, R. T., Winter, M., *et al.* Randomized Trial of a Vaccine Regimen to Prevent Chronic HCV Infection. *New England Journal of Medicine*, **384**(6): 541–549 (2021). doi:10.1056/NEJMoa2023345. 3

[28] Prentoe, J., Velázquez-Moctezuma, R., Foung, S. K. H., Law, M., & Bukh, J. Hypervariable region 1 shielding of hepatitis C virus is a main contributor to genotypic differences in neutralization sensitivity. *Hepatology (Baltimore, Md.)*, **64**(6): 1881–1892 (2016). doi:10.1002/hep.28705. 3, 5

[29] Prentoe, J., Velázquez-Moctezuma, R., Augestad, E. H., Galli, A., *et al.* Hypervariable region 1 and N-linked glycans of hepatitis C regulate virion neutralization by modulating envelope conformations. *Proceedings of the National Academy of Sciences*, **116**(20): 10039–10047 (2019). doi:10.1073/pnas.1822002116. 3, 5

[30] Kumar, A., Hossain, R. A., Yost, S. A., Bu, W., *et al.* Structural insights into hepatitis C virus receptor binding and entry. *Nature*, **598**(7881): 521–525 (2021). doi:10.1038/s41586-021-03913-5. 3, 5, 10, 17

[31] Torrents de la Peña, A., Sliepen, K., Eshun-Wilson, L., Newby, M. L., *et al.* Structure of the hepatitis C virus E1E2 glycoprotein complex. *Science*, **378**(6617): 263–269 (2022). doi:10.1126/science.abn9884. 3, 5, 10

[32] Vietheer, P. T., Boo, I., Gu, J., McCaffrey, K., *et al.* The core domain of hepatitis C virus glycoprotein E2 generates potent cross-neutralizing antibodies in guinea pigs. *Hepatology*, **65**(4): 1117–1131 (2017). doi:10.1002/hep.28989. 3

[33] Donnison, T., McGregor, J., Chinnakannan, S., Hutchings, C., *et al.* A pan-genotype hepatitis C virus viral vector vaccine generates T cells and neutralizing antibodies in mice. *Hepatology*, **76**(4): 1190–1202 (2022). doi:10.1002/hep.32470. 3

[34] Lindenbach, B. D. & Rice, C. M. The ins and outs of hepatitis C virus entry and assembly. *Nature Reviews Microbiology*, **11**(10): 688–700 (2013). doi:10.1038/nrmicro3098. 3, 4, 5, 10

[35] Niepmann, M. Hepatitis C Virus RNA Translation. In Bartenschlager, R. (ed.), Hepatitis C Virus: From Molecular Virology to Antiviral Therapy, volume 369, pp. 143–166. Springer Berlin Heidelberg, Berlin, Heidelberg (2013). ISBN 978-3-642-27339-1 978-3-642-27340-7. doi:10.1007/978-3-642-27340-7_6. Series Title: Current Topics in Microbiology and Immunology. 3, 10

[36] Niepmann, M. & Gerresheim, G. K. Hepatitis C Virus Translation Regulation. *International Journal of Molecular Sciences*, **21**(7): 2328 (2020). doi:10.3390/ijms21072328. 3, 10, 77

[37] Kunden, R. D., Khan, J. Q., Ghezelbash, S., & Wilson, J. A. The Role of the Liver-Specific microRNA, miRNA-122 in the HCV Replication Cycle. *International Journal of Molecular Sciences*, **21**(16): 5677 (2020). doi:10.3390/ijms21165677. 3

[38] Thibault, P. A., Huys, A., Amador-Cañizares, Y., Gailius, J. E., *et al.* Regulation of Hepatitis C Virus Genome Replication by Xrn1 and MicroRNA-122 Binding to Individual Sites in the 5' Untranslated Region. *Journal of Virology*, **89**(12): 6294–6311 (2015). doi:10.1128/JVI.03631-14.

[39] Chahal, J., Gebert, L. F. R., Gan, H. H., Camacho, E., *et al.* miR-122 and Ago interactions with the HCV genome alter the structure of the viral 5' terminus. *Nucleic Acids Research*, **47**(10): 5307–5324 (2019). doi:10.1093/nar/gkz194. 3

[40] Kim, Y. K., Lee, S. H., Kim, C. S., Seol, S. K., & Jang, S. K. Long-range RNA–RNA interaction between the 5' nontranslated region and the core-coding sequences of

hepatitis C virus modulates the IRES-dependent translation. *RNA*, **9**(5): 599–606 (2003). doi:10.1261/rna.2185603. 3, 77

[41] Romero-López, C. & Berzal-Herranz, A. A long-range RNA–RNA interaction between the 5' and 3' ends of the HCV genome. *RNA*, **15**(9): 1740–1752 (2009). doi:10.1261/rna.1680809. 4, 77

[42] Pirakitikulr, N., Kohlway, A., Lindenbach, B. D., & Pyle, A. M. The Coding Region of the HCV Genome Contains a Network of Regulatory RNA Structures. *Molecular Cell*, **62**(1): 111–120 (2016). doi:10.1016/j.molcel.2016.01.024. 3, 4, 77

[43] Ye, L., Ambi, U. B., Olguin-Nava, M., Gribling-Burrer, A.-S., *et al.* RNA Structures and Their Role in Selective Genome Packaging. *Viruses*, **13**(9): 1788 (2021). doi:10.3390/v13091788. 3, 4

[44] Shetty, S., Stefanovic, S., & Mihailescu, M. R. Hepatitis C virus RNA: molecular switches mediated by long-range RNA–RNA interactions? *Nucleic Acids Research*, **41**(4): 2526–2540 (2013). doi:10.1093/nar/gks1318. 3, 4, 77

[45] Lee, H., Shin, H., Wimmer, E., & Paul, A. V. *cis* -Acting RNA Signals in the NS5B C-Terminal Coding Sequence of the Hepatitis C Virus Genome. *Journal of Virology*, **78**(20): 10865–10877 (2004). doi:10.1128/JVI.78.20.10865-10877.2004.

[46] You, S., Stump, D. D., Branch, A. D., & Rice, C. M. A *cis* -Acting Replication Element in the Sequence Encoding the NS5B RNA-Dependent RNA Polymerase Is Required for Hepatitis C Virus RNA Replication. *Journal of Virology*, **78**(3): 1352–1366 (2004). doi:10.1128/JVI.78.3.1352-1366.2004.

[47] Shi, G., Ando, T., Suzuki, R., Matsuda, M., *et al.* Involvement of the 3' Untranslated Region in Encapsidation of the Hepatitis C Virus. *PLOS Pathogens*, **12**(2): e1005441 (2016). doi:10.1371/journal.ppat.1005441. 4

[48] Romero-López, C., Barroso-delJesus, A., García-Sacristán, A., Briones, C., & Berzal-Herranz, A. End-to-end crosstalk within the hepatitis C virus genome mediates the conformational switch of the 3'X-tail region. *Nucleic Acids Research*, **42**(1): 567–582 (2014). doi:10.1093/nar/gkt841. 4

[49] Marques, J. T., Devosse, T., Wang, D., Zamanian-Daryoush, M., *et al.* A structural basis for discriminating between self and nonself double-stranded RNAs in mammalian cells. *Nature Biotechnology*, **24**(5): 559–565 (2006). doi:10.1038/nbt1205. 4

[50] Onoguchi, K., Yoneyama, M., & Fujita, T. Retinoic Acid-Inducible Gene-I-Like Receptors. *Journal of Interferon & Cytokine Research*, **31**(1): 27–31 (2011). doi:10.1089/jir.2010.0057.

[51] Nallagatla, S. R., Hwang, J., Toroney, R., Zheng, X., *et al.* 5'-Triphosphate-Dependent Activation of PKR by RNAs with Short Stem-Loops. *Science*, **318**(5855): 1455–1458 (2007). doi:10.1126/science.1147347.

[52] Saito, T., Owen, D. M., Jiang, F., Marcotrigiano, J., & Gale, M. Innate immunity induced by composition-dependent RIG-I recognition of hepatitis C virus RNA. *Nature*, **454**(7203): 523–527 (2008). doi:10.1038/nature07106. 4, 13

[53] Shulman, Z. & Stern-Ginossar, N. The RNA modification N6-methyladenosine as a novel regulator of the immune system. *Nature Immunology*, **21**(5): 501–512 (2020). doi:10.1038/s41590-020-0650-4. 4

[54] Gokhale, N. S., McIntyre, A. B., McFadden, M. J., Roder, A. E., *et al.* N6 - Methyladenosine in Flaviviridae Viral RNA Genomes Regulates Infection. *Cell Host & Microbe*, **20**(5): 654–665 (2016). doi:10.1016/j.chom.2016.09.015. 4

[55] Kim, G.-W. & Siddiqui, A. N6-methyladenosine modification of HCV RNA genome regulates cap-independent IRES-mediated translation via YTHDC2 recognition. *Proceedings of the National Academy of Sciences*, **118**(10): e2022024118 (2021). doi:10.1073/pnas.2022024118.

[56] Durbin, A. F., Wang, C., Marcotrigiano, J., & Gehrke, L. RNAs Containing Modified Nucleotides Fail To Trigger RIG-I Conformational Changes for Innate Immune Signaling. *mBio*, **7**(5): e00833–16 (2016). doi:10.1128/mBio.00833-16.

[57] Lu, M., Zhang, Z., Xue, M., Zhao, B. S., *et al.* N6-methyladenosine modification enables viral RNA to escape recognition by RNA sensor RIG-I. *Nature Microbiology*, **5**(4): 584–598 (2020). doi:10.1038/s41564-019-0653-9. 4

[58] Lindenbach, B. D. & Rice, C. M. Unravelling hepatitis C virus replication from genome to function. *Nature*, **436**(7053): 933–938 (2005). doi:10.1038/nature04077. 4, 10

[59] Moradpour, D. & Penin, F. Hepatitis C Virus Proteins: From Structure to Function. In Bartenschlager, R. (ed.), Hepatitis C Virus: From Molecular Virology to Antiviral Therapy, volume 369, pp. 113–142. Springer Berlin Heidelberg, Berlin, Heidelberg (2013). ISBN 978-3-642-27339-1 978-3-642-27340-7. doi:10.1007/978-3-642-27340-7_5. Series Title: Current Topics in Microbiology and Immunology. 4, 5, 8, 11

[60] Gawlik, K. & Gallay, P. A. HCV core protein and virus assembly: what we know without structures. *Immunologic Research*, **60**(1): 1–10 (2014). doi:10.1007/s12026-014-8494-3. 4

[61] Fromentin, R., Majeau, N., Gagné, M.-E. L., Boivin, A., *et al.* A method for in vitro assembly of hepatitis C virus core protein and for screening of inhibitors. *Analytical Biochemistry*, **366**(1): 37–45 (2007). doi:10.1016/j.ab.2007.03.033. 4

[62] Boulant, S., Montserret, R., Hope, R. G., Ratinier, M., *et al.* Structural Determinants That Target the Hepatitis C Virus Core Protein to Lipid Droplets. *Journal of Biological Chemistry*, **281**(31): 22236–22247 (2006). doi:10.1074/jbc.M601031200. 4, 11

[63] Hundt, J. Post-translational modifications of hepatitis C viral proteins and their biological significance. *World Journal of Gastroenterology*, **19**(47): 8929 (2013). doi:10.3748/wjg.v19.i47.8929. 4, 5, 7, 10

[64] Shavinskaya, A., Boulant, S., Penin, F., McLauchlan, J., & Bartenschlager, R. The Lipid Droplet Binding Domain of Hepatitis C Virus Core Protein Is a Major Determinant for Efficient Virus Assembly. *Journal of Biological Chemistry*, **282**(51): 37158–37169 (2007). doi:10.1074/jbc.M707329200. 4, 11

[65] Okamoto, K., Mori, Y., Komoda, Y., Okamoto, T., *et al.* Intramembrane Processing by Signal Peptide Peptidase Regulates the Membrane Localization of Hepatitis C Virus Core Protein and Viral Propagation. *Journal of Virology*, **82**(17): 8349–8361 (2008). doi:10.1128/JVI.00306-08. 4

[66] Majeau, N., Fromentin, R., Savard, C., Duval, M., *et al.* Palmitoylation of Hepatitis C Virus Core Protein Is Important for Virion Production. *Journal of Biological Chemistry*, **284**(49): 33915–33925 (2009). doi:10.1074/jbc.M109.018549. 4

[67] Ajjaji, D., Ben M'barek, K., Boson, B., Omrane, M., *et al.* Hepatitis C virus core protein uses triacylglycerols to fold onto the endoplasmic reticulum membrane. *Traffic*, **23**(1): 63–80 (2022). doi:10.1111/tra.12825. 4, 12

[68] Boson, B., Mialon, C., Schichl, K., Denolly, S., & Cosset, F.-L. Nup98 Is Subverted from Annulate Lamellae by Hepatitis C Virus Core Protein to Foster Viral Assembly. *mBio*, **13**(2): e02923–21 (2022). doi:10.1128/mbio.02923-21. 4, 12

[69] Mahmoudvand, S., Shokri, S., Taherkhani, R., & Farshadpour, F. Hepatitis C virus core protein modulates several signaling pathways involved in hepato-

cellular carcinoma. *World Journal of Gastroenterology*, **25**(1): 42–58 (2019). doi:10.3748/wjg.v25.i1.42. 4, 5

[70] Mani, H., Yen, J.-H., Hsu, H.-J., Chang, C.-C., & Liou, J.-W. Hepatitis C virus core protein: Not just a nucleocapsid building block, but an immunity and inflammation modulator. *Tzu Chi Medical Journal*, **34**(2): 139 (2022). doi:10.4103/tcmj.tcmj$_9$7$_2$1. 4, 5

[71] Blindenbacher, A., Duong, F. H., Hunziker, L., Stutvoet, S. T., *et al.* Expression of hepatitis c virus proteins inhibits interferon α signaling in the liver of transgenic mice. *Gastroenterology*, **124**(5): 1465–1475 (2003). doi:10.1016/S0016-5085(03)00290-7. 4, 14

[72] Lin, W., Kim, S. S., Yeung, E., Kamegaya, Y., *et al.* Hepatitis C Virus Core Protein Blocks Interferon Signaling by Interaction with the STAT1 SH2 Domain. *Journal of Virology*, **80**(18): 9226–9235 (2006). doi:10.1128/JVI.00459-06. 4, 14, 78

[73] Chung, Y. M., Park, K. J., Choi, S. Y., Hwang, S. B., & Lee, S. Y. Hepatitis C Virus Core Protein Potentiates TNF-α-Induced NF-κB Activation through TRAF2-IKKβ-Dependent Pathway. *Biochemical and Biophysical Research Communications*, **284**(1): 15–19 (2001). doi:10.1006/bbrc.2001.4936. 5, 81

[74] Devi, P., Punga, T., & Bergqvist, A. Activation of the Ca2+/NFAT Pathway by Assembly of Hepatitis C Virus Core Protein into Nucleocapsid-like Particles. *Viruses*, **14**(4): 761 (2022). doi:10.3390/v14040761.

[75] Saito, K., Meyer, K., Warner, R., Basu, A., *et al.* Hepatitis C Virus Core Protein Inhibits Tumor Necrosis Factor Alpha-Mediated Apoptosis by a Protective Effect Involving Cellular FLICE Inhibitory Protein. *Journal of Virology*, **80**(9): 4372–4379 (2006). doi:10.1128/JVI.80.9.4372-4379.2006.

[76] Imran, M., Waheed, Y., Manzoor, S., Bilal, M., *et al.* Interaction of Hepatitis C virus proteins with pattern recognition receptors. *Virology Journal*, **9**(1): 126 (2012). doi:10.1186/1743-422X-9-126.

[77] Liu, B., Ma, X., Wang, Q., Luo, S., *et al.* Marmoset Viral Hepatic Inflammation Induced by Hepatitis C Virus Core Protein via IL-32. *Frontiers in Cellular and Infection Microbiology*, **10**: 135 (2020). doi:10.3389/fcimb.2020.00135. 5

[78] Vieyres, G., Dubuisson, J., & Pietschmann, T. Incorporation of Hepatitis C Virus E1 and E2 Glycoproteins: The Keystones on a Peculiar Virion. *Viruses*, **6**(3): 1149–1187 (2014). doi:10.3390/v6031149. 5, 11, 12

[79] Shanmugam, S. & Yi, M. Efficiency of E2-p7 Processing Modulates Production of Infectious Hepatitis C Virus. *Journal of Virology*, **87**(20): 11255–11266 (2013). doi:10.1128/JVI.01807-13.

[80] Cocquerel, L. Topological changes in the transmembrane domains of hepatitis C virus envelope glycoproteins. *The EMBO Journal*, **21**(12): 2893–2902 (2002). doi:10.1093/emboj/cdf295. 5

[81] Tong, Y., Lavillette, D., Li, Q., & Zhong, J. Role of Hepatitis C Virus Envelope Glycoprotein E1 in Virus Entry and Assembly. *Frontiers in Immunology*, **9**: 1411 (2018). doi:10.3389/fimmu.2018.01411. 5

[82] Alzahrani, N., Wu, M.-J., Sousa, C. F., Kalinina, O. V., *et al.* SPCS1-Dependent E2-p7 processing determines HCV Assembly efficiency. *PLOS Pathogens*, **18**(2): e1010310 (2022). doi:10.1371/journal.ppat.1010310. 5, 11

[83] Vieyres, G., Thomas, X., Descamps, V., Duverlie, G., *et al.* Characterization of the Envelope Glycoproteins Associated with Infectious Hepatitis C Virus. *Journal of Virology*, **84**(19): 10159–10168 (2010). doi:10.1128/JVI.01180-10. 5, 12

[84] Goffard, A., Callens, N., Bartosch, B., Wychowski, C., *et al.* Role of N-Linked Glycans in the Functions of Hepatitis C Virus Envelope Glycoproteins. *Journal of Virology*, **79**(13): 8400–8409 (2005). doi:10.1128/JVI.79.13.8400-8409.2005. 5

[85] Pileri, P., Uematsu, Y., Campagnoli, S., Galli, G., *et al.* Binding of Hepatitis C Virus to CD81. *Science*, **282**(5390): 938–941 (1998). doi:10.1126/science.282.5390.938. 5, 9, 17

[86] Scarselli, E., Ansuini, H., Cerino, R., Roccasecca, R. M., *et al.* The human scavenger receptor class B type I is a novel candidate receptor for the hepatitis C virus. *The EMBO Journal*, **21**(19): 5017–5025 (2002). doi:10.1093/emboj/cdf529. 9

[87] Cormier, E. G., Tsamis, F., Kajumo, F., Durso, R. J., *et al.* CD81 is an entry coreceptor for hepatitis C virus. *Proceedings of the National Academy of Sciences*, **101**(19): 7270–7274 (2004). doi:10.1073/pnas.0402253101. 5, 9, 17

[88] Yost, S. A., Wang, Y., & Marcotrigiano, J. Hepatitis C Virus Envelope Glycoproteins: A Balancing Act of Order and Disorder. *Frontiers in Immunology*, **9**: 1917 (2018). doi:10.3389/fimmu.2018.01917. 5

[89] Atoom, A. M., Taylor, N. G., & Russell, R. S. The elusive function of the hepatitis C virus p7 protein. *Virology*, **462-463**: 377–387 (2014). doi:10.1016/j.virol.2014.04.018. 5

[90] Montserret, R., Saint, N., Vanbelle, C., Salvay, A. G., *et al.* NMR Structure and Ion Channel Activity of the p7 Protein from Hepatitis C Virus. *Journal of Biological Chemistry*, **285**(41): 31446–31461 (2010). doi:10.1074/jbc.M110.122895. 5

[91] OuYang, B., Xie, S., Berardi, M. J., Zhao, X., *et al.* Unusual architecture of the p7 channel from hepatitis C virus. *Nature*, **498**(7455): 521–525 (2013). doi:10.1038/nature12283. 5

[92] Griffin, S., Clarke, D., McCormick, C., Rowlands, D., & Harris, M. Signal Peptide Cleavage and Internal Targeting Signals Direct the Hepatitis C Virus p7 Protein to Distinct Intracellular Membranes. *Journal of Virology*, **79**(24): 15525–15536 (2005). doi:10.1128/JVI.79.24.15525-15536.2005. 5

[93] Pavlović, D., Neville, D. C. A., Argaud, O., Blumberg, B., *et al.* The hepatitis C virus p7 protein forms an ion channel that is inhibited by long-alkyl-chain iminosugar derivatives. *Proceedings of the National Academy of Sciences*, **100**(10): 6104–6108 (2003). doi:10.1073/pnas.1031527100. 5

[94] Luik, P., Chew, C., Aittoniemi, J., Chang, J., *et al.* The 3-dimensional structure of a hepatitis C virus p7 ion channel by electron microscopy. *Proceedings of the National Academy of Sciences*, **106**(31): 12712–12716 (2009). doi:10.1073/pnas.0905966106.

[95] Clarke, D., Griffin, S., Beales, L., Gelais, C. S., *et al.* Evidence for the Formation of a Heptameric Ion Channel Complex by the Hepatitis C Virus P7 Protein in Vitro. *Journal of Biological Chemistry*, **281**(48): 37057–37068 (2006). doi:10.1074/jbc.M602434200.

[96] Oestringer, B. P., Bolivar, J. H., Hensen, M., Claridge, J. K., *et al.* Re-evaluating the p7 viroporin structure. *Nature*, **562**(7727): E8–E18 (2018). doi:10.1038/s41586-018-0561-9.

[97] Chen, W., OuYang, B., & Chou, J. J. Chen et al. reply. *Nature*, **562**(7727): E19–E20 (2018). doi:10.1038/s41586-018-0562-8.

[98] Chen, W., Dev, J., Mezhyrova, J., Pan, L., *et al.* The Unusual Transmembrane Partition of the Hexameric Channel of the Hepatitis C Virus. *Structure*, **26**(4): 627–634.e4 (2018). doi:10.1016/j.str.2018.02.011.

[99] Lee, H.-R., Lee, G. Y., You, D.-G., Kim, H. K., & Yoo, Y. D. Hepatitis C Virus p7 Induces Membrane Permeabilization by Interacting with Phosphatidylserine. *International Journal of Molecular Sciences*, **21**(3): 897 (2020). doi:10.3390/ijms21030897.

[100] Steinmann, E., Penin, F., Kallis, S., Patel, A. H., *et al.* Hepatitis C Virus p7 Protein Is Crucial for Assembly and Release of Infectious Virions. *PLoS Pathogens*, **3**(7): e103 (2007). doi:10.1371/journal.ppat.0030103. 5, 11, 28

[101] Bentham, M. J., Foster, T. L., McCormick, C., & Griffin, S. Mutations in hepatitis C virus p7 reduce both the egress and infectivity of assembled particles via impaired proton channel function. *Journal of General Virology*, **94**(10): 2236–2248 (2013). doi:10.1099/vir.0.054338-0. 5

[102] Atoom, A. M., Jones, D. M., & Russell, R. S. Evidence suggesting that HCV p7 protects E2 glycoprotein from premature degradation during virus production. *Virus Research*, **176**(1-2): 199–210 (2013). doi:10.1016/j.virusres.2013.06.008.

[103] Wozniak, A. L., Griffin, S., Rowlands, D., Harris, M., *et al.* Intracellular Proton Conductance of the Hepatitis C Virus p7 Protein and Its Contribution to Infectious Virus Production. *PLoS Pathogens*, **6**(9): e1001087 (2010). doi:10.1371/journal.ppat.1001087.

[104] Madan, V. & Bartenschlager, R. Structural and Functional Properties of the Hepatitis C Virus p7 Viroporin. *Viruses*, **7**(8): 4461–4481 (2015). doi:10.3390/v7082826. 5

[105] Boson, B., Granio, O., Bartenschlager, R., & Cosset, F.-L. A Concerted Action of Hepatitis C Virus P7 and Nonstructural Protein 2 Regulates Core Localization at the Endoplasmic Reticulum and Virus Assembly. *PLoS Pathogens*, **7**(7): e1002144 (2011). doi:10.1371/journal.ppat.1002144. 11

[106] Duan, X., Anwar, M. I., Xu, Z., Ma, L., *et al.* Adaptive mutation F772S-enhanced p7-NS4A cooperation facilitates the assembly and release of hepatitis C virus and is associated with lipid droplet enlargement. *Emerging Microbes & Infections*, **7**(1): 1–14 (2018). doi:10.1038/s41426-018-0140-z.

[107] Gentzsch, J., Brohm, C., Steinmann, E., Friesland, M., *et al.* Hepatitis C Virus p7 is Critical for Capsid Assembly and Envelopment. *PLoS Pathogens*, **9**(5): e1003355 (2013). doi:10.1371/journal.ppat.1003355. 11, 12

[108] Tedbury, P., Welbourn, S., Pause, A., King, B., *et al.* The subcellular localization of the hepatitis C virus non-structural protein NS2 is regulated by an ion channel-independent function of the p7 protein. *Journal of General Virology*, **92**(4): 819–830 (2011). doi:10.1099/vir.0.027441-0. 5, 11

[109] Qi, H., Chu, V., Wu, N. C., Chen, Z., *et al.* Systematic identification of anti-interferon function on hepatitis C virus genome reveals p7 as an immune evasion

protein. *Proceedings of the National Academy of Sciences*, **114**(8): 2018–2023 (2017). doi:10.1073/pnas.1614623114. 5

[110] Convery, O., Gargan, S., Kickham, M., Schroder, M., *et al.* The hepatitis C virus (HCV) protein, p7, suppresses inflammatory responses to tumor necrosis factor (TNF)- α *via* signal transducer and activator of transcription (STAT)3 and extracellular signal-regulated kinase (ERK)–mediated induction of suppressor of cytokine signaling (SOCS)3. *The FASEB Journal*, **33**(8): 8732–8744 (2019). doi:10.1096/fj.201800629RR.

[111] Wei, S., Hu, X., Du, L., Zhao, L., *et al.* Inhibitor Development against p7 Channel in Hepatitis C Virus. *Molecules*, **26**(5): 1350 (2021). doi:10.3390/molecules26051350. 5

[112] Suzuki, T. & Suzuki, R. Role of Nonstructural Proteins in HCV Replication. In Miyamura, T., Lemon, S. M., Walker, C. M., & Wakita, T. (eds.), Hepatitis C Virus I, pp. 129–148. Springer Japan, Tokyo (2016). ISBN 978-4-431-56096-8 978-4-431-56098-2. doi:10.1007/978-4-431-56098-2_7. 5, 6, 7, 8

[113] Jirasko, V., Montserret, R., Appel, N., Janvier, A., *et al.* Structural and Functional Characterization of Nonstructural Protein 2 for Its Role in Hepatitis C Virus Assembly. *Journal of Biological Chemistry*, **283**(42): 28546–28562 (2008). doi:10.1074/jbc.M803981200. 6, 11

[114] Phan, T., Beran, R. K. F., Peters, C., Lorenz, I. C., & Lindenbach, B. D. Hepatitis C Virus NS2 Protein Contributes to Virus Particle Assembly via Opposing Epistatic Interactions with the E1-E2 Glycoprotein and NS3-NS4A Enzyme Complexes. *Journal of Virology*, **83**(17): 8379–8395 (2009). doi:10.1128/JVI.00891-09. 5

[115] Jirasko, V., Montserret, R., Lee, J. Y., Gouttenoire, J., *et al.* Structural and Functional Studies of Nonstructural Protein 2 of the Hepatitis C Virus Reveal Its Key Role as Organizer of Virion Assembly. *PLoS Pathogens*, **6**(12): e1001233 (2010). doi:10.1371/journal.ppat.1001233. 6, 11

[116] Lorenz, I. C., Marcotrigiano, J., Dentzer, T. G., & Rice, C. M. Structure of the catalytic domain of the hepatitis C virus NS2-3 protease. *Nature*, **442**(7104): 831–835 (2006). doi:10.1038/nature04975. 6

[117] Schregel, V., Jacobi, S., Penin, F., & Tautz, N. Hepatitis C virus NS2 is a protease stimulated by cofactor domains in NS3. *Proceedings of the National Academy of Sciences*, **106**(13): 5342–5347 (2009). doi:10.1073/pnas.0810950106. 6

[118] Wu, M.-J., Shanmugam, S., Welsch, C., & Yi, M. Palmitoylation of Hepatitis C Virus NS2 Regulates Its Subcellular Localization and NS2-NS3 Autocleavage. *Journal of Virology*, **94**(1): e00906–19 (2019). doi:10.1128/JVI.00906-19.

[119] Isken, O., Walther, T., Wong-Dilworth, L., Rehders, D., *et al.* Identification of NS2 determinants stimulating intrinsic HCV NS2 protease activity. *PLOS Pathogens*, **18**(6): e1010644 (2022). doi:10.1371/journal.ppat.1010644.

[120] Welbourn, S., Green, R., Gamache, I., Dandache, S., *et al.* Hepatitis C Virus NS2/3 Processing Is Required for NS3 Stability and Viral RNA Replication. *Journal of Biological Chemistry*, **280**(33): 29604–29611 (2005). doi:10.1074/jbc.M505019200. 6

[121] Jones, C. T., Murray, C. L., Eastman, D. K., Tassello, J., & Rice, C. M. Hepatitis C Virus p7 and NS2 Proteins Are Essential for Production of Infectious Virus. *Journal of Virology*, **81**(16): 8374–8383 (2007). doi:10.1128/JVI.00690-07. 6, 11

[122] Suzuki, R., Matsuda, M., Watashi, K., Aizaki, H., *et al.* Signal Peptidase Complex Subunit 1 Participates in the Assembly of Hepatitis C Virus through an Interaction with E2 and NS2. *PLoS Pathogens*, **9**(8): e1003589 (2013). doi:10.1371/journal.ppat.1003589. 11

[123] Xiao, F., Wang, S., Barouch-Bentov, R., Neveu, G., *et al.* Interactions between the Hepatitis C Virus Nonstructural 2 Protein and Host Adaptor Proteins 1 and 4 Orchestrate Virus Release. *mBio*, **9**(2): e02233–17 (2018). doi:10.1128/mBio.02233-17. 12

[124] Kumar, S., Barouch-Bentov, R., Xiao, F., Schor, S., *et al.* MARCH8 Ubiquitinates the Hepatitis C Virus Nonstructural 2 Protein and Mediates Viral Envelopment. *Cell Reports*, **26**(7): 1800–1814.e5 (2019). doi:10.1016/j.celrep.2019.01.075. 6

[125] von dem Bussche, A., Machida, R., Li, K., Loevinsohn, G., *et al.* Hepatitis C virus NS2 protein triggers endoplasmic reticulum stress and suppresses its own viral replication. *Journal of Hepatology*, **53**(5): 797–804 (2010). doi:10.1016/j.jhep.2010.05.022. 6

[126] Kaukinen, P., Sillanpää, M., Nousiainen, L., Melén, K., & Julkunen, I. Hepatitis C virus NS2 protease inhibits host cell antiviral response by inhibiting IKKε and TBK1 functions. *Journal of Medical Virology*, **85**(1): 71–82 (2013). doi:10.1002/jmv.23442.

[127] Chen, S., Wu, Z., Wang, M., & Cheng, A. Innate Immune Evasion Mediated by Flaviviridae Non-Structural Proteins. *Viruses*, **9**(10): 291 (2017). doi:10.3390/v9100291. 6, 78

[128] Zhou, H., Qian, Q., Shu, T., Xu, J., *et al.* Hepatitis C Virus NS2 Protein Suppresses RNA Interference in Cells. *Virologica Sinica*, **35**(4): 436–444 (2020). doi:10.1007/s12250-019-00182-5. 6

[129] Raney, K. D., Sharma, S. D., Moustafa, I. M., & Cameron, C. E. Hepatitis C virus non-structural protein 3 (HCV NS3): a multifunctional antiviral target. *The Journal of Biological Chemistry*, **285**(30): 22725–22731 (2010). doi:10.1074/jbc.R110.125294. 6

[130] Bartenschlager, R., Ahlborn-Laake, L., Mous, J., & Jacobsen, H. Kinetic and structural analyses of hepatitis C virus polyprotein processing. *Journal of Virology*, **68**(8): 5045–5055 (1994). doi:10.1128/jvi.68.8.5045-5055.1994. 6

[131] Failla, C., Tomei, L., & De Francesco, R. Both NS3 and NS4A are required for proteolytic processing of hepatitis C virus nonstructural proteins. *Journal of Virology*, **68**(6): 3753–3760 (1994). doi:10.1128/jvi.68.6.3753-3760.1994. 6

[132] Brass, V., Berke, J. M., Montserret, R., Blum, H. E., *et al.* Structural determinants for membrane association and dynamic organization of the hepatitis C virus NS3-4A complex. *Proceedings of the National Academy of Sciences*, **105**(38): 14545–14550 (2008). doi:10.1073/pnas.0807298105. 6

[133] Love, R. A., Parge, H. E., Wickersham, J. A., Hostomsky, Z., *et al.* The Crystal Structure of Hepatitis C Virus NS3 Proteinase Reveals a Trypsin-like Fold and a Structural Zinc Binding Site. *Cell*, **87**(2): 331–342 (1996). doi:10.1016/S0092-8674(00)81350-1. 6

[134] Bartenschlager, R., Ahlborn-Laake, L., Yasargil, K., Mous, J., & Jacobsen, H. Substrate determinants for cleavage in cis and in trans by the hepatitis C virus NS3 proteinase. *Journal of Virology*, **69**(1): 198–205 (1995). doi:10.1128/jvi.69.1.198-205.1995. 6

[135] Lin, C., Prágai, B. M., Grakoui, A., Xu, J., & Rice, C. M. Hepatitis C virus NS3 serine proteinase: trans-cleavage requirements and processing kinetics. *Journal of Virology*, **68**(12): 8147–8157 (1994). doi:10.1128/jvi.68.12.8147-8157.1994. 6

[136] Ferreira, A. R., Magalhães, A. C., Camões, F., Gouveia, A., *et al.* Hepatitis C virus NS3-4A inhibits the peroxisomal MAVS-dependent antiviral signalling response. *Journal of Cellular and Molecular Medicine*, **20**(4): 750–757 (2016). doi:10.1111/jcmm.12801. 6, 14

[137] Gagné, B., Tremblay, N., Park, A. Y., Baril, M., & Lamarre, D. Importin β1 targeting by hepatitis C virus NS3/4A protein restricts IRF3 and NF-κB signaling of IFNB1 antiviral response. *Traffic*, **18**(6): 362–377 (2017). doi:10.1111/tra.12480. 6, 14

[138] Tran, H. T. L., Morikawa, K., Anggakusuma, Zibi, R., *et al.* OCIAD1 is a host mitochondrial substrate of the hepatitis C virus NS3-4A protease. *PLOS ONE*, **15**(7): e0236447 (2020). doi:10.1371/journal.pone.0236447. 6

[139] McCauley, J. A. & Rudd, M. T. Hepatitis C virus NS3/4a protease inhibitors. *Current Opinion in Pharmacology*, **30**: 84–92 (2016). doi:10.1016/j.coph.2016.07.015. 6

[140] Kim, D., Gwack, Y., Han, J., & Choe, J. C-Terminal Domain of the Hepatitis C Virus NS3 Protein Contains an RNA Helicase Activity. *Biochemical and Biophysical Research Communications*, **215**(1): 160–166 (1995). doi:10.1006/bbrc.1995.2447. 6

[141] Dumont, S., Cheng, W., Serebrov, V., Beran, R. K., *et al.* RNA translocation and unwinding mechanism of HCV NS3 helicase and its coordination by ATP. *Nature*, **439**(7072): 105–108 (2006). doi:10.1038/nature04331.

[142] Hara, H., Aizaki, H., Matsuda, M., Shinkai-Ouchi, F., *et al.* Involvement of Creatine Kinase B in Hepatitis C Virus Genome Replication through Interaction with the Viral NS4A Protein. *Journal of Virology*, **83**(10): 5137–5147 (2009). doi:10.1128/JVI.02179-08.

[143] Gu, M. & Rice, C. M. The Spring α-Helix Coordinates Multiple Modes of HCV (Hepatitis C Virus) NS3 Helicase Action. *Journal of Biological Chemistry*, **291**(28): 14499–14509 (2016). doi:10.1074/jbc.M115.704379.

[144] Lebsir, N., Goueslain, L., Farhat, R., Callens, N., *et al.* Functional and Physical Interaction between the Arf Activator GBF1 and Hepatitis C Virus NS3 Protein. *Journal of Virology*, **93**(6): e01459–18 (2019). doi:10.1128/JVI.01459-18. 6

[145] Suzuki, R., Saito, K., Kato, T., Shirakura, M., *et al.* Trans-complemented hepatitis C virus particles as a versatile tool for study of virus assembly and infection. *Virology*, **432**(1): 29–38 (2012). doi:10.1016/j.virol.2012.05.033. 6

[146] Ma, Y., Yates, J., Liang, Y., Lemon, S. M., & Yi, M. NS3 Helicase Domains Involved in Infectious Intracellular Hepatitis C Virus Particle Assembly. *Journal of Virology*, **82**(15): 7624–7639 (2008). doi:10.1128/JVI.00724-08. 11

[147] Jones, D. M., Atoom, A. M., Zhang, X., Kottilil, S., & Russell, R. S. A Genetic Interaction between the Core and NS3 Proteins of Hepatitis C Virus Is Essential for Production of Infectious Virus. *Journal of Virology*, **85**(23): 12351–12361 (2011). doi:10.1128/JVI.05313-11. 11

[148] Chiang, C.-H., Lai, Y.-L., Huang, Y.-N., Yu, C.-C., *et al.* Sequential Phosphorylation of the Hepatitis C Virus NS5A Protein Depends on NS3-Mediated Autocleavage between NS3 and NS4A. *Journal of Virology*, **94**(19): e00420–20 (2020). doi:10.1128/JVI.00420-20. 6, 7

[149] Vazquez, C., Tan, C. Y., & Horner, S. M. Hepatitis C Virus Infection Is Inhibited by a Noncanonical Antiviral Signaling Pathway Targeted by NS3-NS4A. *Journal of Virology*, **93**(23): e00725–19 (2019). doi:10.1128/JVI.00725-19. 6, 78

[150] Zhu, Y.-P., Peng, Z.-G., Wu, Z.-Y., Li, J.-R., *et al.* Host APOBEC3G Protein Inhibits HCV Replication through Direct Binding at NS3. *PLOS ONE*, **10**(3): e0121608 (2015). doi:10.1371/journal.pone.0121608.

[151] Qian, X., Xu, C., Zhao, P., & Qi, Z. Long non-coding RNA GAS5 inhibited hepatitis C virus replication by binding viral NS3 protein. *Virology*, **492**: 155–165 (2016). doi:10.1016/j.virol.2016.02.020. 6

[152] Lundin, M., Monné, M., Widell, A., von Heijne, G., & Persson, M. A. A. Topology of the Membrane-Associated Hepatitis C Virus Protein NS4B. *Journal of Virology*, **77**(9): 5428–5438 (2003). doi:10.1128/JVI.77.9.5428-5438.2003. 6

[153] Gouttenoire, J., Penin, F., & Moradpour, D. Hepatitis C virus nonstructural protein 4B: a journey into unexplored territory. *Reviews in Medical Virology*, **20**(2): 117–129 (2010). doi:10.1002/rmv.640. _eprint: https://onlinelibrary.wiley.com/doi/pdf/10.1002/rmv.640. 6

[154] Elazar, M., Liu, P., Rice, C. M., & Glenn, J. S. An N-Terminal Amphipathic Helix in Hepatitis C Virus (HCV) NS4B Mediates Membrane Association, Correct Localization of Replication Complex Proteins, and HCV RNA Replication. *Journal of Virology*, **78**(20): 11393–11400 (2004). doi:10.1128/JVI.78.20.11393-11400.2004. 6, 10

[155] Yu, G.-Y., Lee, K.-J., Gao, L., & Lai, M. M. C. Palmitoylation and Polymerization of Hepatitis C Virus NS4B Protein. *Journal of Virology*, **80**(12): 6013–6023 (2006). doi:10.1128/JVI.00053-06.

[156] Gouttenoire, J., Roingeard, P., Penin, F., & Moradpour, D. Amphipathic α-Helix AH2 Is a Major Determinant for the Oligomerization of Hepatitis C Virus Nonstructural Protein 4B. *Journal of Virology*, **84**(24): 12529–12537 (2010). doi:10.1128/JVI.01798-10.

[157] Paul, D., Romero-Brey, I., Gouttenoire, J., Stoitsova, S., *et al.* NS4B Self-Interaction through Conserved C-Terminal Elements Is Required for the Establishment of Functional Hepatitis C Virus Replication Complexes. *Journal of Virology*, **85**(14): 6963–6976 (2011). doi:10.1128/JVI.00502-11. 6

[158] Romero-Brey, I., Merz, A., Chiramel, A., Lee, J.-Y., *et al.* Three-Dimensional Architecture and Biogenesis of Membrane Structures Associated with Hepatitis C Virus Replication. *PLoS Pathogens*, **8**(12): e1003056 (2012). doi:10.1371/journal.ppat.1003056. 10

[159] Paul, D. & Bartenschlager, R. Flaviviridae Replication Organelles: Oh, What a Tangled Web We Weave. *Annual Review of Virology*, **2**(1): 289–310 (2015). doi:10.1146/annurev-virology-100114-055007. 6, 7, 10

[160] Einav, S., Elazar, M., Danieli, T., & Glenn, J. S. A Nucleotide Binding Motif in Hepatitis C Virus (HCV) NS4B Mediates HCV RNA Replication. *Journal of Virology*, **78**(20): 11288–11295 (2004). doi:10.1128/JVI.78.20.11288-11295.2004. 6

[161] David, N., Yaffe, Y., Hagoel, L., Elazar, M., *et al.* The interaction between the Hepatitis C proteins NS4B and NS5A is involved in viral replication. *Virology*, **475**: 139–149 (2015). doi:10.1016/j.virol.2014.10.021. 7, 8

[162] Biswas, A., Treadaway, J., & Tellinghuisen, T. L. Interaction between Nonstructural Proteins NS4B and NS5A Is Essential for Proper NS5A Localization and Hepatitis C Virus RNA Replication. *Journal of Virology*, **90**(16): 7205–7218 (2016). doi:10.1128/JVI.00037-16. 7, 8

[163] Kong, L., Fujimoto, A., Nakamura, M., Aoyagi, H., *et al.* Prolactin Regulatory Element Binding Protein Is Involved in Hepatitis C Virus Replication by Interaction with NS4B. *Journal of Virology*, **90**(6): 3093–3111 (2016). doi:10.1128/JVI.01540-15. 6, 10

[164] Jones, D. M., Patel, A. H., Targett-Adams, P., & McLauchlan, J. The Hepatitis C Virus NS4B Protein Can *trans* -Complement Viral RNA Replication and Modulates Production of Infectious Virus. *Journal of Virology*, **83**(5): 2163–2177 (2009). doi:10.1128/JVI.01885-08. 7

[165] Gouttenoire, J., Montserret, R., Paul, D., Castillo, R., *et al.* Aminoterminal Amphipathic α-Helix AH1 of Hepatitis C Virus Nonstructural Protein 4B Possesses a Dual Role in RNA Replication and Virus Production. *PLoS Pathogens*, **10**(11): e1004501 (2014). doi:10.1371/journal.ppat.1004501. 7

[166] Su, W.-C., Chao, T.-C., Huang, Y.-L., Weng, S.-C., *et al.* Rab5 and Class III Phosphoinositide 3-Kinase Vps34 Are Involved in Hepatitis C Virus NS4B-Induced Autophagy. *Journal of Virology*, **85**(20): 10561–10571 (2011). doi:10.1128/JVI.00173-11. 7

[167] Wang, L., Tian, Y., & Ou, J.-h. J. HCV Induces the Expression of Rubicon and UVRAG to Temporally Regulate the Maturation of Autophagosomes and Viral Replication. *PLOS Pathogens*, **11**(3): e1004764 (2015). doi:10.1371/journal.ppat.1004764. 7, 11

[168] Ding, Q., Cao, X., Lu, J., Huang, B., *et al.* Hepatitis C virus NS4B blocks the interaction of STING and TBK1 to evade host innate immunity. *Journal of Hepatology*, **59**(1): 52–58 (2013). doi:10.1016/j.jhep.2013.03.019. 7, 14

[169] Nitta, S., Sakamoto, N., Nakagawa, M., Kakinuma, S., *et al.* Hepatitis C virus NS4B protein targets STING and abrogates RIG-I-mediated type I interferon-dependent innate immunity. *Hepatology*, **57**(1): 46–58 (2013). doi:10.1002/hep.26017. 14

[170] Yi, G., Wen, Y., Shu, C., Han, Q., *et al.* Hepatitis C Virus NS4B Can Suppress STING Accumulation To Evade Innate Immune Responses. *Journal of Virology*, **90**(1): 254–265 (2016). doi:10.1128/JVI.01720-15.

[171] Liang, Y., Cao, X., Ding, Q., Zhao, Y., *et al.* Hepatitis C virus NS4B induces the degradation of TRIF to inhibit TLR3-mediated interferon signaling pathway. *PLOS Pathogens*, **14**(5): e1007075 (2018). doi:10.1371/journal.ppat.1007075. 13

[172] Li, S., Ye, L., Yu, X., Xu, B., *et al.* Hepatitis C virus NS4B induces unfolded protein response and endoplasmic reticulum overload response-dependent NF-κB activation. *Virology*, **391**(2): 257–264 (2009). doi:10.1016/j.virol.2009.06.039. 16

[173] Kong, L., Li, S., Huang, M., Xiong, Y., *et al.* The Roles of Endoplasmic Reticulum Overload Response Induced by HCV and NS4B Protein in Human Hepatocyte Viability and Virus Replication. *PLOS ONE*, **10**(4): e0123190 (2015). doi:10.1371/journal.pone.0123190.

[174] Kong, L., Li, S., Yu, X., Fang, X., *et al.* Hepatitis C virus and its protein NS4B activate the cancer-related STAT3 pathway via the endoplasmic reticulum overload

response. *Archives of Virology*, **161**(8): 2149–2159 (2016). doi:10.1007/s00705-016-2892-x.

[175] Jiang, X.-H., Xie, Y.-T., Cai, Y.-P., Ren, J., & Ma, T. Effects of hepatitis C virus core protein and nonstructural protein 4B on the Wnt/β-catenin pathway. *BMC Microbiology*, **17**(1): 124 (2017). doi:10.1186/s12866-017-1032-4. 7

[176] Penin, F., Brass, V., Appel, N., Ramboarina, S., *et al.* Structure and Function of the Membrane Anchor Domain of Hepatitis C Virus Nonstructural Protein 5A. *Journal of Biological Chemistry*, **279**(39): 40835–40843 (2004). doi:10.1074/jbc.M404761200. 7

[177] Ross-Thriepland, D. & Harris, M. Hepatitis C virus NS5A: enigmatic but still promiscuous 10 years on! *Journal of General Virology*, **96**(4): 727–738 (2015). doi:10.1099/jgv.0.000009. 7

[178] Tellinghuisen, T. L., Marcotrigiano, J., & Rice, C. M. Structure of the zinc-binding domain of an essential component of the hepatitis C virus replicase. *Nature*, **435**(7040): 374–379 (2005). doi:10.1038/nature03580. 7

[179] Liang, Y., Ye, H., Kang, C. B., & Yoon, H. S. Domain 2 of Nonstructural Protein 5A (NS5A) of Hepatitis C Virus Is Natively Unfolded. *Biochemistry*, **46**(41): 11550–11558 (2007). doi:10.1021/bi700776e. 7

[180] Liang, Y., Kang, C., & Yoon, H. S. Molecular and Structural Characterization of the Domain 2 of Hepatitis C Virus Non-structural Protein 5A. *Molecules and Cells*, **1**(22): 13–20 (2006). 7

[181] Feuerstein, S., Solyom, Z., Aladag, A., Favier, A., *et al.* Transient Structure and SH3 Interaction Sites in an Intrinsically Disordered Fragment of the Hepatitis C Virus Protein NS5A. *Journal of Molecular Biology*, **420**(4-5): 310–323 (2012). doi:10.1016/j.jmb.2012.04.023. 7

[182] Bacarizo, J., Martínez-Rodríguez, S., & Cámara-Artigas, A. Structure of the c-Src-SH3 domain in complex with a proline-rich motif of NS5A protein from the hepatitis C virus. *Journal of Structural Biology*, **189**(1): 67–72 (2015). doi:10.1016/j.jsb.2014.11.004.

[183] Sólyom, Z., Ma, P., Schwarten, M., Bosco, M., *et al.* The Disordered Region of the HCV Protein NS5A: Conformational Dynamics, SH3 Binding, and Phosphorylation. *Biophysical Journal*, **109**(7): 1483–1496 (2015). doi:10.1016/j.bpj.2015.06.040. 7

[184] Hanoulle, X., Verdegem, D., Badillo, A., Wieruszeski, J.-M., *et al.* Domain 3 of non-structural protein 5A from hepatitis C virus is natively unfolded. *Biochemical and Biophysical Research Communications*, **381**(4): 634–638 (2009). doi:10.1016/j.bbrc.2009.02.108. 7

[185] Lim, P. J., Chatterji, U., Cordek, D., Sharma, S. D., *et al.* Correlation between NS5A Dimerization and Hepatitis C Virus Replication. *Journal of Biological Chemistry*, **287**(36): 30861–30873 (2012). doi:10.1074/jbc.M112.376822. 7

[186] Yin, C., Goonawardane, N., Stewart, H., & Harris, M. A role for domain I of the hepatitis C virus NS5A protein in virus assembly. *PLOS Pathogens*, **14**(1): e1006834 (2018). doi:10.1371/journal.ppat.1006834. 7

[187] Shanmugam, S., Nichols, A. K., Saravanabalaji, D., Welsch, C., & Yi, M. HCV NS5A dimer interface residues regulate HCV replication by controlling its self-interaction, hyperphosphorylation, subcellular localization and interaction with cyclophilin A. *PLOS Pathogens*, **14**(7): e1007177 (2018). doi:10.1371/journal.ppat.1007177. 7

[188] Shirota, Y., Luo, H., Qin, W., Kaneko, S., *et al.* Hepatitis C Virus (HCV) NS5A Binds RNA-dependent RNA Polymerase (RdRP) NS5B and Modulates RNA-dependent RNA Polymerase Activity. *Journal of Biological Chemistry*, **277**(13): 11149–11155 (2002). doi:10.1074/jbc.M111392200. 7

[189] Oliver Koch, J. & Bartenschlager, R. Modulation of Hepatitis C Virus NS5A Hyperphosphorylation by Nonstructural Proteins NS3, NS4A, and NS4B. *Journal of Virology*, **73**(9): 7138–7146 (1999). doi:10.1128/JVI.73.9.7138-7146.1999. 7

[190] Appel, N., Pietschmann, T., & Bartenschlager, R. Mutational Analysis of Hepatitis C Virus Nonstructural Protein 5A: Potential Role of Differential Phosphorylation in RNA Replication and Identification of a Genetically Flexible Domain. *Journal of Virology*, **79**(5): 3187–3194 (2005). doi:10.1128/JVI.79.5.3187-3194.2005. 7

[191] Yu, C.-C., Lin, P.-C., Chiang, C.-H., Jen, S.-T., *et al.* Sequential Phosphorylation of Hepatitis C Virus NS5A Protein Requires the ATP-Binding Domain of NS3 Helicase. *Journal of Virology*, **96**(7): e00107–22 (2022). doi:10.1128/jvi.00107-22. 7

[192] Ross-Thriepland, D., Mankouri, J., & Harris, M. Serine Phosphorylation of the Hepatitis C Virus NS5A Protein Controls the Establishment of Replication Complexes. *Journal of Virology*, **89**(6): 3123–3135 (2015). doi:10.1128/JVI.02995-14. 7

[193] Kandangwa, M. & Liu, Q. HCV NS5A hyperphosphorylation is involved in viral translation modulation. *Biochemical and Biophysical Research Communications*, **520**(1): 192–197 (2019). doi:10.1016/j.bbrc.2019.09.105. 7

[194] Kim, J., Lee, D., & Choe, J. Hepatitis C Virus NS5A Protein Is Phosphorylated by Casein Kinase II. *Biochemical and Biophysical Research Communications*, **257**(3): 777–781 (1999). doi:10.1006/bbrc.1999.0460. 7

[195] Reiss, S., Harak, C., Romero-Brey, I., Radujkovic, D., *et al.* The Lipid Kinase Phosphatidylinositol-4 Kinase III Alpha Regulates the Phosphorylation Status of Hepatitis C Virus NS5A. *PLoS Pathogens*, **9**(5): e1003359 (2013). doi:10.1371/journal.ppat.1003359. 7

[196] Shi, S. T., Polyak, S. J., Tu, H., Taylor, D. R., *et al.* Hepatitis C Virus NS5A Colocalizes with the Core Protein on Lipid Droplets and Interacts with Apolipoproteins. *Virology*, **292**(2): 198–210 (2002). doi:10.1006/viro.2001.1225. 7, 11, 12

[197] Masaki, T., Suzuki, R., Murakami, K., Aizaki, H., *et al.* Interaction of Hepatitis C Virus Nonstructural Protein 5A with Core Protein Is Critical for the Production of Infectious Virus Particles. *Journal of Virology*, **82**(16): 7964–7976 (2008). doi:10.1128/JVI.00826-08. 11

[198] Cai, H., Yao, W., Li, L., Li, X., *et al.* Cell-death-inducing DFFA-like Effector B Contributes to the Assembly of Hepatitis C Virus (HCV) Particles and Interacts with HCV NS5A. *Scientific Reports*, **6**(1): 27778 (2016). doi:10.1038/srep27778. 7

[199] Street, A., Macdonald, A., Crowder, K., & Harris, M. The Hepatitis C Virus NS5A Protein Activates a Phosphoinositide 3-Kinase-dependent Survival Signaling Cascade. *Journal of Biological Chemistry*, **279**(13): 12232–12241 (2004). doi:10.1074/jbc.M312245200. 7

[200] Xie, Z., Xiao, Z., & Wang, F. Hepatitis C Virus Nonstructural 5A Protein (HCV-NS5A) Inhibits Hepatocyte Apoptosis through the NF-kappab/miR-503/bcl-2 Pathway. *Molecules and Cells* (2017). doi:10.14348/molcells.2017.2299.

[201] Chen, W.-C., Tseng, C.-K., Chen, Y.-H., Lin, C.-K., *et al.* HCV NS5A Up-Regulates COX-2 Expression via IL-8-Mediated Activation of the ERK/JNK MAPK Pathway. *PLOS ONE*, **10**(7): e0133264 (2015). doi:10.1371/journal.pone.0133264.

[202] Gong, G., Waris, G., Tanveer, R., & Siddiqui, A. Human hepatitis C virus NS5A protein alters intracellular calcium levels, induces oxidative stress, and activates

STAT-3 and NF-κB. *Proceedings of the National Academy of Sciences*, **98**(17): 9599–9604 (2001). doi:10.1073/pnas.171311298.

[203] Gale, M. J., Jr, Korth, M. J., & Katze, M. G. Repression of the PKR protein kinase by the hepatitis C virus NS5A protein: a potential mechanism of interferon resistance. *Clinical and Diagnostic Virology*, **10**(2-3): 157–162 (1998). doi:10.1016/S0928-0197(98)00034-8.

[204] Çevik, R. E., Cesarec, M., Da Silva Filipe, A., Licastro, D., *et al.* Hepatitis C Virus NS5A Targets Nucleosome Assembly Protein NAP1L1 To Control the Innate Cellular Response. *Journal of Virology*, **91**(18): e00880–17 (2017). doi:10.1128/JVI.00880-17. 7

[205] Bley, H., Schöbel, A., & Herker, E. Whole Lotta Lipids—From HCV RNA Replication to the Mature Viral Particle. *International Journal of Molecular Sciences*, **21**(8): 2888 (2020). doi:10.3390/ijms21082888. 7, 12

[206] Matsui, C., Deng, L., Minami, N., Abe, T., *et al.* Hepatitis C Virus NS5A Protein Promotes the Lysosomal Degradation of Hepatocyte Nuclear Factor 1α via Chaperone-Mediated Autophagy. *Journal of Virology*, **92**(13): e00639–18 (2018). doi:10.1128/JVI.00639-18.

[207] Parvaiz, F. Hepatitis C virus NS5A promotes insulin resistance through IRS-1 serine phosphorylation and increased gluconeogenesis. *World Journal of Gastroenterology*, **21**(43): 12361 (2015). doi:10.3748/wjg.v21.i43.12361.

[208] Reiss, S., Rebhan, I., Backes, P., Romero-Brey, I., *et al.* Recruitment and Activation of a Lipid Kinase by Hepatitis C Virus NS5A Is Essential for Integrity of the Membranous Replication Compartment. *Cell Host & Microbe*, **9**(1): 32–45 (2011). doi:10.1016/j.chom.2010.12.002. 10, 28

[209] Zhao, Y., Wang, Q., Qiu, G., Zhou, S., *et al.* RACK1 Promotes Autophagy by Enhancing the Atg14L-Beclin 1-Vps34-Vps15 Complex Formation upon Phosphorylation by AMPK. *Cell Reports*, **13**(7): 1407–1417 (2015). doi:10.1016/j.celrep.2015.10.011.

[210] Lee, J. S., Tabata, K., Twu, W.-I., Rahman, M. S., *et al.* RACK1 mediates rewiring of intracellular networks induced by hepatitis C virus infection. *PLOS Pathogens*, **15**(9): e1008021 (2019). doi:10.1371/journal.ppat.1008021. 7, 11

[211] Hwang, S. B., Park, K.-J., Kim, Y.-S., Sung, Y. C., & Lai, M. M. Hepatitis C Virus NS5B Protein Is a Membrane-Associated Phosphoprotein with a Predominantly Per-

inuclear Localization. *Virology*, **227**(2): 439–446 (1997). doi:10.1006/viro.1996.8357. 8

[212] Lesburg, C. A., Cable, M. B., Ferrari, E., Hong, Z., *et al.* Crystal structure of the RNA-dependent RNA polymerase from hepatitis C virus reveals a fully encircled active site. *Nature Structural Biology*, **6**(10): 937–943 (1999). doi:10.1038/13305. 8

[213] Ago, H., Adachi, T., Yoshida, A., Yamamoto, M., *et al.* Crystal structure of the RNA-dependent RNA polymerase of hepatitis C virus. *Structure*, **7**(11): 1417–1426 (1999). doi:10.1016/S0969-2126(00)80031-3.

[214] Bressanelli, S., Tomei, L., Roussel, A., Incitti, I., *et al.* Crystal structure of the RNA-dependent RNA polymerase of hepatitis C virus. *Proceedings of the National Academy of Sciences*, **96**(23): 13034–13039 (1999). doi:10.1073/pnas.96.23.13034. 8

[215] Ranjith-Kumar, C. T., Kim, Y.-C., Gutshall, L., Silverman, C., *et al.* Mechanism of De Novo Initiation by the Hepatitis C Virus RNA-Dependent RNA Polymerase: Role of Divalent Metals. *Journal of Virology*, **76**(24): 12513–12525 (2002). doi:10.1128/JVI.76.24.12513-12525.2002. 8

[216] Biswal, B. K., Cherney, M. M., Wang, M., Chan, L., *et al.* Crystal Structures of the RNA-dependent RNA Polymerase Genotype 2a of Hepatitis C Virus Reveal Two Conformations and Suggest Mechanisms of Inhibition by Non-nucleoside Inhibitors. *Journal of Biological Chemistry*, **280**(18): 18202–18210 (2005). doi:10.1074/jbc.M413410200. 8

[217] Ferrari, E., He, Z., Palermo, R. E., & Huang, H.-C. Hepatitis C Virus NS5B Polymerase Exhibits Distinct Nucleotide Requirements for Initiation and Elongation. *Journal of Biological Chemistry*, **283**(49): 33893–33901 (2008). doi:10.1074/jbc.M803094200.

[218] Mosley, R. T., Edwards, T. E., Murakami, E., Lam, A. M., *et al.* Structure of Hepatitis C Virus Polymerase in Complex with Primer-Template RNA. *Journal of Virology*, **86**(12): 6503–6511 (2012). doi:10.1128/JVI.00386-12. 8

[219] Paul, D., Madan, V., & Bartenschlager, R. Hepatitis C Virus RNA Replication and Assembly: Living on the Fat of the Land. *Cell Host & Microbe*, **16**(5): 569–579 (2014). doi:10.1016/j.chom.2014.10.008. 8, 10, 11

[220] Shimakami, T., Hijikata, M., Luo, H., Ma, Y. Y., *et al.* Effect of Interaction between Hepatitis C Virus NS5A and NS5B on Hepatitis C Virus RNA Replication with

the Hepatitis C Virus Replicon. *Journal of Virology*, **78**(6): 2738–2748 (2004). doi:10.1128/JVI.78.6.2738-2748.2004.

[221] Ishido, S., Fujita, T., & Hotta, H. Complex Formation of NS5B with NS3 and NS4A Proteins of Hepatitis C Virus. *Biochemical and Biophysical Research Communications*, **244**(1): 35–40 (1998). doi:10.1006/bbrc.1998.8202.

[222] Moradpour, D., Brass, V., Bieck, E., Friebe, P., *et al.* Membrane Association of the RNA-Dependent RNA Polymerase Is Essential for Hepatitis C Virus RNA Replication. *Journal of Virology*, **78**(23): 13278–13284 (2004). doi:10.1128/JVI.78.23.13278-13284.2004. 8

[223] Aligeti, M., Roder, A., & Horner, S. M. Cooperation between the Hepatitis C Virus p7 and NS5B Proteins Enhances Virion Infectivity. *Journal of Virology*, **89**(22): 11523–11533 (2015). doi:10.1128/JVI.01185-15. 8

[224] Anwar, M. I., Li, N., Zhou, Q., Chen, M., *et al.* PPP2R5D promotes hepatitis C virus infection by binding to viral NS5B and enhancing viral RNA replication. *Virology Journal*, **19**(1): 118 (2022). doi:10.1186/s12985-022-01848-5.

[225] Aweya, J. J., Sze, C. W., Bayega, A., Mohd-Ismail, N. K., *et al.* NS5B induces up-regulation of the BH3-only protein, BIK, essential for the hepatitis C virus RNA replication and viral release. *Virology*, **474**: 41–51 (2015). doi:10.1016/j.virol.2014.10.027.

[226] Kyono, K., Miyashiro, M., & Taguchi, I. Human Eukaryotic Initiation Factor 4AII Associates with Hepatitis C Virus NS5B Protein in Vitro. *Biochemical and Biophysical Research Communications*, **292**(3): 659–666 (2002). doi:10.1006/bbrc.2002.6702. 8

[227] Moriyama, M., Kato, N., Otsuka, M., Shao, R.-X., *et al.* Interferon-beta is activated by hepatitis C virus NS5B and inhibited by NS4A, NS4B, and NS5A. *Hepatology International*, **1**(2): 302–310 (2007). doi:10.1007/s12072-007-9003-8. 8

[228] Itsui, Y., Sakamoto, N., Kakinuma, S., Nakagawa, M., *et al.* Antiviral effects of the interferon-induced protein guanylate binding protein 1 and its interaction with the hepatitis C virus NS5B protein. *Hepatology*, **50**(6): 1727–1737 (2009). doi:10.1002/hep.23195. 8

[229] Cosset, F.-L., Mialon, C., Boson, B., Granier, C., & Denolly, S. HCV Interplay with Lipoproteins: Inside or Outside the Cells? *Viruses*, **12**(4): 434 (2020). doi:10.3390/v12040434. 8, 12

[230] Bartenschlager, R., Penin, F., Lohmann, V., & André, P. Assembly of infectious hepatitis C virus particles. *Trends in Microbiology*, **19**(2): 95–103 (2011). doi:10.1016/j.tim.2010.11.005. 8

[231] Dey, D., Poudyal, S., Rehman, A., & Hasan, S. S. Structural and biochemical insights into flavivirus proteins. *Virus Research*, **296**: 198343 (2021). doi:10.1016/j.virusres.2021.198343. 8

[232] Gastaminza, P., Dryden, K. A., Boyd, B., Wood, M. R., *et al.* Ultrastructural and Biophysical Characterization of Hepatitis C Virus Particles Produced in Cell Culture. *Journal of Virology*, **84**(21): 10999–11009 (2010). doi:10.1128/JVI.00526-10. 8

[233] Catanese, M. T., Uryu, K., Kopp, M., Edwards, T. J., *et al.* Ultrastructural analysis of hepatitis C virus particles. *Proceedings of the National Academy of Sciences*, **110**(23): 9505–9510 (2013). doi:10.1073/pnas.1307527110. 8

[234] Gastaminza, P., Kapadia, S. B., & Chisari, F. V. Differential Biophysical Properties of Infectious Intracellular and Secreted Hepatitis C Virus Particles. *Journal of Virology*, **80**(22): 11074–11081 (2006). doi:10.1128/JVI.01150-06. 8

[235] Jiang, J. & Luo, G. Apolipoprotein E but Not B Is Required for the Formation of Infectious Hepatitis C Virus Particles. *Journal of Virology*, **83**(24): 12680–12691 (2009). doi:10.1128/JVI.01476-09. 8, 12

[236] Fukuhara, T., Wada, M., Nakamura, S., Ono, C., *et al.* Amphipathic α-Helices in Apolipoproteins Are Crucial to the Formation of Infectious Hepatitis C Virus Particles. *PLoS Pathogens*, **10**(12): e1004534 (2014). doi:10.1371/journal.ppat.1004534.

[237] Fukuhara, T., Ono, C., Puig-Basagoiti, F., & Matsuura, Y. Roles of Lipoproteins and Apolipoproteins in Particle Formation of Hepatitis C Virus. *Trends in Microbiology*, **23**(10): 618–629 (2015). doi:10.1016/j.tim.2015.07.007. 8, 9, 12

[238] Calattini, S., Fusil, F., Mancip, J., Dao Thi, V. L., *et al.* Functional and Biochemical Characterization of Hepatitis C Virus (HCV) Particles Produced in a Humanized Liver Mouse Model. *Journal of Biological Chemistry*, **290**(38): 23173–23187 (2015). doi:10.1074/jbc.M115.662999. 8

[239] Merz, A., Long, G., Hiet, M.-S., Brügger, B., *et al.* Biochemical and Morphological Properties of Hepatitis C Virus Particles and Determination of Their Lipidome. *Journal of Biological Chemistry*, **286**(4): 3018–3032 (2011). doi:10.1074/jbc.M110.175018. 8

[240] Aizaki, H., Morikawa, K., Fukasawa, M., Hara, H., *et al.* Critical Role of Virion-Associated Cholesterol and Sphingolipid in Hepatitis C Virus Infection. *Journal of Virology*, **82**(12): 5715–5724 (2008). doi:10.1128/JVI.02530-07. 8

[241] Vieyres, G. & Pietschmann, T. HCV Pit Stop at the Lipid Droplet: Refuel Lipids and Put on a Lipoprotein Coat before Exit. *Cells*, **8**(3): 233 (2019). doi:10.3390/cells8030233. 8

[242] Shimotohno, K. HCV Assembly and Egress via Modifications in Host Lipid Metabolic Systems. *Cold Spring Harbor Perspectives in Medicine*, **11**(1): a036814 (2021). doi:10.1101/cshperspect.a036814. 12

[243] Sidorkiewicz, M. Hepatitis C Virus Uses Host Lipids to Its Own Advantage. *Metabolites*, **11**(5): 273 (2021). doi:10.3390/metabo11050273. 8, 11, 50

[244] Denolly, S., Granier, C., Fontaine, N., Pozzetto, B., *et al.* A serum protein factor mediates maturation and apoB-association of HCV particles in the extracellular milieu. *Journal of Hepatology*, **70**(4): 626–638 (2019). doi:10.1016/j.jhep.2018.11.033. 8, 12

[245] Gerold, G., Moeller, R., & Pietschmann, T. Hepatitis C Virus Entry: Protein Interactions and Fusion Determinants Governing Productive Hepatocyte Invasion. *Cold Spring Harbor Perspectives in Medicine*, **10**(2): a036830 (2020). doi:10.1101/cshperspect.a036830. 9, 10

[246] Colpitts, C., Tsai, P.-L., & Zeisel, M. Hepatitis C Virus Entry: An Intriguingly Complex and Highly Regulated Process. *International Journal of Molecular Sciences*, **21**(6): 2091 (2020). doi:10.3390/ijms21062091. 9, 10

[247] Jiang, J., Cun, W., Wu, X., Shi, Q., *et al.* Hepatitis C Virus Attachment Mediated by Apolipoprotein E Binding to Cell Surface Heparan Sulfate. *Journal of Virology*, **86**(13): 7256–7267 (2012). doi:10.1128/JVI.07222-11. 9

[248] Jiang, J., Wu, X., Tang, H., & Luo, G. Apolipoprotein E Mediates Attachment of Clinical Hepatitis C Virus to Hepatocytes by Binding to Cell Surface Heparan Sulfate Proteoglycan Receptors. *PLoS ONE*, **8**(7): e67982 (2013). doi:10.1371/journal.pone.0067982.

[249] Brown, M. S. & Goldstein, J. L. A Receptor-Mediated Pathway for Cholesterol Homeostasis. *Science*, **232**(4746): 34–47 (1986). doi:10.1126/science.3513311.

[250] Milne, R., Théolis, R., Maurice, R., Pease, R. J., *et al.* The Use of Monoclonal Antibodies to Localize the Low Density Lipoprotein Receptor-binding Domain of Apolipoprotein B. *Journal of Biological Chemistry*, **264**(33): 19754–19760 (1989). doi:10.1016/S0021-9258(19)47176-7. 9

[251] Barth, H., Schäfer, C., Adah, M. I., Zhang, F., *et al.* Cellular Binding of Hepatitis C Virus Envelope Glycoprotein E2 Requires Cell Surface Heparan Sulfate. *Journal of Biological Chemistry*, **278**(42): 41003–41012 (2003). doi:10.1074/jbc.M302267200. 9

[252] Dreux, M., Dao Thi, V. L., Fresquet, J., Guérin, M., *et al.* Receptor Complementation and Mutagenesis Reveal SR-BI as an Essential HCV Entry Factor and Functionally Imply Its Intra- and Extra-Cellular Domains. *PLoS Pathogens*, **5**(2): e1000310 (2009). doi:10.1371/journal.ppat.1000310. 9

[253] Lupberger, J., Zeisel, M. B., Xiao, F., Thumann, C., *et al.* EGFR and EphA2 are host factors for hepatitis C virus entry and possible targets for antiviral therapy. *Nature Medicine*, **17**(5): 589–595 (2011). doi:10.1038/nm.2341. 9

[254] Zona, L., Lupberger, J., Sidahmed-Adrar, N., Thumann, C., *et al.* HRas Signal Transduction Promotes Hepatitis C Virus Cell Entry by Triggering Assembly of the Host Tetraspanin Receptor Complex. *Cell Host & Microbe*, **13**(3): 302–313 (2013). doi:10.1016/j.chom.2013.02.006. 9

[255] Brazzoli, M., Bianchi, A., Filippini, S., Weiner, A., *et al.* CD81 Is a Central Regulator of Cellular Events Required for Hepatitis C Virus Infection of Human Hepatocytes. *Journal of Virology*, **82**(17): 8316–8329 (2008). doi:10.1128/JVI.00665-08. 9, 17

[256] Harris, H. J., Farquhar, M. J., Mee, C. J., Davis, C., *et al.* CD81 and Claudin 1 Coreceptor Association: Role in Hepatitis C Virus Entry. *Journal of Virology*, **82**(10): 5007–5020 (2008). doi:10.1128/JVI.02286-07. 9

[257] Harris, H. J., Davis, C., Mullins, J. G., Hu, K., *et al.* Claudin Association with CD81 Defines Hepatitis C Virus Entry. *Journal of Biological Chemistry*, **285**(27): 21092–21102 (2010). doi:10.1074/jbc.M110.104836.

[258] Evans, M. J., von Hahn, T., Tscherne, D. M., Syder, A. J., *et al.* Claudin-1 is a hepatitis C virus co-receptor required for a late step in entry. *Nature*, **446**(7137): 801–805 (2007). doi:10.1038/nature05654. 9

[259] Hopcraft, S. E. & Evans, M. J. Selection of a hepatitis C virus with altered entry factor requirements reveals a genetic interaction between the E1 glycoprotein and

claudins: HEPATOLOGY, Vol. XX, No. X, 2015. *Hepatology*, **62**(4): 1059–1069 (2015). doi:10.1002/hep.27815.

[260] Douam, F., Dao Thi, V. L., Maurin, G., Fresquet, J., *et al.* Critical interaction between E1 and E2 glycoproteins determines binding and fusion properties of hepatitis C virus during cell entry: Hepatology. *Hepatology*, **59**(3): 776–788 (2014). doi:10.1002/hep.26733. 9, 10

[261] Ploss, A., Evans, M. J., Gaysinskaya, V. A., Panis, M., *et al.* Human occludin is a hepatitis C virus entry factor required for infection of mouse cells. *Nature*, **457**(7231): 882–886 (2009). doi:10.1038/nature07684. 9

[262] Benedicto, I., Molina-Jiménez, F., Bartosch, B., Cosset, F.-L., *et al.* The Tight Junction-Associated Protein Occludin Is Required for a Postbinding Step in Hepatitis C Virus Entry and Infection. *Journal of Virology*, **83**(16): 8012–8020 (2009). doi:10.1128/JVI.00038-09.

[263] Sourisseau, M., Michta, M. L., Zony, C., Israelow, B., *et al.* Temporal Analysis of Hepatitis C Virus Cell Entry with Occludin Directed Blocking Antibodies. *PLoS Pathogens*, **9**(3): e1003244 (2013). doi:10.1371/journal.ppat.1003244. 9

[264] Haid, S., Grethe, C., Dill, M. T., Heim, M., *et al.* Isolate-dependent use of claudins for cell entry by hepatitis C virus: HEPATOLOGY, Vol. 58, No. X, 2013 HAID ET AL. *Hepatology*, **59**(1): 24–34 (2014). doi:10.1002/hep.26567. 9

[265] Blanchard, E., Belouzard, S., Goueslain, L., Wakita, T., *et al.* Hepatitis C Virus Entry Depends on Clathrin-Mediated Endocytosis. *Journal of Virology*, **80**(14): 6964–6972 (2006). doi:10.1128/JVI.00024-06. 9

[266] Farquhar, M. J., Hu, K., Harris, H. J., Davis, C., *et al.* Hepatitis C Virus Induces CD81 and Claudin-1 Endocytosis. *Journal of Virology*, **86**(8): 4305–4316 (2012). doi:10.1128/JVI.06996-11.

[267] Liu, S., Kuo, W., Yang, W., Liu, W., *et al.* The second extracellular loop dictates Occludin-mediated HCV entry. *Virology*, **407**(1): 160–170 (2010). doi:10.1016/j.virol.2010.08.009. 9

[268] Kamal, A. & Goldstein, L. S. Connecting vesicle transport to the cytoskeleton. *Current Opinion in Cell Biology*, **12**(4): 503–508 (2000). doi:10.1016/S0955-0674(00)00123-X. 9

[269] Lavillette, D., Pécheur, E.-I., Donot, P., Fresquet, J., *et al.* Characterization of Fusion Determinants Points to the Involvement of Three Discrete Regions of Both E1 and E2 Glycoproteins in the Membrane Fusion Process of Hepatitis C Virus. *Journal of Virology*, **81**(16): 8752–8765 (2007). doi:10.1128/JVI.02642-06. 10

[270] Maurin, G., Fresquet, J., Granio, O., Wychowski, C., *et al.* Identification of Interactions in the E1E2 Heterodimer of Hepatitis C Virus Important for Cell Entry. *Journal of Biological Chemistry*, **286**(27): 23865–23876 (2011). doi:10.1074/jbc.M110.213942.

[271] Douam, F., Fusil, F., Enguehard, M., Dib, L., *et al.* A protein coevolution method uncovers critical features of the Hepatitis C Virus fusion mechanism. *PLOS Pathogens*, **14**(3): e1006908 (2018). doi:10.1371/journal.ppat.1006908. 10

[272] Sharma, N. R., Mateu, G., Dreux, M., Grakoui, A., *et al.* Hepatitis C Virus Is Primed by CD81 Protein for Low pH-dependent Fusion. *Journal of Biological Chemistry*, **286**(35): 30361–30376 (2011). doi:10.1074/jbc.M111.263350. 10

[273] Cunha, E. S., Sfriso, P., Rojas, A. L., Roversi, P., *et al.* Mechanism of Structural Tuning of the Hepatitis C Virus Human Cellular Receptor CD81 Large Extracellular Loop. *Structure*, **25**(1): 53–65 (2017). doi:10.1016/j.str.2016.11.003. 10

[274] Perin, P. M., Haid, S., Brown, R. J., Doerrbecker, J., *et al.* Flunarizine prevents hepatitis C virus membrane fusion in a genotype-dependent manner by targeting the potential fusion peptide within E1. *Hepatology*, **63**(1): 49–62 (2016). doi:10.1002/hep.28111. 10

[275] Tong, Y., Chi, X., Yang, W., & Zhong, J. Functional Analysis of Hepatitis C Virus (HCV) Envelope Protein E1 Using a *trans* -Complementation System Reveals a Dual Role of a Putative Fusion Peptide of E1 in both HCV Entry and Morphogenesis. *Journal of Virology*, **91**(7): e02468–16 (2017). doi:10.1128/JVI.02468-16. 10

[276] Lohmann, V. Hepatitis C Virus RNA Replication. In Bartenschlager, R. (ed.), Hepatitis C Virus: From Molecular Virology to Antiviral Therapy, volume 369, pp. 167–198. Springer Berlin Heidelberg, Berlin, Heidelberg (2013). ISBN 978-3-642-27339-1 978-3-642-27340-7. doi:10.1007/978-3-642-27340-7_7. Series Title: Current Topics in Microbiology and Immunology. 10

[277] Paul, D., Hoppe, S., Saher, G., Krijnse-Locker, J., & Bartenschlager, R. Morphological and Biochemical Characterization of the Membranous Hepatitis C Virus Replication Compartment. *Journal of Virology*, **87**(19): 10612–10627 (2013). doi:10.1128/JVI.01370-13. 10

[278] Stoeck, I. K., Lee, J.-Y., Tabata, K., Romero-Brey, I., *et al.* Hepatitis C Virus Replication Depends on Endosomal Cholesterol Homeostasis. *Journal of Virology*, **92**(1): e01196–17 (2018). doi:10.1128/JVI.01196-17. 50

[279] Wang, H. & Tai, A. W. Continuous de novo generation of spatially segregated hepatitis C virus replication organelles revealed by pulse-chase imaging. *Journal of Hepatology*, **66**(1): 55–66 (2017). doi:10.1016/j.jhep.2016.08.018. 10, 11

[280] Park, C.-Y., Jun, H.-J., Wakita, T., Cheong, J. H., & Hwang, S. B. Hepatitis C Virus Nonstructural 4B Protein Modulates Sterol Regulatory Element-binding Protein Signaling via the AKT Pathway. *Journal of Biological Chemistry*, **284**(14): 9237–9246 (2009). doi:10.1074/jbc.M808773200. 11

[281] Schaefer, E. & Chung, R. HCV and Host Lipids: An Intimate Connection. *Seminars in Liver Disease*, **33**(04): 358–368 (2013). doi:10.1055/s-0033-1358524. 11, 50

[282] Chu, J. Y. K. & Ou, J.-h. J. Autophagy in HCV Replication and Protein Trafficking. *International Journal of Molecular Sciences*, **22**(3): 1089 (2021). doi:10.3390/ijms22031089. 11, 75

[283] Chan, S. & Ou, J.-h. Hepatitis C Virus-Induced Autophagy and Host Innate Immune Response. *Viruses*, **9**(8): 224 (2017). doi:10.3390/v9080224.

[284] Bunz, M., Ritter, M., & Schindler, M. HCV egress – unconventional secretion of assembled viral particles. *Trends in Microbiology*, **30**(4): 364–378 (2022). doi:10.1016/j.tim.2021.08.005. 11, 12

[285] Shinohara, Y., Imajo, K., Yoneda, M., Tomeno, W., *et al.* Unfolded protein response pathways regulate Hepatitis C virus replication via modulation of autophagy. *Biochemical and Biophysical Research Communications*, **432**(2): 326–332 (2013). doi:10.1016/j.bbrc.2013.01.103. 11

[286] Huang, H., Kang, R., Wang, J., Luo, G., *et al.* Hepatitis C virus inhibits AKT-tuberous sclerosis complex (TSC), the mechanistic target of rapamycin (MTOR) pathway, through endoplasmic reticulum stress to induce autophagy. *Autophagy*, **9**(2): 175–195 (2013). doi:10.4161/auto.22791.

[287] Sir, D., Kuo, C.-f., Tian, Y., Liu, H. M., *et al.* Replication of Hepatitis C Virus RNA on Autophagosomal Membranes. *Journal of Biological Chemistry*, **287**(22): 18036–18043 (2012). doi:10.1074/jbc.M111.320085.

[288] Wang, L. & James Ou, J.-h. Hepatitis C virus and autophagy. *Biological Chemistry*, **396**(11): 1215–1222 (2015). doi:10.1515/hsz-2015-0172. 11

[289] Hansen, M. D., Johnsen, I. B., Stiberg, K. A., Sherstova, T., *et al.* Hepatitis C virus triggers Golgi fragmentation and autophagy through the immunity-related GTPase M. *Proceedings of the National Academy of Sciences*, **114**(17) (2017). doi:10.1073/pnas.1616683114. 11, 13

[290] Wang, L., Kim, J. Y., Liu, H. M., Lai, M. M. C., & Ou, J.-h. J. HCV-induced autophagosomes are generated via homotypic fusion of phagophores that mediate HCV RNA replication. *PLOS Pathogens*, **13**(9): e1006609 (2017). doi:10.1371/journal.ppat.1006609. 11, 12

[291] Jones-Jamtgaard, K. N., Wozniak, A. L., Koga, H., Ralston, R., & Weinman, S. A. Hepatitis C virus infection increases autophagosome stability by suppressing lysosomal fusion through an Arl8b-dependent mechanism. *Journal of Biological Chemistry*, **294**(39): 14257–14266 (2019). doi:10.1074/jbc.RA119.008229. 11, 12

[292] Ren, H., Elgner, F., Jiang, B., Himmelsbach, K., *et al.* The Autophagosomal SNARE Protein Syntaxin 17 Is an Essential Factor for the Hepatitis C Virus Life Cycle. *Journal of Virology*, **90**(13): 5989–6000 (2016). doi:10.1128/JVI.00551-16. 12

[293] Itakura, E., Kishi-Itakura, C., & Mizushima, N. The Hairpin-type Tail-Anchored SNARE Syntaxin 17 Targets to Autophagosomes for Fusion with Endosomes/Lysosomes. *Cell*, **151**(6): 1256–1269 (2012). doi:10.1016/j.cell.2012.11.001. 11, 12

[294] Lee, J.-Y., Cortese, M., Haselmann, U., Tabata, K., *et al.* Spatiotemporal Coupling of the Hepatitis C Virus Replication Cycle by Creating a Lipid Droplet- Proximal Membranous Replication Compartment. *Cell Reports*, **27**(12): 3602–3617.e5 (2019). doi:10.1016/j.celrep.2019.05.063. 11, 28, 77

[295] Counihan, N. A., Rawlinson, S. M., & Lindenbach, B. D. Trafficking of Hepatitis C Virus Core Protein during Virus Particle Assembly. *PLoS Pathogens*, **7**(10): e1002302 (2011). doi:10.1371/journal.ppat.1002302. 11

[296] Neveu, G., Barouch-Bentov, R., Ziv-Av, A., Gerber, D., *et al.* Identification and Targeting of an Interaction between a Tyrosine Motif within Hepatitis C Virus Core Protein and AP2M1 Essential for Viral Assembly. *PLoS Pathogens*, **8**(8): e1002845 (2012). doi:10.1371/journal.ppat.1002845.

[297] Mousseau, G., Kota, S., Takahashi, V., Frick, D. N., & Strosberg, A. D. Dimerization-driven interaction of hepatitis C virus core protein with NS3 helicase. *Journal of General Virology*, **92**(1): 101–111 (2011). doi:10.1099/vir.0.023325-0. 11

[298] Pietschmann, T., Kaul, A., Koutsoudakis, G., Shavinskaya, A., *et al.* Construction and characterization of infectious intragenotypic and intergenotypic hepatitis C virus chimeras. *Proceedings of the National Academy of Sciences of the United States of America*, **103**(19): 7408–7413 (2006). doi:10.1073/pnas.0504877103. 12, 34

[299] Steinmann, E., Doerrbecker, J., Friesland, M., Riebesehl, N., *et al.* Characterization of Hepatitis C Virus Intra- and Intergenotypic Chimeras Reveals a Role of the Glycoproteins in Virus Envelopment. *Journal of Virology*, **87**(24): 13297–13306 (2013). doi:10.1128/JVI.01708-13. 12

[300] Menzel, N., Fischl, W., Hueging, K., Bankwitz, D., *et al.* MAP-Kinase Regulated Cytosolic Phospholipase A2 Activity Is Essential for Production of Infectious Hepatitis C Virus Particles. *PLoS Pathogens*, **8**(7): e1002829 (2012). doi:10.1371/journal.ppat.1002829. 12

[301] Lee, J.-Y., Acosta, E. G., Stoeck, I. K., Long, G., *et al.* Apolipoprotein E Likely Contributes to a Maturation Step of Infectious Hepatitis C Virus Particles and Interacts with Viral Envelope Glycoproteins. *Journal of Virology*, **88**(21): 12422–12437 (2014). doi:10.1128/JVI.01660-14. 12

[302] Chang, K.-S., Jiang, J., Cai, Z., & Luo, G. Human Apolipoprotein E Is Required for Infectivity and Production of Hepatitis C Virus in Cell Culture. *Journal of Virology*, **81**(24): 13783–13793 (2007). doi:10.1128/JVI.01091-07. 12

[303] Syed, G. H., Khan, M., Yang, S., & Siddiqui, A. Hepatitis C Virus Lipoviroparticles Assemble in the Endoplasmic Reticulum (ER) and Bud off from the ER to the Golgi Compartment in COPII Vesicles. *Journal of Virology*, **91**(15): e00499–17 (2017). doi:10.1128/JVI.00499-17. 12

[304] Coller, K. E., Heaton, N. S., Berger, K. L., Cooper, J. D., *et al.* Molecular Determinants and Dynamics of Hepatitis C Virus Secretion. *PLoS Pathogens*, **8**(1): e1002466 (2012). doi:10.1371/journal.ppat.1002466. 12

[305] Takacs, C. N., Andreo, U., Dao Thi, V. L., Wu, X., *et al.* Differential Regulation of Lipoprotein and Hepatitis C Virus Secretion by Rab1b. *Cell Reports*, **21**(2): 431–441 (2017). doi:10.1016/j.celrep.2017.09.053. 12

[306] Bishé, B., Syed, G. H., Field, S. J., & Siddiqui, A. Role of Phosphatidylinositol 4-Phosphate (PI4P) and Its Binding Protein GOLPH3 in Hepatitis C Virus Secretion. *Journal of Biological Chemistry*, **287**(33): 27637–27647 (2012). doi:10.1074/jbc.M112.346569. 12

[307] Lai, C.-K., Jeng, K.-S., Machida, K., & Lai, M. M. C. Hepatitis C Virus Egress and Release Depend on Endosomal Trafficking of Core Protein. *Journal of Virology*, **84**(21): 11590–11598 (2010). doi:10.1128/JVI.00587-10. 12

[308] Mankouri, J., Walter, C., Stewart, H., Bentham, M., *et al.* Release of Infectious Hepatitis C Virus from Huh7 Cells Occurs via a *trans* -Golgi Network-to-Endosome Pathway Independent of Very-Low-Density Lipoprotein Secretion. *Journal of Virology*, **90**(16): 7159–7170 (2016). doi:10.1128/JVI.00826-16. 12, 13

[309] Ploen, D., Hafirassou, M. L., Himmelsbach, K., Schille, S. A., *et al.* TIP47 is associated with the Hepatitis C virus and its interaction with Rab9 is required for release of viral particles. *European Journal of Cell Biology*, **92**(12): 374–382 (2013). doi:10.1016/j.ejcb.2013.12.003.

[310] Elgner, F., Hildt, E., & Bender, D. Relevance of Rab Proteins for the Life Cycle of Hepatitis C Virus. *Frontiers in Cell and Developmental Biology*, **6**: 166 (2018). doi:10.3389/fcell.2018.00166. 12, 13

[311] Corless, L., Crump, C. M., Griffin, S. D. C., & Harris, M. Vps4 and the ESCRT-III complex are required for the release of infectious hepatitis C virus particles. *Journal of General Virology*, **91**(2): 362–372 (2010). doi:10.1099/vir.0.017285-0. 12

[312] Ariumi, Y., Kuroki, M., Maki, M., Ikeda, M., *et al.* The ESCRT System Is Required for Hepatitis C Virus Production. *PLoS ONE*, **6**(1): e14517 (2011). doi:10.1371/journal.pone.0014517.

[313] Tamai, K., Shiina, M., Tanaka, N., Nakano, T., *et al.* Regulation of hepatitis C virus secretion by the Hrs-dependent exosomal pathway. *Virology*, **422**(2): 377–385 (2012). doi:10.1016/j.virol.2011.11.009.

[314] Barouch-Bentov, R., Neveu, G., Xiao, F., Beer, M., *et al.* Hepatitis C Virus Proteins Interact with the Endosomal Sorting Complex Required for Transport (ESCRT) Machinery via Ubiquitination To Facilitate Viral Envelopment. *mBio*, **7**(6): e01456–16 (2016). doi:10.1128/mBio.01456-16. 12

[315] Elgner, F., Donnerhak, C., Ren, H., Medvedev, R., *et al.* Characterization of α-taxilin as a novel factor controlling the release of hepatitis C virus. *Biochemical Journal*, **473**(2): 145–155 (2016). doi:10.1042/BJ20150717. 12

[316] Bayer, K., Banning, C., Bruss, V., Wiltzer-Bach, L., & Schindler, M. Hepatitis C Virus Is Released via a Noncanonical Secretory Route. *Journal of Virology*, **90**(23): 10558–10573 (2016). doi:10.1128/JVI.01615-16. 12, 28

[317] Adams, A., Weinman, S. A., & Wozniak, A. L. Caspase-1 regulates cellular trafficking via cleavage of the Rab7 adaptor protein RILP. *Biochemical and Biophysical Research Communications*, **503**(4): 2619–2624 (2018). doi:10.1016/j.bbrc.2018.08.013. 13

[318] Wozniak, A. L., Long, A., Jones-Jamtgaard, K. N., & Weinman, S. A. Hepatitis C virus promotes virion secretion through cleavage of the Rab7 adaptor protein RILP. *Proceedings of the National Academy of Sciences*, **113**(44): 12484–12489 (2016). doi:10.1073/pnas.1607277113. 13

[319] Ao, X., Zou, L., & Wu, Y. Regulation of autophagy by the Rab GTPase network. *Cell Death & Differentiation*, **21**(3): 348–358 (2014). doi:10.1038/cdd.2013.187. 13

[320] Morgan, N. E., Cutrona, M. B., & Simpson, J. C. Multitasking Rab Proteins in Autophagy and Membrane Trafficking: A Focus on Rab33b. *International Journal of Molecular Sciences*, **20**(16): 3916 (2019). doi:10.3390/ijms20163916. 13

[321] Daussy, C. F., Monard, S. C., Guy, C., Muñoz-González, S., *et al.* The Inflammasome Components NLRP3 and ASC Act in Concert with IRGM To Rearrange the Golgi Apparatus during Hepatitis C Virus Infection. *Journal of Virology*, **95**(3): e00826–20 (2021). doi:10.1128/JVI.00826-20. 13

[322] Kawai, T. & Akira, S. TLR signaling. *Seminars in Immunology*, **19**(1): 24–32 (2007). doi:10.1016/j.smim.2006.12.004. 13

[323] Uehata, T. & Takeuchi, O. RNA Recognition and Immunity—Innate Immune Sensing and Its Posttranscriptional Regulation Mechanisms. *Cells*, **9**(7): 1701 (2020). doi:10.3390/cells9071701. 13

[324] Li, X.-D., Sun, L., Seth, R. B., Pineda, G., & Chen, Z. J. Hepatitis C virus protease NS3/4A cleaves mitochondrial antiviral signaling protein off the mitochondria to evade innate immunity. *Proceedings of the National Academy of Sciences*, **102**(49): 17717–17722 (2005). doi:10.1073/pnas.0508531102. 13, 14

[325] Chan, S. T., Lee, J., Narula, M., & Ou, J.-H. J. Suppression of Host Innate Immune Response by Hepatitis C Virus via Induction of Autophagic Degradation of TRAF6. *Journal of Virology*, **90**(23): 10928–10935 (2016). doi:10.1128/JVI.01365-16. 13, 14

[326] Abe, T., Kaname, Y., Hamamoto, I., Tsuda, Y., *et al.* Hepatitis C Virus Nonstructural Protein 5A Modulates the Toll-Like Receptor-MyD88-Dependent Signaling Pathway in Macrophage Cell Lines. *Journal of Virology*, **81**(17): 8953–8966 (2007). doi:10.1128/JVI.00649-07. 13

[327] Kato, H. & Fujita, T. Cytoplasmic Viral RNA Sensors: RIG-I-Like Receptors. In Encyclopedia of Immunobiology, pp. 352–359. Elsevier (2016). ISBN 978-0-08-092152-5. doi:10.1016/B978-0-12-374279-7.02005-1. 13

[328] Cao, X., Ding, Q., Lu, J., Tao, W., *et al.* MDA5 plays a critical role in interferon response during hepatitis C virus infection. *Journal of Hepatology*, **62**(4): 771–778 (2015). doi:10.1016/j.jhep.2014.11.007. 13

[329] Gokhale, N. S., Vazquez, C., & Horner, S. M. Hepatitis C virus: strategies to evade antiviral responses. *Future Virology*, **9**(12): 1061–1075 (2014). doi:10.2217/fvl.14.89. 13, 14

[330] Lee, J. & Ou, J.-H. J. Hepatitis C virus and intracellular antiviral response. *Current Opinion in Virology*, **52**: 244–249 (2022). doi:10.1016/j.coviro.2021.12.010. 13, 14

[331] Foy, E., Li, K., Sumpter, R., Loo, Y.-M., *et al.* Control of antiviral defenses through hepatitis C virus disruption of retinoic acid-inducible gene-I signaling. *Proceedings of the National Academy of Sciences*, **102**(8): 2986–2991 (2005). doi:10.1073/pnas.0408707102. 14

[332] Otsuka, M., Kato, N., Moriyama, M., Taniguchi, H., *et al.* Interaction between the HCV NS3 protein and the host TBK1 protein leads to inhibition of cellular antiviral responses. *Hepatology*, **41**(5): 1004–1012 (2005). doi:10.1002/hep.20666. 14

[333] Sung, P. S. & Shin, E.-C. Interferon Response in Hepatitis C Virus-Infected Hepatocytes: Issues to Consider in the Era of Direct-Acting Antivirals. *International Journal of Molecular Sciences*, **21**(7): 2583 (2020). doi:10.3390/ijms21072583. 14

[334] Mesev, E. V., LeDesma, R. A., & Ploss, A. Decoding type I and III interferon signalling during viral infection. *Nature Microbiology*, **4**(6): 914–924 (2019). doi:10.1038/s41564-019-0421-x. 14

[335] Hofmann, S., Kedersha, N., Anderson, P., & Ivanov, P. Molecular mechanisms of stress granule assembly and disassembly. *Biochimica et Biophysica Acta (BBA) - Molecular Cell Research*, **1868**(1): 118876 (2021). doi:10.1016/j.bbamcr.2020.118876. 14, 16, 63

[336] Shimoike, T., McKenna, S. A., Lindhout, D. A., & Puglisi, J. D. Translational insensitivity to potent activation of PKR by HCV IRES RNA. *Antiviral Research*, **83**(3): 228–237 (2009). doi:10.1016/j.antiviral.2009.05.004. 14, 16

[337] Arnaud, N., Dabo, S., Maillard, P., Budkowska, A., *et al.* Hepatitis C Virus Controls Interferon Production through PKR Activation. *PLoS ONE*, **5**(5): e10575 (2010). doi:10.1371/journal.pone.0010575.

[338] Dabo, S. & Meurs, E. dsRNA-Dependent Protein Kinase PKR and its Role in Stress, Signaling and HCV Infection. *Viruses*, **4**(11): 2598–2635 (2012). doi:10.3390/v4112598.

[339] Kim, J. H., Park, S. M., Park, J. H., Keum, S. J., & Jang, S. K. eIF2A mediates translation of hepatitis C viral mRNA under stress conditions: eIF2A mediates eIF2-independent translation. *The EMBO Journal*, **30**(12): 2454–2464 (2011). doi:10.1038/emboj.2011.146.

[340] Munir, M. & Berg, M. The multiple faces of proteinkinase R in antiviral defense. *Virulence*, **4**(1): 85–89 (2013). doi:10.4161/viru.23134. 14

[341] Klein, P., Kallenberger, S. M., Roth, H., Roth, K., *et al.* Temporal control of the integrated stress response by a stochastic molecular switch. *Science Advances*, **8**(12): eabk2022 (2022). doi:10.1126/sciadv.abk2022. 14, 16, 80

[342] Arnaud, N., Dabo, S., Akazawa, D., Fukasawa, M., *et al.* Hepatitis C Virus Reveals a Novel Early Control in Acute Immune Response. *PLoS Pathogens*, **7**(10): e1002289 (2011). doi:10.1371/journal.ppat.1002289. 14

[343] Bonnet, M. C., Weil, R., Dam, E., Hovanessian, A. G., & Meurs, E. F. PKR Stimulates NF-κB Irrespective of Its Kinase Function by Interacting with the IκB Kinase Complex. *Molecular and Cellular Biology*, **20**(13): 4532–4542 (2000). doi:10.1128/MCB.20.13.4532-4542.2000. 14

[344] Gil, J., Alcamí, J., & Esteban, M. Activation of NF-κB by the dsRNA-dependent protein kinase, PKR involves the IκB kinase complex. *Oncogene*, **19**(11): 1369–1378 (2000). doi:10.1038/sj.onc.1203448. 14

[345] Gale, M. J., Korth, M. J., Tang, N. M., Tan, S.-L., *et al.* Evidence That Hepatitis C Virus Resistance to Interferon Is Mediated through Repression of the PKR Protein Kinase by the Nonstructural 5A Protein. *Virology*, **230**(2): 217–227 (1997). doi:10.1006/viro.1997.8493. 14, 78

[346] Taylor, D. R., Shi, S. T., Romano, P. R., Barber, G. N., & Lai, M. M. C. Inhibition of the Interferon- Inducible Protein Kinase PKR by HCV E2 Protein. *Science*, **285**(5424): 107–110 (1999). doi:10.1126/science.285.5424.107. 14

[347] Blackham, S. L. & McGarvey, M. J. A host cell RNA-binding protein, Staufen1, has a role in hepatitis C virus replication before virus assembly. *The Journal of General Virology*, **94**(Pt 11): 2429–2436 (2013). doi:10.1099/vir.0.051383-0. 14, 79

[348] Dixit, U., Pandey, A. K., Mishra, P., Sengupta, A., & Pandey, V. N. Staufen1 promotes HCV replication by inhibiting protein kinase R and transporting viral RNA to the site of translation and replication in the cells. *Nucleic Acids Research*, **44**(11): 5271–5287 (2016). doi:10.1093/nar/gkw312. 14, 79, 80

[349] Wilkins, C., Woodward, J., Lau, D. T.-Y., Barnes, A., *et al.* IFITM1 is a tight junction protein that inhibits hepatitis C virus entry. *Hepatology*, **57**(2): 461–469 (2013). doi:10.1002/hep.26066. 14

[350] Yao, L., Dong, H., Zhu, H., Nelson, D., *et al.* Identification of the IFITM3 gene as an inhibitor of hepatitis C viral translation in a stable STAT1 cell line: Anti-HCV activities by STAT1 and 1-8U genes. *Journal of Viral Hepatitis*, **18**(10): e523–e529 (2011). doi:10.1111/j.1365-2893.2011.01452.x. 14

[351] Walter, P. & Ron, D. The Unfolded Protein Response: From Stress Pathway to Homeostatic Regulation. *Science*, **334**(6059): 1081–1086 (2011). doi:10.1126/science.1209038. 15, 63

[352] Chan, S.-W. Unfolded protein response in hepatitis C virus infection. *Frontiers in Microbiology*, **5** (2014). doi:10.3389/fmicb.2014.00233. 15

[353] Ríos-Ocampo, W. A., Navas, M.-C., Faber, K. N., Daemen, T., & Moshage, H. The cellular stress response in hepatitis C virus infection: A balancing act to promote viral persistence and host cell survival. *Virus Research*, **263**: 1–8 (2019). doi:10.1016/j.virusres.2018.12.013. 15

[354] Bertolotti, A., Zhang, Y., Hendershot, L. M., Harding, H. P., & Ron, D. Dynamic interaction of BiP and ER stress transducers in the unfolded-protein response. *Nature Cell Biology*, **2**(6): 326–332 (2000). doi:10.1038/35014014. 15

[355] Shen, J., Chen, X., Hendershot, L., & Prywes, R. ER Stress Regulation of ATF6 Localization by Dissociation of BiP/GRP78 Binding and Unmasking of Golgi Localization Signals. *Developmental Cell*, **3**(1): 99–111 (2002). doi:10.1016/S1534-5807(02)00203-4. 15

[356] Schindler, A. J. & Schekman, R. In vitro reconstitution of ER-stress induced ATF6 transport in COPII vesicles. *Proceedings of the National Academy of Sciences*, **106**(42): 17775–17780 (2009). doi:10.1073/pnas.0910342106. 15

[357] Haze, K., Yoshida, H., Yanagi, H., Yura, T., & Mori, K. Mammalian Transcription Factor ATF6 Is Synthesized as a Transmembrane Protein and Activated by Proteolysis in Response to Endoplasmic Reticulum Stress. *Molecular Biology of the Cell*, **10**(11): 3787–3799 (1999). doi:10.1091/mbc.10.11.3787. 15

[358] Harding, H. P., Zhang, Y., & Ron, D. Protein translation and folding are coupled by an endoplasmic-reticulum-resident kinase. *Nature*, **397**(6716): 271–274 (1999). doi:10.1038/16729. 15

[359] Harding, H. P., Novoa, I., Zhang, Y., Zeng, H., *et al.* Regulated Translation Initiation Controls Stress-Induced Gene Expression in Mammalian Cells. *Molecular Cell*, **6**(5): 1099–1108 (2000). doi:10.1016/S1097-2765(00)00108-8. 15

[360] Ohoka, N., Yoshii, S., Hattori, T., Onozaki, K., & Hayashi, H. TRB3, a novel ER stress-inducible gene, is induced via ATF4–CHOP pathway and is involved in cell death. *The EMBO Journal*, **24**(6): 1243–1255 (2005). doi:10.1038/sj.emboj.7600596. 15

[361] Tallóczy, Z., Jiang, W., Virgin, H. W., Leib, D. A., *et al.* Regulation of starvation- and virus-induced autophagy by the eIF2α kinase signaling pathway. *Proceedings of the National Academy of Sciences*, **99**(1): 190–195 (2002). doi:10.1073/pnas.012485299. 15

[362] Novoa, I., Zeng, H., Harding, H. P., & Ron, D. Feedback Inhibition of the Unfolded Protein Response by GADD34-Mediated Dephosphorylation of eIF2α. *Journal of Cell Biology*, **153**(5): 1011–1022 (2001). doi:10.1083/jcb.153.5.1011. 15

[363] Connor, J. H., Weiser, D. C., Li, S., Hallenbeck, J. M., & Shenolikar, S. Growth Arrest and DNA Damage-Inducible Protein GADD34 Assembles a Novel Signaling Complex Containing Protein Phosphatase 1 and Inhibitor 1. *Molecular and Cellular Biology*, **21**(20): 6841–6850 (2001). doi:10.1128/MCB.21.20.6841-6850.2001. 15

[364] Korennykh, A. V., Egea, P. F., Korostelev, A. A., Finer-Moore, J., *et al.* The unfolded protein response signals through high-order assembly of Ire1. *Nature*, **457**(7230): 687–693 (2009). doi:10.1038/nature07661. 15

[365] Ali, M. M. U., Bagratuni, T., Davenport, E. L., Nowak, P. R., *et al.* Structure of the Ire1 autophosphorylation complex and implications for the unfolded protein response: Structure of the Ire1 autophosphorylation complex and implications for the UPR. *The EMBO Journal*, **30**(5): 894–905 (2011). doi:10.1038/emboj.2011.18. 15

[366] Hollien, J. & Weissman, J. S. Decay of Endoplasmic Reticulum-Localized mRNAs During the Unfolded Protein Response. *Science*, **313**(5783): 104–107 (2006). doi:10.1126/science.1129631. 15

[367] Hollien, J., Lin, J. H., Li, H., Stevens, N., *et al.* Regulated Ire1-dependent decay of messenger RNAs in mammalian cells. *Journal of Cell Biology*, **186**(3): 323–331 (2009). doi:10.1083/jcb.200903014.

[368] Iwawaki, T., Hosoda, A., Okuda, T., Kamigori, Y., *et al.* Translational control by the ER transmembrane kinase/ribonuclease IRE1 under ER stress. *Nature Cell Biology*, **3**(2): 158–164 (2001). doi:10.1038/35055065. 15

[369] Darling, N. J. & Cook, S. J. The role of MAPK signalling pathways in the response to endoplasmic reticulum stress. *Biochimica et Biophysica Acta (BBA) - Molecular Cell Research*, **1843**(10): 2150–2163 (2014). doi:10.1016/j.bbamcr.2014.01.009. 15, 81

[370] Tardif, K. D., Mori, K., Kaufman, R. J., & Siddiqui, A. Hepatitis C Virus Suppresses the IRE1-XBP1 Pathway of the Unfolded Protein Response. *Journal of Biological Chemistry*, **279**(17): 17158–17164 (2004). doi:10.1074/jbc.M312144200. 15, 81, 83

[371] Pal, S., Polyak, S. J., Bano, N., Qiu, W. C., *et al.* Hepatitis C virus induces oxidative stress, DNA damage and modulates the DNA repair enzyme NEIL1: HCV modulates NEIL1. *Journal of Gastroenterology and Hepatology*, **25**(3): 627–634 (2010). doi:10.1111/j.1440-1746.2009.06128.x. 16

[372] Ivanov, A. V., Smirnova, O. A., Ivanova, O. N., Masalova, O. V., *et al.* Hepatitis C Virus Proteins Activate NRF2/ARE Pathway by Distinct ROS-Dependent and Independent Mechanisms in HUH7 Cells. *PLoS ONE*, **6**(9): e24957 (2011). doi:10.1371/journal.pone.0024957. 16

[373] Ivanov, A., Bartosch, B., Smirnova, O., Isaguliants, M., & Kochetkov, S. HCV and Oxidative Stress in the Liver. *Viruses*, **5**(2): 439–469 (2013). doi:10.3390/v5020439. 16

[374] Ivanov, A., Smirnova, O., Petrushanko, I., Ivanova, O., *et al.* HCV Core Protein Uses Multiple Mechanisms to Induce Oxidative Stress in Human Hepatoma Huh7 Cells. *Viruses*, **7**(6): 2745–2770 (2015). doi:10.3390/v7062745. 16

[375] Korenaga, M., Wang, T., Li, Y., Showalter, L. A., *et al.* Hepatitis C Virus Core Protein Inhibits Mitochondrial Electron Transport and Increases Reactive Oxygen

Species (ROS) Production. *Journal of Biological Chemistry*, **280**(45): 37481–37488 (2005). doi:10.1074/jbc.M506412200. 16

[376] Piccoli, C., Scrima, R., Quarato, G., D'Aprile, A., *et al.* Hepatitis C virus protein expression causes calcium-mediated mitochondrial bioenergetic dysfunction and nitro-oxidative stress. *Hepatology*, **46**(1): 58–65 (2007). doi:10.1002/hep.21679. 16

[377] Carvajal-Yepes, M., Himmelsbach, K., Schaedler, S., Ploen, D., *et al.* Hepatitis C Virus Impairs the Induction of Cytoprotective Nrf2 Target Genes by Delocalization of Small Maf Proteins. *Journal of Biological Chemistry*, **286**(11): 8941–8951 (2011). doi:10.1074/jbc.M110.186684. 16

[378] Jack, S. C. & Chan, S.-W. The role of PERK and GCN2 in basal and hydrogen peroxide-regulated translation from the hepatitis C virus internal ribosome entry site. *Virus Genes*, **43**(2): 208–214 (2011). doi:10.1007/s11262-011-0629-1. 16

[379] Verfaillie, T., Rubio, N., Garg, A. D., Bultynck, G., *et al.* PERK is required at the ER-mitochondrial contact sites to convey apoptosis after ROS-based ER stress. *Cell Death & Differentiation*, **19**(11): 1880–1891 (2012). doi:10.1038/cdd.2012.74. 16

[380] Di Bona, D., Cippitelli, M., Fionda, C., Cammà, C., *et al.* Oxidative stress inhibits IFN-α-induced antiviral gene expression by blocking the JAK–STAT pathway. *Journal of Hepatology*, **45**(2): 271–279 (2006). doi:10.1016/j.jhep.2006.01.037. 16

[381] Protter, D. S. & Parker, R. Principles and Properties of Stress Granules. *Trends in Cell Biology*, **26**(9): 668–679 (2016). doi:10.1016/j.tcb.2016.05.004. 16

[382] Sano, R. & Reed, J. C. ER stress-induced cell death mechanisms. *Biochimica et Biophysica Acta (BBA) - Molecular Cell Research*, **1833**(12): 3460–3470 (2013). doi:10.1016/j.bbamcr.2013.06.028. 16

[383] Ruggieri, A., Dazert, E., Metz, P., Hofmann, S., *et al.* Dynamic Oscillation of Translation and Stress Granule Formation Mark the Cellular Response to Virus Infection. *Cell Host & Microbe*, **12**(1): 71–85 (2012). doi:10.1016/j.chom.2012.05.013. 16, 80

[384] Liu, X. & Green, R. M. Endoplasmic reticulum stress and liver diseases. *Liver Research*, **3**(1): 55–64 (2019). doi:10.1016/j.livres.2019.01.002. 16, 17

[385] Wei, J. & Fang, D. Endoplasmic Reticulum Stress Signaling and the Pathogenesis of Hepatocarcinoma. *International Journal of Molecular Sciences*, **22**(4): 1799 (2021). doi:10.3390/ijms22041799.

[386] Kim, J. Y., Garcia-Carbonell, R., Yamachika, S., Zhao, P., *et al.* ER Stress Drives Lipogenesis and Steatohepatitis via Caspase-2 Activation of S1P. *Cell*, **175**(1): 133–145.e15 (2018). doi:10.1016/j.cell.2018.08.020.

[387] Urra, H., Dufey, E., Avril, T., Chevet, E., & Hetz, C. Endoplasmic Reticulum Stress and the Hallmarks of Cancer. *Trends in Cancer*, **2**(5): 252–262 (2016). doi:10.1016/j.trecan.2016.03.007. 16, 17

[388] Valgimigli, M., Valgimigli, L., Trerè, D., Gaiani, S., *et al.* Oxidative Stress EPR Measurement in Human Liver by Radical-probe Technique. Correlation with Etiology, Histology and Cell Proliferation. *Free Radical Research*, **36**(9): 939–948 (2002). doi:10.1080/10715602100006653. 17

[389] Shuda, M., Kondoh, N., Imazeki, N., Tanaka, K., *et al.* Activation of the ATF6, XBP1 and grp78 genes in human hepatocellular carcinoma: a possible involvement of the ER stress pathway in hepatocarcinogenesis. *Journal of Hepatology*, **38**(5): 605–614 (2003). doi:10.1016/S0168-8278(03)00029-1.

[390] Asselah, T., Bièche, I., Mansouri, A., Laurendeau, I., *et al.* In vivo hepatic endoplasmic reticulum stress in patients with chronic hepatitis C. *The Journal of Pathology*, **221**(3): 264–274 (2010). doi:10.1002/path.2703.

[391] McPherson, S., Powell, E. E., Barrie, H. D., Clouston, A. D., *et al.* No evidence of the unfolded protein response in patients with chronic hepatitis C virus infection: Unfolded protein response and HCV. *Journal of Gastroenterology and Hepatology*, **26**(2): 319–327 (2011). doi:10.1111/j.1440-1746.2010.06368.x. 17

[392] Gillman, R., Lopes Floro, K., Wankell, M., & Hebbard, L. The role of DNA damage and repair in liver cancer. *Biochimica et Biophysica Acta (BBA) - Reviews on Cancer*, **1875**(1): 188493 (2021). doi:10.1016/j.bbcan.2020.188493. 17

[393] Machida, K., McNamara, G., Cheng, K. T.-H., Huang, J., *et al.* Hepatitis C Virus Inhibits DNA Damage Repair through Reactive Oxygen and Nitrogen Species and by Interfering with the ATM-NBS1/Mre11/Rad50 DNA Repair Pathway in Monocytes and Hepatocytes. *The Journal of Immunology*, **185**(11): 6985–6998 (2010). doi:10.4049/jimmunol.1000618.

[394] Nguyen, T. T. T., Park, E.-M., Lim, Y.-S., & Hwang, S. B. Nonstructural Protein 5A Impairs DNA Damage Repair: Implications for Hepatitis C Virus-Mediated Hepatocarcinogenesis. *Journal of Virology*, **92**(11): e00178–18 (2018). doi:10.1128/JVI.00178-18.

[395] Pham, H. T., Nguyen, T. T. T., Nguyen, L. P., Han, S.-S., *et al.* Hepatitis C Virus Downregulates Ubiquitin-Conjugating Enzyme E2S Expression To Prevent Proteasomal Degradation of NS5A, Leading to Host Cells More Sensitive to DNA Damage. *Journal of Virology*, **93**(2): e01240–18 (2019). doi:10.1128/JVI.01240-18. 17

[396] Carnero, E., Barriocanal, M., Prior, C., Pablo Unfried, J., *et al.* Long noncoding RNA EGOT negatively affects the antiviral response and favors HCV replication. *EMBO reports*, **17**(7): 1013–1028 (2016). doi:10.15252/embr.201541763. 17

[397] Levy, S. & Shoham, T. The tetraspanin web modulates immune-signalling complexes. *Nature Reviews Immunology*, **5**(2): 136–148 (2005). doi:10.1038/nri1548. 17

[398] Charrin, S., Jouannet, S., Boucheix, C., & Rubinstein, E. Tetraspanins at a glance. *Journal of Cell Science*, p. jcs.154906 (2014). doi:10.1242/jcs.154906. 17, 18

[399] Zimmerman, B., Kelly, B., McMillan, B. J., Seegar, T. C. M., *et al.* Crystal Structure of a Full-Length Human Tetraspanin Reveals a Cholesterol-Binding Pocket. *Cell*, **167**(4): 1041–1051.e11 (2016). doi:10.1016/j.cell.2016.09.056. 17, 46, 74

[400] Umeda, R., Satouh, Y., Takemoto, M., Nakada-Nakura, Y., *et al.* Structural insights into tetraspanin CD9 function. *Nature Communications*, **11**(1): 1606 (2020). doi:10.1038/s41467-020-15459-7. 17

[401] Caparotta, M. & Masone, D. Cholesterol plays a decisive role in tetraspanin assemblies during bilayer deformations. *Biosystems*, **209**: 104505 (2021). doi:10.1016/j.biosystems.2021.104505.

[402] Palor, M., Stejskal, L., Mandal, P., Lenman, A., *et al.* Cholesterol sensing by CD81 is important for hepatitis C virus entry. *Journal of Biological Chemistry*, **295**(50): 16931–16948 (2020). doi:10.1074/jbc.RA120.014761. 17, 74

[403] Susa, K. J., Rawson, S., Kruse, A. C., & Blacklow, S. C. Cryo-EM structure of the B cell co-receptor CD19 bound to the tetraspanin CD81. *Science*, **371**(6526): 300–305 (2021). doi:10.1126/science.abd9836. 17, 18, 74

[404] Florin, L. & Lang, T. Tetraspanin Assemblies in Virus Infection. *Frontiers in Immunology*, **9**: 1140 (2018). doi:10.3389/fimmu.2018.01140. 17

[405] Hantak, M. P., Qing, E., Earnest, J. T., & Gallagher, T. Tetraspanins: Architects of Viral Entry and Exit Platforms. *Journal of Virology*, **93**(6): e01429–17 (2019). doi:10.1128/JVI.01429-17. 17, 18

[406] Raaben, M., Jae, L. T., Herbert, A. S., Kuehne, A. I., *et al.* NRP2 and CD63 Are Host Factors for Lujo Virus Cell Entry. *Cell Host & Microbe*, **22**(5): 688–696.e5 (2017). doi:10.1016/j.chom.2017.10.002.

[407] Fast, L., Mikuličić, S., Fritzen, A., Schwickert, J., *et al.* Inhibition of Tetraspanin Functions Impairs Human Papillomavirus and Cytomegalovirus Infections. *International Journal of Molecular Sciences*, **19**(10): 3007 (2018). doi:10.3390/ijms19103007. 17

[408] Ninomiya, M., Inoue, J., Krueger, E. W., Chen, J., *et al.* The Exosome-Associated Tetraspanin CD63 Contributes to the Efficient Assembly and Infectivity of the Hepatitis B Virus. *Hepatology Communications*, **5**(7): 1238–1251 (2021). doi:10.1002/hep4.1709. 17

[409] Rocha-Perugini, V., Suárez, H., Álvarez, S., López-Martín, S., *et al.* CD81 association with SAMHD1 enhances HIV-1 reverse transcription by increasing dNTP levels. *Nature Microbiology*, **2**(11): 1513–1522 (2017). doi:10.1038/s41564-017-0019-0. 17

[410] Lasswitz, L., Zapatero-Belinchón, F. J., Moeller, R., Hülskötter, K., *et al.* The Tetraspanin CD81 Is a Host Factor for Chikungunya Virus Replication. *mBio*, **13**(3): e00731–22 (2022). doi:10.1128/mbio.00731-22. 18

[411] Dharan, R., Goren, S., Cheppali, S. K., Shendrik, P., *et al.* Transmembrane proteins tetraspanin 4 and CD9 sense membrane curvature. *Proceedings of the National Academy of Sciences*, **119**(43): e2208993119 (2022). doi:10.1073/pnas.2208993119. 18

[412] Zhang, Y.-Y., Zhang, B.-H., Ishii, K., & Liang, T. J. Novel Function of CD81 in Controlling Hepatitis C Virus Replication. *Journal of Virology*, **84**(7): 3396–3407 (2010). doi:10.1128/JVI.02391-09. 18

[413] Masciopinto, F., Giovani, C., Campagnoli, S., Galli-Stampino, L., *et al.* Association of hepatitis C virus envelope proteins with exosomes. *European Journal of Immunology*, **34**(10): 2834–2842 (2004). doi:10.1002/eji.200424887. 18

[414] Dreux, M., Garaigorta, U., Boyd, B., Décembre, E., *et al.* Short-Range Exosomal Transfer of Viral RNA from Infected Cells to Plasmacytoid Dendritic Cells Triggers Innate Immunity. *Cell Host & Microbe*, **12**(4): 558–570 (2012). doi:10.1016/j.chom.2012.08.010. 18

[415] Ramakrishnaiah, V., Thumann, C., Fofana, I., Habersetzer, F., *et al.* Exosome-mediated transmission of hepatitis C virus between human hepatoma Huh7.5 cells.

Proceedings of the National Academy of Sciences, **110**(32): 13109–13113 (2013). doi:10.1073/pnas.1221899110. 18, 76

[416] Ke, P.-Y. & Chen, S. S.-L. Active RNA Replication of Hepatitis C Virus Downregulates CD81 Expression. *PLoS ONE*, **8**(1): e54866 (2013). doi:10.1371/journal.pone.0054866. 18, 73

[417] Zheng, Y., Ye, L.-B., Liu, J., Jing, W., *et al.* Gene Expression Profiles of HeLa Cells Impacted by Hepatitis C Virus Non-structural Protein NS4B. *BMB Reports*, **38**(2): 151–160 (2005). doi:10.5483/BMBRep.2005.38.2.151. 18, 73

[418] Tscherne, D. M., Evans, M. J., von Hahn, T., Jones, C. T., *et al.* Superinfection Exclusion in Cells Infected with Hepatitis C Virus. *Journal of Virology*, **81**(8): 3693–3703 (2007). doi:10.1128/JVI.01748-06. 18, 73

[419] Park, J. H., Park, S., Yang, J.-S., Kwon, O. S., *et al.* Discovery of Cellular Proteins Required for the Early Steps of HCV Infection Using Integrative Genomics. *PLoS ONE*, **8**(4): e60333 (2013). doi:10.1371/journal.pone.0060333. 18

[420] Lussignol, M., Kopp, M., Molloy, K., Vizcay-Barrena, G., *et al.* Proteomics of HCV virions reveals an essential role for the nucleoporin Nup98 in virus morphogenesis. *Proceedings of the National Academy of Sciences*, **113**(9): 2484–2489 (2016). doi:10.1073/pnas.1518934113. 18

[421] Gallard, C., Lebsir, N., Khursheed, H., Reungoat, E., *et al.* Heparanase-1 is upregulated by hepatitis C virus and favors its replication. *Journal of Hepatology*, **77**(1): 29–41 (2022). doi:10.1016/j.jhep.2022.01.008. 18, 73, 74

[422] Hagen, N., Bayer, K., Rösch, K., & Schindler, M. The Intraviral Protein Interaction Network of Hepatitis C Virus. *Molecular & Cellular Proteomics*, **13**(7): 1676–1689 (2014). doi:10.1074/mcp.M113.036301. 26, 27

[423] Banse, P., Moeller, R., Bruening, J., Lasswitz, L., *et al.* CD81 Receptor Regions outside the Large Extracellular Loop Determine Hepatitis C Virus Entry into Hepatoma Cells. *Viruses*, **10**(4): 207 (2018). doi:10.3390/v10040207. 27, 74

[424] Schaller, T., Appel, N., Koutsoudakis, G., Kallis, S., *et al.* Analysis of hepatitis C virus superinfection exclusion by using novel fluorochrome gene-tagged viral genomes. *Journal of Virology*, **81**(9): 4591–4603 (2007). doi:10.1128/JVI.02144-06. 28, 73, 74, 77

[425] García-Mediavilla, M. V., Pisonero-Vaquero, S., Lima-Cabello, E., Benedicto, I., *et al.* Liver X receptor α-mediated regulation of lipogenesis by core and NS5A proteins contributes to HCV-induced liver steatosis and HCV replication. *Laboratory Investigation*, **92**(8): 1191–1202 (2012). doi:10.1038/labinvest.2012.88. 29

[426] Chang, G.-W., Hsiao, C.-C., Peng, Y.-M., Vieira Braga, F. A., *et al.* The Adhesion G Protein-Coupled Receptor GPR56/ADGRG1 Is an Inhibitory Receptor on Human NK Cells. *Cell Reports*, **15**(8): 1757–1770 (2016). doi:10.1016/j.celrep.2016.04.053. 29

[427] Ghezzi, M. C., Raponi, G., Angeletti, S., & Mancini, C. Serum-Mediated Enhancement of TNF-α Release by Human Monocytes Stimulated with the Yeast Form of *Candida albicans*. *The Journal of Infectious Diseases*, **178**(6): 1743–1749 (1998). doi:10.1086/314484. 29

[428] Schnupf, P. & Sansonetti, P. J. Quantitative RT-PCR profiling of the Rabbit Immune Response: Assessment of Acute Shigella flexneri Infection. *PLoS ONE*, **7**(6): e36446 (2012). doi:10.1371/journal.pone.0036446. 29

[429] Businger, R., Deutschmann, J., Gruska, I., Milbradt, J., *et al.* Human cytomegalovirus overcomes SAMHD1 restriction in macrophages via pUL97. *Nature Microbiology*, **4**(12): 2260–2272 (2019). doi:10.1038/s41564-019-0557-8. 29

[430] Yoon, S.-B., Park, Y.-H., Choi, S.-A., Yang, H.-J., *et al.* Real-time PCR quantification of spliced X-box binding protein 1 (XBP1) using a universal primer method. *PLOS ONE*, **14**(7): e0219978 (2019). doi:10.1371/journal.pone.0219978. 29, 30

[431] Savic, S., Ouboussad, L., Dickie, L. J., Geiler, J., *et al.* TLR dependent XBP-1 activation induces an autocrine loop in rheumatoid arthritis synoviocytes. *Journal of Autoimmunity*, **50**(100): 59–66 (2014). doi:10.1016/j.jaut.2013.11.002. 30

[432] Bond, S. R. & Naus, C. C. RF-Cloning.org: an online tool for the design of restriction-free cloning projects. *Nucleic Acids Research*, **40**(Web Server issue): W209–213 (2012). doi:10.1093/nar/gks396. 32

[433] Sanjana, N. E., Shalem, O., & Zhang, F. Improved vectors and genome-wide libraries for CRISPR screening. *Nature Methods*, **11**(8): 783–784 (2014). doi:10.1038/nmeth.3047. 32

[434] Shalem, O., Sanjana, N. E., Hartenian, E., Shi, X., *et al.* Genome-scale CRISPR-Cas9 knockout screening in human cells. *Science (New York, N.Y.)*, **343**(6166): 84–87 (2014). doi:10.1126/science.1247005. 32

[435] Labun, K., Montague, T. G., Krause, M., Torres Cleuren, Y. N., *et al.* CHOPCHOP v3: expanding the CRISPR web toolbox beyond genome editing. *Nucleic Acids Research*, **47**(W1): W171–W174 (2019). doi:10.1093/nar/gkz365. 32

[436] Kurz, S. Characterization of fluorescently labeled HCV genomes to investigate HCV-host interactions. Master's thesis, Ludwig-Maximilians-Universität München, München (2014). 43, 73, 85

[437] Bunz, M. Importance of CD63 and CD81 in HCV Assembly and Release. Master's thesis, Universität Tübingen, Tübingen (2018). 43, 85

[438] Thorne, N., Inglese, J., & Auld, D. S. Illuminating insights into firefly luciferase and other bioluminescent reporters used in chemical biology. *Chemistry & Biology*, **17**(6): 646–657 (2010). doi:10.1016/j.chembiol.2010.05.012. 52, 75

[439] Neil, S. J., Sandrin, V., Sundquist, W. I., & Bieniasz, P. D. An Interferon-α-Induced Tethering Mechanism Inhibits HIV-1 and Ebola Virus Particle Release but Is Counteracted by the HIV-1 Vpu Protein. *Cell Host & Microbe*, **2**(3): 193–203 (2007). doi:10.1016/j.chom.2007.08.001. 56

[440] Neil, S. J. D., Zang, T., & Bieniasz, P. D. Tetherin inhibits retrovirus release and is antagonized by HIV-1 Vpu. *Nature*, **451**(7177): 425–430 (2008). doi:10.1038/nature06553. 56

[441] Almasi, S. & Jasmin, B. J. The multifunctional RNA-binding protein Staufen1: an emerging regulator of oncogenesis through its various roles in key cellular events. *Cellular and Molecular Life Sciences*, **78**(23): 7145–7160 (2021). doi:10.1007/s00018-021-03965-w. 63, 79

[442] Schmitz, M., Shaban, M., Albert, B., Gökçen, A., & Kracht, M. The Crosstalk of Endoplasmic Reticulum (ER) Stress Pathways with NF-κB: Complex Mechanisms Relevant for Cancer, Inflammation and Infection. *Biomedicines*, **6**(2): 58 (2018). doi:10.3390/biomedicines6020058. 64, 80

[443] Eisele, M. The role of CD81 in the regulation of the NF-κB pathway in regard to HCV. Bachelor's Thesis, Universität Tübingen, Tübingen (2022). 64

[444] Susa, K. J., Seegar, T. C., Blacklow, S. C., & Kruse, A. C. A dynamic interaction between CD19 and the tetraspanin CD81 controls B cell co-receptor trafficking. *eLife*, **9**: e52337 (2020). doi:10.7554/eLife.52337. 73

[445] Zhang, X.-F., Zhang, S., Guo, Q., Sun, R., *et al.* A New Mechanistic Model for Viral Cross Protection and Superinfection Exclusion. *Frontiers in Plant Science*, **9**: 40 (2018). doi:10.3389/fpls.2018.00040. 74

[446] Folimonova, S. Y. Superinfection exclusion is an active virus-controlled function that requires a specific viral protein. *Journal of Virology*, **86**(10): 5554–5561 (2012). doi:10.1128/JVI.00310-12.

[447] Biryukov, J. & Meyers, C. Superinfection Exclusion between Two High-Risk Human Papillomavirus Types during a Coinfection. *Journal of Virology*, **92**(8): e01993–17 (2018). doi:10.1128/JVI.01993-17.

[448] Kirchberger, P. C., Martinez, Z. A., Luker, L. J., & Ochman, H. Defensive hypervariable regions confer superinfection exclusion in microviruses. *Proceedings of the National Academy of Sciences*, **118**(28): e2102786118 (2021). doi:10.1073/pnas.2102786118. 74

[449] Lim, J., Petersen, M., Bunz, M., Simon, C., & Schindler, M. Flow cytometry based-FRET: basics, novel developments and future perspectives. *Cellular and Molecular Life Sciences*, **79**(4): 217 (2022). doi:10.1007/s00018-022-04232-2. 74

[450] Sun, Y., Wallrabe, H., Booker, C. F., Day, R. N., & Periasamy, A. Three-Color Spectral FRET Microscopy Localizes Three Interacting Proteins in Living Cells. *Biophysical Journal*, **99**(4): 1274–1283 (2010). doi:10.1016/j.bpj.2010.06.004.

[451] Woehler, A. Simultaneous Quantitative Live Cell Imaging of Multiple FRET-Based Biosensors. *PLoS ONE*, **8**(4): e61096 (2013). doi:10.1371/journal.pone.0061096. 74

[452] Timpe, J. M., Stamataki, Z., Jennings, A., Hu, K., *et al.* Hepatitis C virus cell-cell transmission in hepatoma cells in the presence of neutralizing antibodies. *Hepatology*, **47**(1): 17–24 (2007). doi:10.1002/hep.21959. 76

[453] Brimacombe, C. L., Grove, J., Meredith, L. W., Hu, K., *et al.* Neutralizing Antibody-Resistant Hepatitis C Virus Cell-to-Cell Transmission. *Journal of Virology*, **85**(1): 596–605 (2011). doi:10.1128/JVI.01592-10. 76

[454] Ciesek, S., Westhaus, S., Wicht, M., Wappler, I., *et al.* Impact of Intra- and Interspecies Variation of Occludin on Its Function as Coreceptor for Authentic Hepatitis C Virus Particles. *Journal of Virology*, **85**(15): 7613–7621 (2011). doi:10.1128/JVI.00212-11.

[455] Catanese, M. T., Loureiro, J., Jones, C. T., Dorner, M., *et al.* Different Requirements for Scavenger Receptor Class B Type I in Hepatitis C Virus Cell-Free versus Cell-to-Cell Transmission. *Journal of Virology*, **87**(15): 8282–8293 (2013). doi:10.1128/JVI.01102-13. 76

[456] Valli, M. B., Crema, A., Lanzilli, G., Serafino, A., *et al.* Molecular and cellular determinants of cell-to-cell transmission of HCV in vitro. *Journal of Medical Virology*, **79**(10): 1491–1499 (2007). doi:10.1002/jmv.20947.

[457] Fan, H., Qiao, L., Kang, K.-D., Fan, J., *et al.* Attachment and Postattachment Receptors Important for Hepatitis C Virus Infection and Cell-to-Cell Transmission. *Journal of Virology*, **91**(13): e00280–17 (2017). doi:10.1128/JVI.00280-17. 76

[458] Witteveldt, J., Evans, M. J., Bitzegeio, J., Koutsoudakis, G., *et al.* CD81 is dispensable for hepatitis C virus cell-to-cell transmission in hepatoma cells. *Journal of General Virology*, **90**(1): 48–58 (2009). doi:10.1099/vir.0.006700-0.

[459] Potel, J., Rassam, P., Montpellier, C., Kaestner, L., *et al.* EWI-2wint promotes CD81 clustering that abrogates Hepatitis C Virus entry: Dynamics and partitioning of CD81. *Cellular Microbiology*, **15**(7): 1234–1252 (2013). doi:10.1111/cmi.12112.

[460] Fénéant, L., Levy, S., & Cocquerel, L. CD81 and Hepatitis C Virus (HCV) Infection. *Viruses*, **6**(2): 535–572 (2014). doi:10.3390/v6020535. 76

[461] Jeppesen, D. K., Fenix, A. M., Franklin, J. L., Higginbotham, J. N., *et al.* Reassessment of Exosome Composition. *Cell*, **177**(2): 428–445.e18 (2019). doi:10.1016/j.cell.2019.02.029. 76

[462] Rogers, T. B., Inesi, G., Wade, R., & Lederer, W. J. Use of thapsigargin to study Ca2+ homeostasis in cardiac cells. *Bioscience Reports*, **15**(5): 341–349 (1995). doi:10.1007/BF01788366. 79

[463] Groenendyk, J., Agellon, L. B., & Michalak, M. Calcium signaling and endoplasmic reticulum stress. In International Review of Cell and Molecular Biology, volume 363, pp. 1–20. Elsevier (2021). ISBN 978-0-12-824036-6. doi:10.1016/bs.ircmb.2021.03.003. 79

[464] Reyland, M., E. Protein kinase C isoforms: Multi-functional regulators of cell life and death. *Frontiers in Bioscience*, **Volume**(14): 2386 (2009). doi:10.2741/3385. 81

[465] Fink, S. L., Jayewickreme, T. R., Molony, R. D., Iwawaki, T., *et al.* IRE1α promotes viral infection by conferring resistance to apoptosis. *Science Signaling*, **10**(482): eaai7814 (2017). doi:10.1126/scisignal.aai7814. 81, 83

[466] Renner, F. & Schmitz, M. L. Autoregulatory feedback loops terminating the NF-κB response. *Trends in Biochemical Sciences*, **34**(3): 128–135 (2009). doi:10.1016/j.tibs.2008.12.003. 82

[467] Song, X., Yao, Z., Yang, J., Zhang, Z., *et al.* HCV core protein binds to gC1qR to induce A20 expression and inhibit cytokine production through MAPKs and NF-κB signaling pathways. *Oncotarget*, **7**(23): 33796–33808 (2016). doi:10.18632/oncotarget.9304. 83

[468] Lee, J., Chan, S. T., Kim, J. Y., & Ou, J.-h. J. Hepatitis C Virus Induces the Ubiquitin-Editing Enzyme A20 via Depletion of the Transcription Factor Upstream Stimulatory Factor 1 To Support Its Replication. *mBio*, **10**(4): e01660–19 (2019). doi:10.1128/mBio.01660-19. 83